

Effet de la température sur la rétention de U(VI) par SrTiO_3

G. Garcia-Rosales

▶ **To cite this version:**

G. Garcia-Rosales. Effet de la température sur la rétention de U(VI) par SrTiO_3. Radiochimie. Université Paris Sud - Paris XI, 2007. Français. NNT : . tel-00200303

HAL Id: tel-00200303
https://theses.hal.science/tel-00200303

Submitted on 17 Jan 2008

HAL is a multi-disciplinary open access archive for the deposit and dissemination of scientific research documents, whether they are published or not. The documents may come from teaching and research institutions in France or abroad, or from public or private research centers.

L'archive ouverte pluridisciplinaire **HAL**, est destinée au dépôt et à la diffusion de documents scientifiques de niveau recherche, publiés ou non, émanant des établissements d'enseignement et de recherche français ou étrangers, des laboratoires publics ou privés.

N° d'ordre : 8859

UNIVERSITE PARIS SUD 11
UFR SCIENTIFIQUE D'ORSAY

THESE

Présentée

Pour obtenir

LE GRADE DE DOCTEUR EN SCIENCES
DE L'UNIVERSITE PARIS SUD 11 ORSAY

PAR

Genoveva GARCIA ROSALES

« Effet de la Température sur la rétention de U(VI) par $SrTiO_3$ »

Soutenue le 28 de Novembre 2007 devant la Commission d'examen :

M. Eric SIMONI	Directeur de Thèse
M. Jean-Jacques EHRHARDT	Rapporteur
M. Nicolas MARMIER	Rapporteur
M. Hubert CATALETTE	Examinateur
Mme. Mireille DEL NERO	Examinateur
M. Romuald DROT	

REMERCIEMENTS

Je tiens à remercier le Gouvernement du Mexique pour le support financier qu'il m'a accordé à travers le CONACYT (Conseo Nacional de Ciencia y Tecnologia). Je tiens, à ce titre, à adresser ma gratitude à Madame Ivonne Hank Rhon, présidente de la fondation « Cuauhtémoc Hank Rhon » pour sa confiance et son soutien tout au long de ma formation.

Je tiens à remercier toutes les personnes ayant contribué à la réalisation et au bon déroulement de ce travail.

Je remercie tout particulièrement Monsieur le Professeur Eric SIMONI pour m'avoir accueillie au sein du laboratoire de Radiochimie de l'Institut de Physique Nucléaire d'Orsay et pour avoir dirigé ce travail avec un grand professionnalisme et un grand sens des responsabilités. J'ai tout particulièrement apprécié sa considération envers moi et le temps consacré à ma formation.

Je remercie, pour leur encadrement, Madame Florence MERCIER-BION et tout particulièrement Monsieur Romuald DROT à qui je voudrais adresser mes sincères remerciements pour son encadrement tout au long de ces trois années où sa capacité à travailler, sa patience, sa compétence, son goût pour l'enseignement et le partage des connaissances ont su rendre ce travail enrichissant et passionnant.

J'adresse mes sincères remerciements à Monsieur Jean-Jacques EHRHARDT et Monsieur le Professeur Nicolas MARMIER pour avoir bien voulu juger ce travail en tant que rapporteurs. Je tiens également à remercier Monsieur Hubert CATALETTE et Madame Mireille DEL NERO pour avoir participé à ce jury de thèse.

Je remercie également Monsieur Jacques LAMBERT et tout le laboratoire de chimie Physique et Microbiologie pour l'environnement de Nancy pour m'avoir permis de réaliser des expériences par XPS. Que Madame Valérie BOSSE de l'Ecole de Mines de Nantes soit également remerciée pour m'avoir accueillie dans son laboratoire à fin de réaliser des mesures d'ICP-MS.

J’associe également à ces remerciements, Monsieur Eduardo Ordóñez Regil pour m’avoir soutenue au cours de ces trois années, qu’il soit remercié pour son amitié et pour m’avoir permis de réaliser des expériences au sein de l’ININ (Instituto Nacional de Investigaciones Nucleares).

Je tiens à remercier Monsieur Gérard Lagarde pour son aide précieuse dans les expériences de SLRT et particulièrement dans les études réalisées sur le transfert d’énergie. J’associe à ces remerciements l’ensemble des personnes du Groupe de Radiochimie de l’IPN : Mesdames, Céline CANNES, Blandine FOUREST, Claire LE NAOUR, ainsi que Messieurs Nicolas Dacheux, Ahmet ÖZGÜMÜS, Jérôme ROQUES, et Vladimir SLADKOV. Que mesdames Nicole Barre et Nicole Tourne soient également remerciées pour leur soutien et amitié ainsi que mes amies Nina HINGANT et Natasha BUDANOVA avec qui j’ai partagé des moments importants de ma vie et à qui je suis reconnaissante autant pour son amitié que pour son soutien inconditionnel.

Je remercie avec amitié les thésards et post-doc du groupe de Radiochimie : Maria Vita DI GIANDOMINICO, Marie-Olga SORNEIN, Mickael MENDES, Erwan DU FOU DE KERDANIEL, Thu Hang PHAM et Edouard VEILLY. Je voudrais également remercier la gentillesse de Claire TAMAIN et Johan VANDENBORRE ainsi que ma chère amie Irène.

Finalement, mon plus grand merci s’adresse à ma famille et spécialement à mes parents Tomás et Lilia qui m’ont toujours soutenue et qui m’ont permis d’arriver jusqu’ici, à mes frères et sœurs : Roberto, Miguel Angel, Elizabeth, Nohémi et Lilia. Un grand merci pour leur patience et leurs conseils. J’associe à ces remerciements mes amis du Mexique qui, de loin, m’ont manifesté leur fidèle amitié jour après jour : Elizabeth ROMERO, Irma GARCIA, Dolores TENORIO, Camelia ARZATE, Carmen et Olga GARCIA et Maricruz ROMERO.

A mes parents

Lilia et Tomás

SOMMAIRE

TABLE DES MATIERES

INTRODUCTION GENERALE…….…….... 19

Références…….…… 24

CHAPITRE I : ETUDE STRUCTURALE ET PROPRIETES DE SURFACE DU SOLIDE $SrTiO_3$……..…… 25

CARACTERISTIQUES STRUCTURALES DU SUBSTRAT $SrTiO_3$……. 27

Diffraction des rayons X par la poudre $SrTiO_3$……... 28

Spectroscopie Infrarouge (FTIR)…….….. 28

Microscopie électronique à Balayage (MEB)……...…….… 29

Conclusion…….... 31

Réactivité de surface vis-à vis de la molécule d'eau……..……..... 31

Références…….…… 36

ACID–BASE PROPERTIES OF STRONTIUM TITANATE SUBSTRATE *versus* TEMPERATURE……...……..……..... 37

Abstract……..…….. 37

1. Introduction……..... 38

2 Materials and methods……..... 39

2.1 Materials……..……..... 39

2.2 Methods……..…….. 39

3. Results and Discussion……...……...….. 40

3.1 Surface acidity constants……...……...……..…..... 40

3.2 Enthalpy and entropy changes……...……...……..……..... 43

IV Conclusion……..……...……... 44

References..... 49

RESUME DU CHAPITRE I……...…….…... 51

CHAPITRE II : SAUTS DE SORPTION ET ETUDE STRUCTURALE EN FONCTION DE LA TEMPERATURE……..…..... 53

INTERACTION BETWEEN U(VI) AND $SrTiO_3$ SURFACES *versus* TEMPERATURE..... 55
Abstract..... 55
I. Introduction..... 56
2. Materials and methods..... 57
2.1 Materials and Characterization..... 57
2.2 Sorption Procedure..... 57
2.3 Time-Resolved Laser-Induced fluorescence Spectroscopy (TRLIFS)..... 58
2.4 Modelling of the adsorption results..... 59
3. Results and Discussion..... 59
3.1 Uranyl sorption edges..... 60
3.2 Spectroscopic measurements..... 60
3.3 Modelling of the macroscopic retention data..... 61
IV. Conclusion..... 65
References..... 73
RESUME DU CHAPITRE II..... 77

CHAPITRE III : TRANSFERT D'ENERGIE ENTRE DES IONS Tb^{3+} ET Eu^{3+} SORBES SUR $SrTiO_3$ 79

ENERGY TRANSFERT FROM Tb^{3+} TO Eu^{3+} IONS SORBED ONTO $SrTiO_3$ SURFACE..... 81
Abstract..... 81
1. Introduction..... 82
2. Experimental details..... 83
2.1 Samples preparation..... 83
2.2 Techniques..... 84
2.2.1 Time-Resolved Laser-induced Fluorescence Spectroscopy (TRLIFS)..... 84
2.2.2 Ion Coupled Plasma Mass Spectrometry (ICPMS)..... 85
3. Results and Discussion..... 85
3.1 Sorption of Tb^{3+} and Eu^{3+} onto $SrTiO_3$ surfaces..... 85
3.2 Evidence of the energy transfer between Tb^{3+} and Eu^{3+} sorbed onto $SrTiO_3$ surfaces..... 85

87

4. Application of the energy transfer process: determination of the distance between Tb^{3+} and Eu^{3+} ions sorbed onto $SrTiO_3$……..

4.1 Presentation of the formalism used for the calculations…….……..... 87

IV Conclusion..... 90

References……. 97

RESUME DU CHAPITRE III……..…….. 99

CONCLUSION GENERALE..... 101

ANNEXE 107

RESUME GENERAL..... 111

ABSTRACT..... 113

TABLE DES ILLUSTRATIONS

LISTE DES FIGURES

CHAPITRE I

ETUDE STRUCTURALE ET PROPRIETES DE SURFACE DU SOLIDE $SrTiO_3$

Figure 1 : Représentation de la cellule unitaire du $SrTiO_3$……..……..……..... 27
Figure 2 : Diagramme de diffraction des rayons X par la poudre de $SrTiO_3$……..... 28
Figure 3 : Spectre infrarouge du $SrTiO_3$: a)solide non hydraté. b) solide hydraté dans $NaClO_4$ 0.1 M… 29
Figure 4 : Clichés de microscopie électronique à balayage……..…… 30
Figure 5 : Faces cristallographiques du $SrTiO_3$……..……..... 32
Figure 6 : Spectre XPS du pic O_{1S} de la poudre $SrTiO_3$ hydraté…….…...……...……. 34
Figure 7 : Spectre XPS du pic O_{1S} du monocristal face (100) de $SrTiO_3$ hydraté : a) incidence normale b) angle d'irradiation à 60°C entre la surface de l'échantillon et la normale à l'échantillon..... 35

ACID–BASE PROPERTIES OF STRONTIUM TITANATE SUBSTRATE *versus* TEMPERATURE

Figure 1 : Potentiometric titration curves of strontium titanate suspensions (100 $g.L^{-1}$) in KNO_3 0.1 M medium between 25°C and 90°C representing the net number of added base *versus* the pH..... 45
Figure 2 : Potentiometric titrations data of strontium titanate suspensions (100 g/L) at 25°C and 90°C in KNO_3 0.1 M medium. Experimental (dots) and CCM calculated curves (line)..... 46
Figure 3 : log K versus 1/T relation for the titanium and strontium surface sites protonation and deprotonation reactions at the $SrTiO_3$ surface……..... 47

CHAPITRE II

Figure 1 : Sorption edges of strontium titanate suspensions (20 $g.L^{-1}$) in $NaClO_4$ 0.1 M initial concentration of 10^{-4}M, between 25°C and 90°C representing the adsorbed uranyl % *versus* the pH..... 66
Figure 2 : Calculated U profile as a function of pH between 25 and 90°C. Solution composition: $U_{Total}=10^{-4}$ M. $NaClO_4$ 0.1 M. Values calculated using data Grenthe et al (1992). Activity correction made with the Davis equation…..……..…..……..……... 67

Figure 3 : Fluorescence spectra of the uranyl ions sorbed onto $SrTiO_3$, λ_{ex}=430 nm between 25 and 90°C for different retention rates……..……..……... 68

Figure 4 : Experimental data and calculated curves for uranyl sorption onto ≡Sr-OH/UO_2^{2+} and ≡Ti-OH /UO_2^{2+} (10 mL of uranyl solution 10^{-4}M 0.2 g. of $SrTiO_3$ powder) between 25 and 90°C……..... 69

Figure 5 : log K versus 1/T relation for the titanate $SrTiO_3$/ UO_2^{2+} reactions sorption …… 70

CHAPITRE III

Figure 1 : (a) Emission spectrum at 25°C of Tb^{3+} sorbed onto $SrTiO_3$ (10^{-4} M) under 487 nm excitation; (b) excitation spectrum of Eu^{3+} sorbed onto $SrTiO_3$ (10^{-4} M) by monitoring the transition $^5D_0 \rightarrow {}^7F_4$ of Eu^{3+} at 700 nm. The spectra correspond to 1000 accumulations……..……..... 92

Figure 2 : Energy level diagrams of Tb^{3+} and Eu^{3+} ions……..……..……..... 93

Figure 3 : Comparison of different excitation spectra: (a) that of Tb^{3+} (by monitoring the emission line $^5D_4 \rightarrow {}^7F_5$ of Tb^{3+} at 544 nm) for $SrTiO_3$ sorbed with Tb^{3+} 10^{-4} M; that of Eu^{3+} (by Monitoring the emission line $^5D_4 \rightarrow {}^7F_4$ of Eu^{3+} at 700 nm) for $SrTiO_3$ sorbed with Eu^{3+} 10^{-4} M; (c) that of Eu^{3+} (by monitoring the emission line $^5D_4 \rightarrow {}^7F_4$ of Eu^{3+} at 700 nm) for $SrTiO_3$ sorbed with the mixture Tb^{3+} 10^{-4} M / $Eu^{3+}10^{-4}$ ……..…… 94

Figure 4 : Luminescence spectra at 25°C (at an excitation wavelength of 487 nm) for only Tb^{3+} sorbed onto $SrTiO_3$, for only Eu^{3+} sorbed onto $SrTiO_3$ and for Tb^{3+}/Eu^{3+} sorbed onto $SrTiO_3$….…….……... 95

Figure 5 : Logarithmic plot of the fluorescence decay of Tb^{3+} ions at room temperature for different systems: for $SrTiO_3$ only sorbed with $Tb^{3+}$and for $SrTiO_3$ sorbed with Tb^{3+} 10^{-4} M/Eu^{3+} mixtures ([Eu^{3+}] from 10^{-6} M to 10^{-2} M) by monitoring the emission line $^5D_4 \rightarrow {}^7F_5$ of Tb^{3+} at 544 nm. The excitation wavelength is of 487 nm……..……..…… 95

ANNEXE

Figure 1 : Dispositif expérimental (autoclave) permettant de réaliser les expériences de titrage et de sorption en température…….. 110

LISTE DES TABLEAUX

CHAPITRE I

ACID–BASE PROPERTIES OF STRONTIUM TITANATE SUBSTRATE *versus* TEMPERATURE

Table 1. Calculated (intrinsic or chemical) surface reaction constants for the titanium and strontium surface sites, *versus* temperature……...……. 48
Table 2. Enthalpy and entropy changes values corresponding to the protonation and deprotonation reactions of the titanium and strontium surface sites……...……...…… 48

CHAPITRE II

Table 1. Calculated (intrinsic or chemical) surface reaction constants for the titanium and strontium surface sites, *versus* temperature……...……. 71
Table 2. Emission lifetimes recorded for U(VI) ions sorbed onto $SrTiO_3$ in $NaClO_4$ at 25, 50, 75 and 90 % sorption……...……... 71
Table 3. Calculated U equilibrium constants between 25 and 90 °C. Solution composition: $U_{Total}= 10^{-4}$ M, $NaClO_4$ 0.1 M. Values calculated using data Grenthe et al. (1992). Activity correction made with the Davis equation…..……...…...……...……... 72
Table 4. Sorption constant calculated values of uranium sorption onto $SrTiO_3$, versus temperature…… 72
Table 5. Enthalpy and entropy changes values corresponding to the uranium sorption reactions of the titanium and strontium surface sites…….…….……. 72

CHAPITRE III

Table 1. Lifetimes of Tb^{3+} ions (by monitoring the fluorescence at 544 nm) in $SrTiO_3$ only contacted with Tb^{3+} at different aqueous concentrations and at pH = 4 in $NaClO_4$ 0.1M……...…. 96
Table 2. Number of acceptor ions Eu^{3+} sorbed onto $SrTiO_3$ (in atoms per cm^3) obtained from ICPMS measurements…….……..... 96
Table 3. Values of R calculated in this work for the energy transfer from Tb^{3+} to Eu^{3+} sorbed onto $SrTiO_3$ and comparison to the other values obtained from the literature for interactions between lanthanide ions such as $Pr^{3+}\rightarrow Nd^{3+}$, $Er^{3+}\rightarrow Er^{3+}$ and $Nd^{3+}\rightarrow Yb^{3+}$ in co-doped solids as LaF_3 and $LiLaP_4O_{12}$……...……... 96

INTRODUCTION GENERALE

INTRODUCTION GENERALE

Dans la société actuelle, l'industrie nucléaire s'est développée, au cours de ces dernières années, dans différents domaines utilisant les radioisotopes : l'industrie, la médecine, la recherche et surtout la production d'énergie électrique à travers le processus de fission nucléaire. Cette dernière activité (notamment le retraitement du combustible irradié) est celle qui génère des déchets composés de radioisotopes à vie longue de haute activité. Bien que ces isotopes constituent une proportion relativement faible, leur toxicité subsiste sur des échelles de temps particulièrement longues, obligeant à trouver des moyens de construire des installations spécifiques et fiables pour leur confinement en couches géologiques [1-5].

Le principe d'un stockage géologique profond des déchets nucléaires [6] reposant sur le concept multi-barrières où les colis sont entourés de barrières technologiques et naturelles destinées à limiter le transfert de radionuclides vers la biosphère, est actuellement la solution adoptée. Ceci permet d'éviter le danger que représente l'infiltration des eaux souterraines sur le site de confinement. En effet, la présence d'eau peut être la principale cause de dégradation des colis de déchets, induisant leur migration dans l'environnement [7,8].

La migration des radionucléides est un processus dynamique mettant principalement en jeu la solubilité de l'ion métallique et sa sorption sur des surfaces minérales. La sorption de ces radionucléides est donc un processus indispensable à étudier afin d'évaluer le plus précisément possible la migration de ces radioisotopes. A ce sujet, plusieurs études ont été réalisées sur différents solides comme les argiles [9,10], le granite, la diorite [11], les phosphates [12], les hydroxyapatites [13]. Dans ces différentes études, ont été pris en compte divers facteurs mis en jeu pendant le processus de fixation, comme le pH, la force ionique et les conditions rédox du milieu ainsi que le comportement des surfaces minérales vis-à-vis de l'eau. De plus, l'utilisation de méthodes d'analyse comme notamment la spectroscopie Laser Résolue en Temps (SLRT), l'absorption X (EXAFS) et la spectroscopie de photoélectrons (XPS) dans des milieux hétérogènes, a permis de mieux comprendre à une échelle moléculaire la réactivité des actinides et des produits de fission (complexation, solubilité, adsorption) vis-à-vis de nombreux minéraux. Des codes de calculs fondés sur la loi d'action de masse, ont été utilisés pour simuler les données de rétention, permettant ainsi de définir précisément les équilibres de sorption des ions métalliques sur différents matériaux [14-17]. Les résultats obtenus au cours des caractérisations structurales (SLRT, EXAFS) ont été

utilisés comme contraintes lors de la simulation des données macroscopiques (saut de sorption, par exemple). Cependant, la plus grande partie de ces études a été réalisée entre 25 et 30°C, alors que, lors d'un stockage en milieu géologique profond, les déchets nucléaires se trouvent à des températures voisines de 100°C. Ainsi, la température est un paramètre important qui doit être pris en compte dans les processus de rétention [18,19].

Dans le cadre de cette thèse, nous nous sommes intéressés à l'effet de la température sur les mécanismes régissant la sorption de l'U(VI) en phase aqueuse sur la surface minérale de $SrTiO_3$ sous forme de poudre, en considérant comme variables le pH et la température (25, 50, 75 et 90 °C).

L'uranium hexavalent est un ion parfaitement adapté aux études par SLRT car il a un bon rendement de fluorescence, ce qui est un avantage non négligeable eu égard à la faible concentration d'ions métalliques sorbés à la surface du minéral. Le solide $SrTiO_3$ a été choisi non seulement pour sa simplicité cristallographique mais également pour sa très faible solubilité et sa stabilité thermique et chimique. La simplicité de sa structure cristallographique facilitera l'interprétation des mécanismes de sorption de l'uranyle sorbé [20].

La première partie de ce mémoire rassemblera toutes les données issues de la littérature sur $SrTiO_3$, soit sous forme de poudres, soit de monocristaux correspondant aux faces (100), (110) et (111). La poudre de $SrTiO_3$ a été caractérisée en utilisant plusieurs techniques structurales (DRX, FTIR), morphologique (MEB), surfacique (BET) montrant le bon degré de pureté du matériau. Pour suivre l'état d'hydratation de la surface, la spectroscopie XPS a été utilisée. Par ailleurs, nous nous sommes intéressés aux propriétés de surface de $SrTiO_3$, lorsque celui-ci est en contact avec une solution aqueuse, afin de mieux comprendre les mécanismes d'hydratation. En utilisant des titrages potentiométriques de surface, les concentrations en sites actifs ont été déterminées. Le calcul des constantes de protonation et de déprotonation a été réalisé en utilisant la modélisation des courbes de titrage potentiométriques (25-90°C) au moyen du code FITEQL en appliquant un modèle à 1 pK. Les valeurs des constantes d'équilibre obtenues nous ont permis de déterminer les valeurs des variations d'entropie et d'enthalpie d'hydratation en utilisant la relation de van't Hoff.

Dans la deuxième partie de ce travail, les sauts de sorption de l'ion uranyle sur $SrTiO_3$ sont présentés à 25, 50, 75 et 90 °C. Ensuite, une étude spectroscopique (SLRT) a été menée, pour l'identification des espèces formées à la surface de $SrTiO_3$ sur des échantillons *in-situ* et séchés entre 25 et 90 C°. En tenant compte des données spectroscopiques obtenues à différentes températures, ainsi que des valeurs des pK des sites de surface issues de la

modélisation des courbes de titrages potentiométriques, les constantes de sorption ont été déterminées lors de la modélisation des sauts de sorption de 25 à 90°C. Les valeurs des variations d'entropie et d'enthalpie de sorption de l'ion uranyle ont été obtenues en utilisant, là encore, la relation de van't Hoff.

La dernière partie de ce mémoire, sera consacrée à l'étude du transfert d'énergie entre deux ions lanthanides ($Tb^{3+} \rightarrow Eu^{3+}$) sorbés à la surface de $SrTiO_3$ sous forme pulvérulente afin d'essayer d'évaluer la distance entre deux ions métalliques sorbés à la surface de $SrTiO_3$. Après la mise en évidence d'un transfert d'énergie non radiatif entre ces deux lanthanides, nous avons obtenu le rayon de leur sphère d'interaction, en appliquant les modèles de Inokuti-Hirayama et Dexter. Cette étude a été entreprise afin de mieux comprendre les mécanismes de fixation des ions sur la surface de $SrTiO_3$ et a permis de vérifier que les mesures des temps de vie associés aux spectres d'émission des ions sorbés rendent bien compte de la présence de deux sites de surface.

REFERENCES

[1] W. Brewitz, U. Noseck *C. R. Physique* 3 (2002) 879.

[2] M.Tallec, J. M Capdevila *C. R. Physique* 3 (2002) 851.

[3] T. Hedman, A. Nystrom, C. Thegerstrom, *C.R. Physique* 3 (2002) 901-913.

[4] P. Trocellier Ann. *Chim. Sci. Mat*., 2000, ***25***, p. 321-337.

[5] R. Drot, E. Simoni, M. Alnot, J. J. Ehrhardt *Colloid Interface Sci* 205 (1998) 410-416.

[6] International Atomic Energy Agency Technical Reports Series (2003) 413.

[7] A. Browski *Adv. Colloid Interface Sci.* 93 (2001) 135.

[8] G. Sposito *Chemical Equilibria and Kinetics in Soils*, Oxford University Press, Oxford (1994).

[9] S. Motellier, J. Ly, L. Gorgeon, Y. Charles, D. Hainos, P. Meier *J. Applied Geochemistry* 18 (2003) 1517–1530.

[10] J. Weil, P. Ishegem, L. Wang *Soc. Sym. Proc. Series* 506 (1998) 881.

[11] J.A. Berry H.E. Bischop, M.M. Cooper, P.R. Fozard, J. W. McMillan *Radiochim. Acta* 66/67 (1994) 243.

[12] R. Drot , E. Simoni, C. Denauwer *C. R. Acad. Sci. Paris 2* (1999) 11 l-1 17.

[13] T. Ohnuki, N. Kozai, H. Isobe, T. Murakami, S. Yamamoto, Y. Aoki, H. Naramoto *J. Nucl. Sci. Technol.* 34 (1997) 58.

[14] P. Toulhoat *C. R. Physique* 3 (2002) 975.

[15] P. Toulhoat, B. Grambow, E. Simoni *L'actualité chimique* 285/286 (2005) 41.

[16] T. E. Payne, P.L . Airey *Physics and Chemistry of the Earth* 31 (2006) 572-586.

[17] S. McGrellis, J. N. Serafini, J. J. Jean, J. L. Pastol., M. Fedoroff *Sep. and Purif. Technol.* 24 **(**2001) 129-138.

[18] N. Finck, R. Drot, F. Mercier-Bion, E. Simoni, H. Catalette *Colloid Interface Sci.* 312 (2007) 230–236.

[19] E. Tertre, G. Berger, E. Simoni, S. Castet, E. Giffaut, M. Loubet and H. Catalette *Geochim. Cosmochim. Acta*, 70 (2006) 4563-4578.

[20] Z. Wang, S. Karato, K. Fujino *Phys. Earth Planet. Interiors* 79 (1993) 299.

CHAPITRE I :

ETUDE STRUCTURALE ET PROPRIETES DE SURFACE DU SOLIDE $SrTiO_3$.

CARACTERISTIQUES STRUCTURALES DU SUBSTRAT $SrTiO_3$

Le solide $SrTiO_3$ a fait l'objet de nombreuses études utilisant ses caractéristiques thermiques, mécaniques, magnétiques, optiques et chimiques. Par exemple, il est étudié entre autres pour ses propriétés de photoélectrolyse ou de matrice d'incorporation de certains actinides, par substitution de l'ion Sr^{2+}.

$SrTiO_3$ fait partie de la famille des pérovskites de type ABO_3 (Pm3m), dont les principaux minéraux représentatifs sont la Tausonite, la Fabulite, la Marvelite et la Zeathite [1]. Ses caractéristiques cristallographiques correspondent à la fiche JCPDS 35-0734, où la maille élémentaire peut être décrite par un cube (volume = 59.3 $Å^3$), dont les huit sommets sont occupés par les ions Sr^{2+} (r = 1.440 Å), entourés de 12 atomes d'oxygène. Les 6 ions oxygène O^{2-} (r = 1.360 Å) occupent les milieux des arêtes et les ions Ti^{4+} (r = 0.605 Å) se situent au centre du cube en coordinence 6 (Figure 1). Idéalement, les ions sont en contact les uns avec les autres et les longueurs des liaisons sont : Ti-O=1.9505 Å, Sr–O =2.7584 Å, O-O=3.905 Å [2].

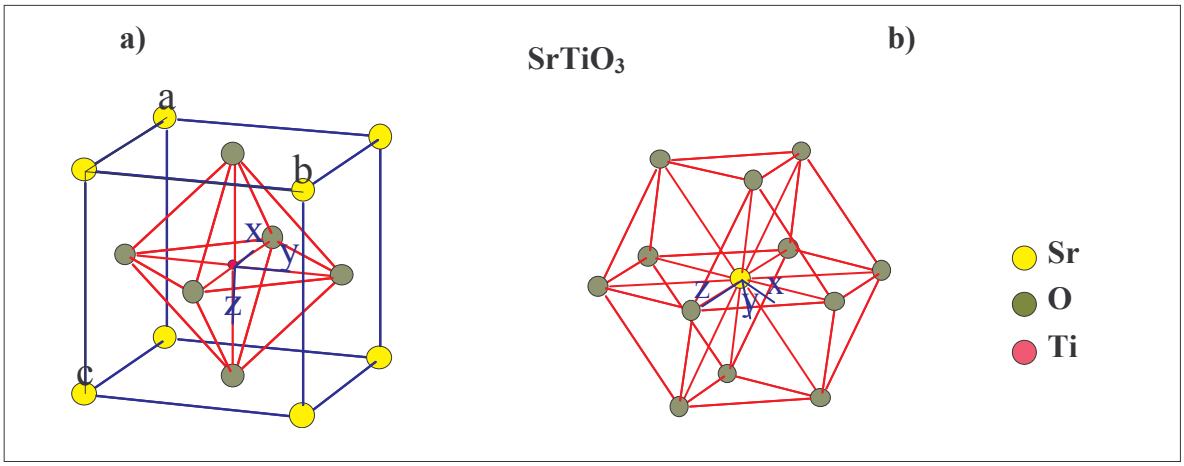


Fig 1. : Représentation de la cellule unitaire du $SrTiO_3$.

Les paramètres de maille sont a = b = c = 3.905Å [3], les angles $\alpha = \beta = \gamma = 90°$ et la densité théorique est de 5,12 g/cm^3. Les orientations préférentielles sont : la face (100) composée par des couches successives de « SrO » et « TiO_2 » ; la face (110) formée par des couches de « $(SrTiO)^{2+}$ » et « O^{2-} » [4,5] et la face (111) constituée de couches de « $(SrO_3)^{-4}$ » et « Ti^{4+} » [6]. La face (100) est la face majoritaire. Elle représente un plan de clivage imparfait avec fracture conchoïdale [7].

Diffraction des rayons X par la poudre $SrTiO_3$

Le solide étudié est distribué par la société Aldrich® sous la référence EC235-044. Le diagramme de diffraction des rayons X par la poudre correspondant à ce substrat est présenté sur la figure 2. Ce diagramme a été obtenu au moyen d'un appareil Bruker D8 Advance utilisant la raie K_α du cuivre et un filtre Ni. Tous les pics observés ont pu être indexés en accord avec la fiche JCPDS 35-0734. Le résultat indique que le matériau présente une bonne cristallinité (pics fins) avec absence de phases secondaires en quantités notables.

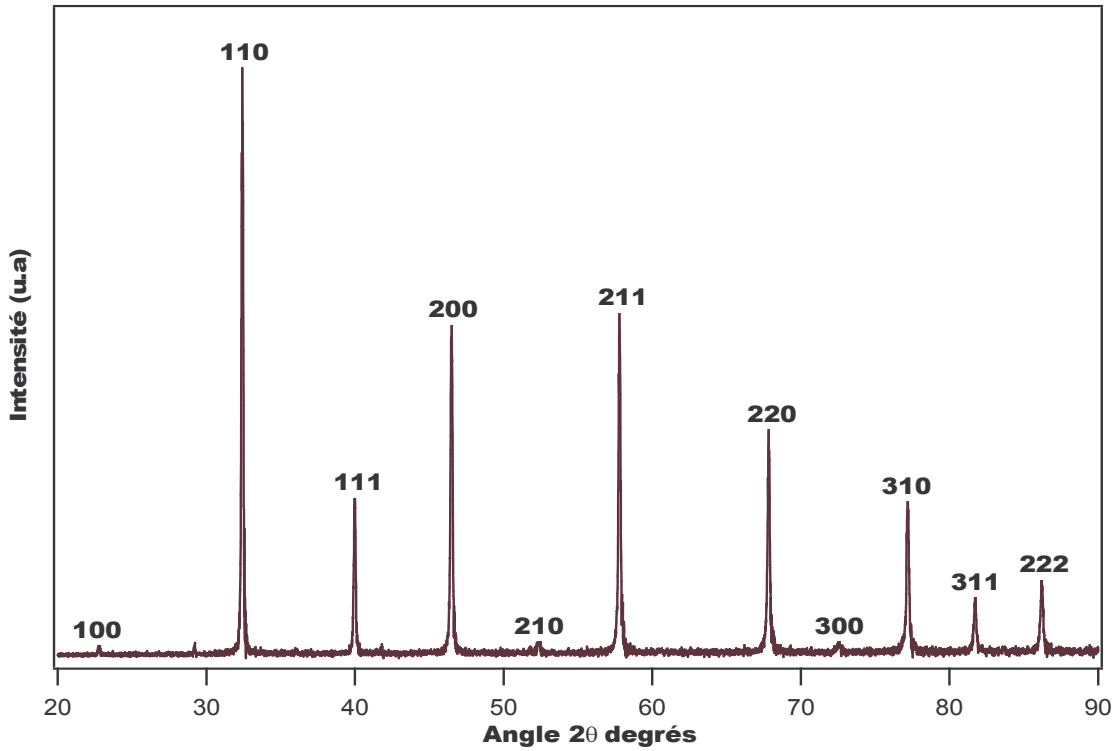


Fig. 2 : Diagramme de diffraction des rayons X par la poudre de $SrTiO_3$.

Spectroscopie infrarouge (FTIR)

Afin de compléter la caractérisation du substrat, des analyses par spectroscopie infrarouge ont été réalisées. Pour ces analyses, deux échantillons de $SrTiO_3$ ont été préparés : Fig. 3a) le solide non hydraté et Fig. 3b) le solide hydraté dans une solution dont le pH a été maintenu à 3. Chaque échantillon a été pastillé dans du bromure de potassium avec une proportion de 1 à 2% en masse. Les spectres obtenus dans la gamme 4000 à 500 cm^{-1}, ont été acquis avec un spectrophotomètre PERKIN–ELMER modèle 1600 FTIR HITACHI-I2001. Les spectres obtenus (Figure 3) sont comparables à ceux répertoriés dans la littérature pour $SrTiO_3$ [8-9]. Ce résultat montre clairement l'absence de phases secondaires en concordance avec les résultats obtenus par DRX.

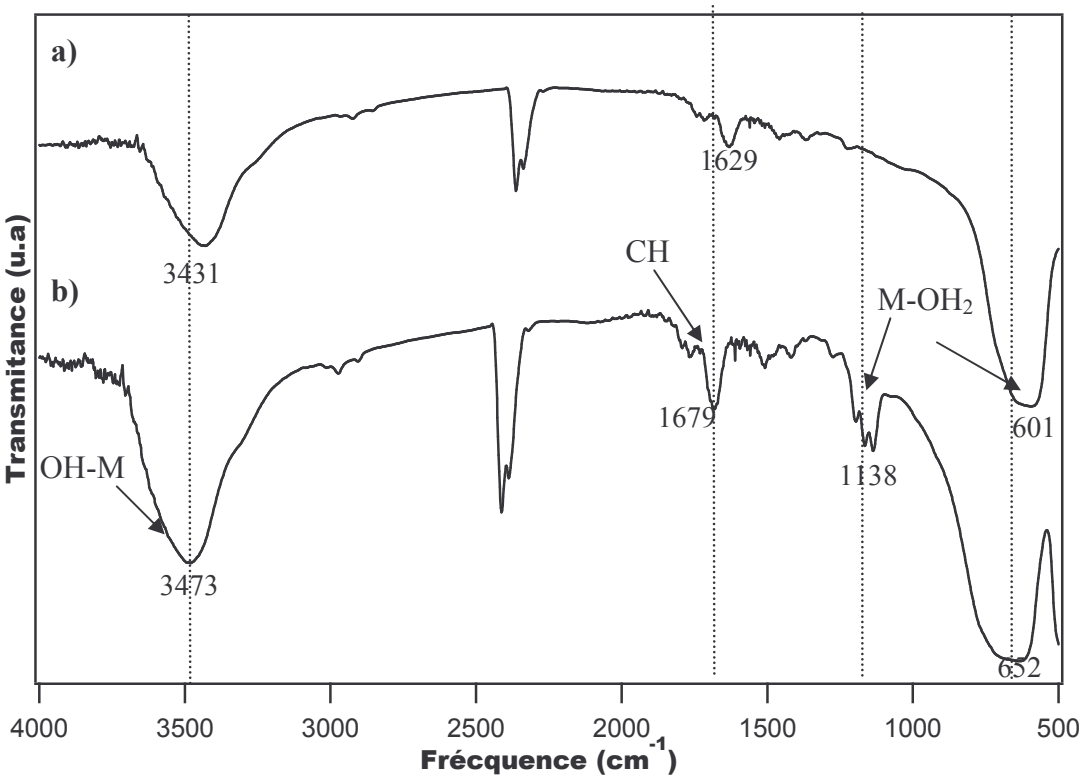


Fig. 3 : Spectres infrarouge du $SrTiO_3$: a) Solide non hydraté b) Solide hydraté dans $NaClO_4$ 0.1M.

L'échantillon hydraté (Figure 3b) présente une augmentation de trois raies principales : la raie à 1138 cm^{-1} et 652 peuvent être attribuée à des groupements doublement protonés (Ti-OH_2), la raie à 3473 cm^{-1} correspond à des groupements hydroxyle (OH^-) liés à des métaux de surface. La présence de la raie à 1679 cm^{-1} est attribuée à des espèces de surface carbonatées, présentes en tant qu'impuretés à la surface du solide. L'origine de cette contamination est probablement la pollution en hydrocarbures de l'atmosphère.

Microscopie électronique à Balayage (MEB)

Les expériences de microscopie électronique à balayage ont été effectuées sur un microscope électronique à balayage Philips XL30, avec une tension d'accélération des électrons de 25 kV, au Laboratoire de Synthèse et caractérisation des Matériaux de l'Institut National d'Investigations Nucléaires du Mexique (ININ, Toluca). L'analyse élémentaire ponctuelle de $SrTiO_3$ a été obtenue en utilisant un spectromètre à dispersion en énergie (EDS) de rayons X, EDAX modèle DX-4.

Pour l'analyse, la poudre de $SrTiO_3$ a été recouverte d'une couche d'or de 20 nm d'épaisseur pour rendre la surface électroniquement conductrice. Les images obtenues en mode électrons secondaires (figure 4) montrent une répartition relativement homogène avec des grains sphériques et lisses. La variation de taille des particules est de 0,4 à 1,2 µm environ.

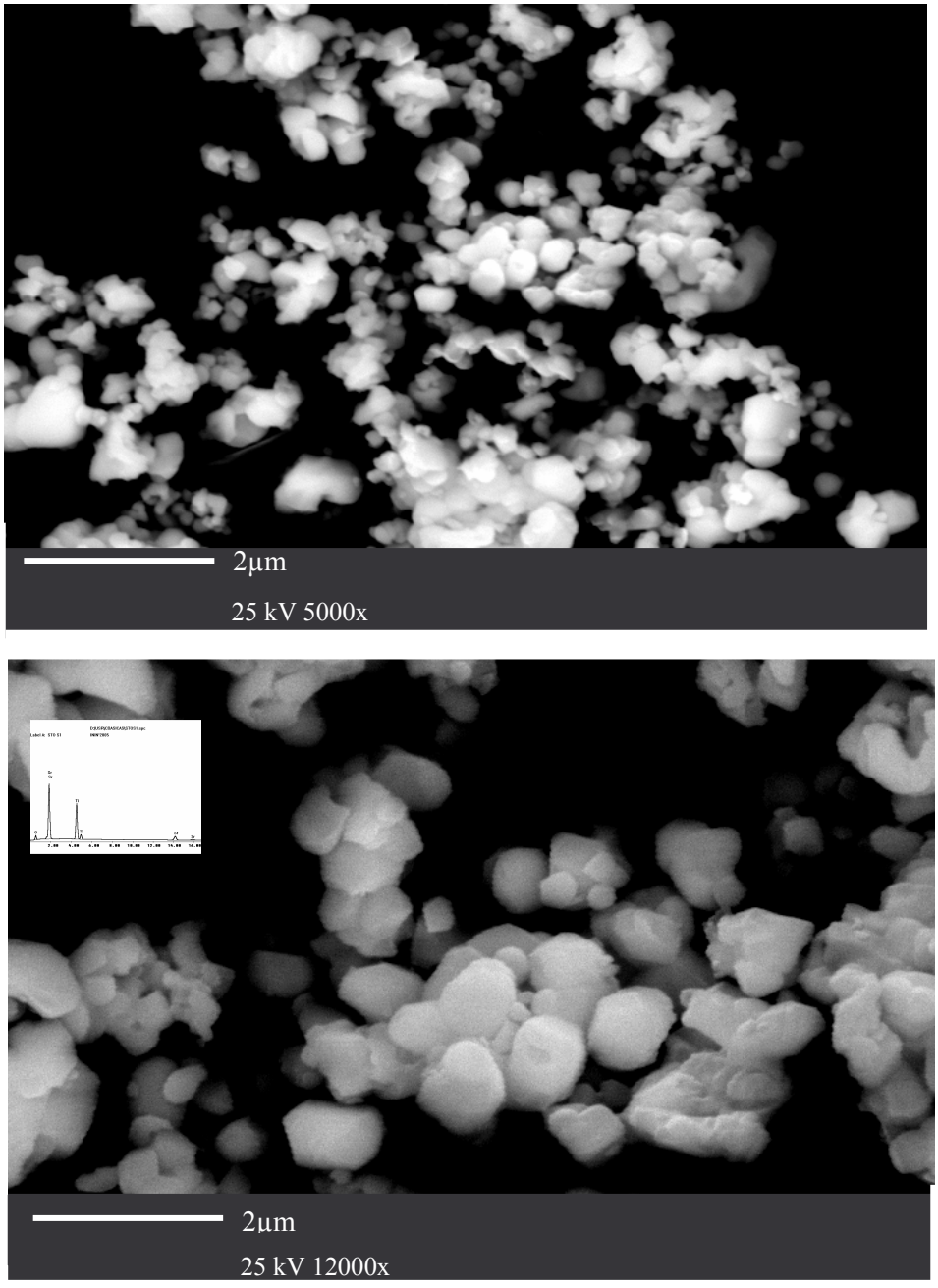


Fig. 4 : Clichés de microscopie électronique à balayage (MEB).

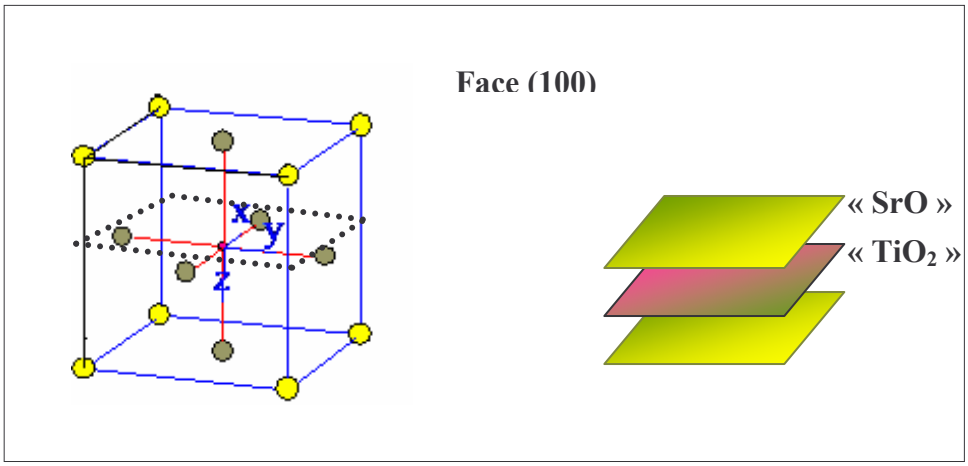
Les résultats des analyses semi quantitatives ponctuelles réalisées sur 10 points différents à la surface de l'échantillon, indiquent que les teneurs massiques élémentaires sont les suivantes : Oxygène : 18.26 %, Titane : 27.81 % et Strontium : 53.93%, mettant en évidence l'absence de phase secondaire, en accord avec les résultats précédents.

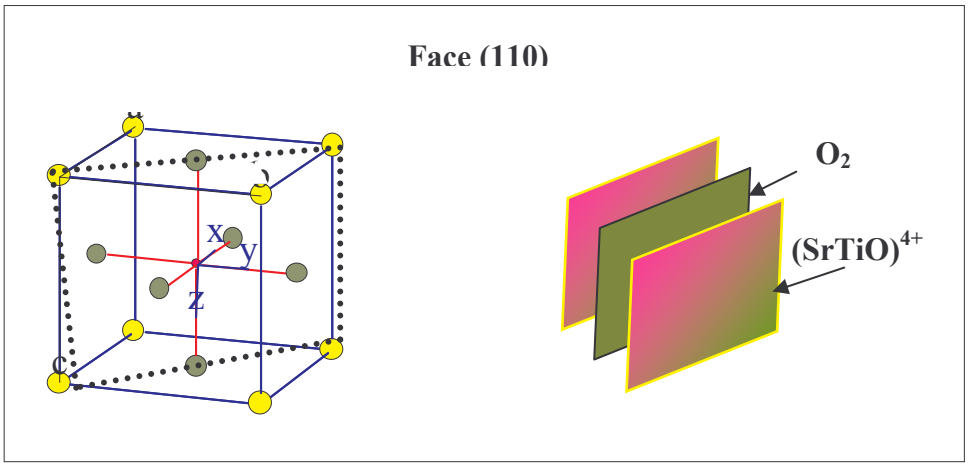
Conclusion

L'ensemble des résultats obtenus au cours de cette étude, nous a permis de montrer que le substrat ne présente pas de phases secondaires en quantité notable. Ce résultat est important, car la présence de phases secondaires dans le matériau aurait pu rendre plus délicate l'interprétation des résultats lors de l'étude de la sorption de l'ion uranyle sur $SrTiO_3$.

Réactivité de surface vis-à-vis de la molécule d'eau.

Le composé $SrTiO_3$ étant utilisé dans des processus de photodécomposition de l'eau en hydrogène et oxygène, il existe de nombreuses études visant à comprendre l'interaction des molécules d'eau avec la surface de $SrTiO_3$, particulièrement à l'état monocristallin (faces (100), (110) et (111) Fig.5) [10-13]. Elles n'ont cependant pas encore permis d'aboutir à un consensus sur les mécanismes prépondérants. En effet, comme pour tous les oxydes, il existe deux types d'interaction de la molécule d'eau avec la surface de $SrTiO_3$: i) la molécule H_2O se dissocie en deux entités pour aboutir à la création d'un groupement hydroxyle OH^-, situé sur un atome de titane ou sur un atome de strontium (appelé OH terminal), alors que l'atome d'hydrogène se fixe sur un atome d'oxygène de surface, coordiné à des atomes de Sr ou de Ti ; ii) la molécule H_2O interagit sans dissociation avec les ions métalliques en surface du solide. Ces mécanismes dépendent principalement de l'état de surface du substrat. Il est en effet bien connu que la présence de défauts en surface d'un substrat favorise de façon significative les mécanismes dissociatifs [14-18].





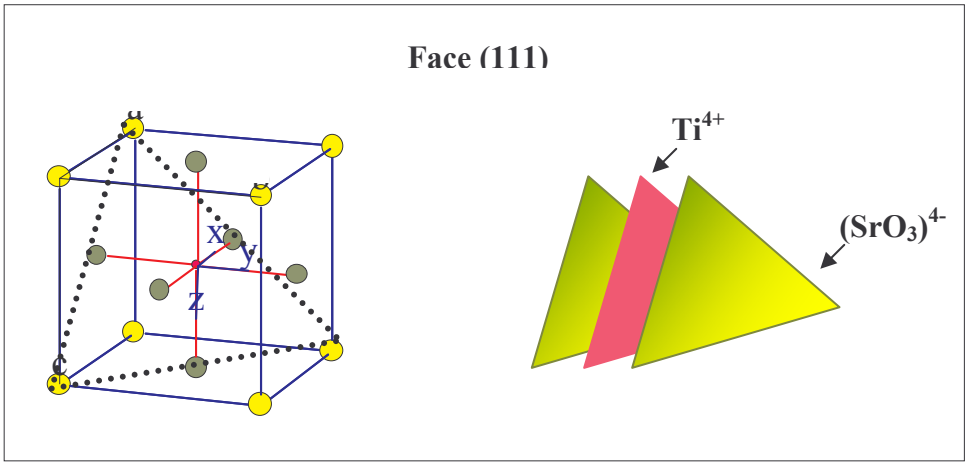


Fig. 5 : Faces cristallographiques du $SrTiO_3$ [19].

Par microscopie à effet tunnel, il a été par exemple montré que les molécules d'eau se dissocient sur les lacunes en oxygène [20]. Cependant, des études XPS ont mis en évidence que ces types de défauts seraient guéris par la présence d'eau [21,22]. L'apparition de groupements hydroxyle comblerait ainsi tous ces défauts de surface [23]. Parallèlement, des calculs de chimie quantique ont montré que la dissociation de l'eau se produit principalement à faible taux de recouvrement, tandis qu'à fort taux de recouvrement, l'eau reste moléculaire sur la surface [24]. Toutefois, bien que certains résultats de la littérature soient contradictoires, nous pouvons considérer dans ce travail que, le solide étudié étant en suspension dans l'eau, la majorité des défauts surfaciques sont guéris par la dissociation des molécules d'eau et que par conséquent, la surface de $SrTiO_3$ peut être considérée comme uniformément hydroxylée (le taux de protonation dépendant du pH de la suspension). Le solide devra donc, préalablement à toute autre expérience, subir une étape d'hydratation. Afin de soutenir cette hypothèse, le solide hydraté a été analysé par spectroscopie de photoélectrons X.

Ces expériences XPS ont été effectuées au laboratoire de Chimie Physique et Microbiologie pour l'Environnement de Nancy (LCPME), sur un spectromètre KRATOS type AXIS Ultra DLD avec un analyseur hémisphérique à 180° en utilisant la raie monochromatée $K\alpha_1$ de l'aluminium, d'énergie 1486,6 eV, sous un atmosphère ultravide de 10^{-9} Torr. En raison du caractère non conducteur des échantillons, il a été nécessaire de corriger les différents spectres obtenus de l'effet de charge, en utilisant le pic du carbone C1s de contamination, situé à 284,6 eV. La recomposition des pics photoélectriques a été effectuée à l'aide du logiciel XPSPeak [25], en considérant un bruit de fond de type Shirley et un pourcentage Lorentzienne-Gaussienne de 40%.

Le solide $SrTiO_3$ a été hydraté suivant la méthodologie suivante : 200 mg de poudre ont été mis en contact avec 10 mL de $NaClO_4$ de concentration 0,1 M pendant 24 heures, sous agitation permanente. Après filtration, le solide a été lavé avec de l'eau distillée pour éliminer l'excès de sodium et ensuite a été placé dans un dessiccateur.

Sur la figure 6, est présenté le spectre XPS correspondant au composé $SrTiO_3$. La decomposition du spectre indique clairement la présence de quatre pics : le premier, situé à 529,0 eV, a été attribué aux oxygènes du matériau massif. La raie à 530,4 eV est attribuée aux oxygènes des groupements de surface « ≡Ti-OH » et celle située à 531,6 eV correspond aux atomes d'oxygène des groupements surfaciques « ≡Sr-OH ». Finalement à 532,6 eV, se trouve la composante correspondant à l'eau physisorbée.

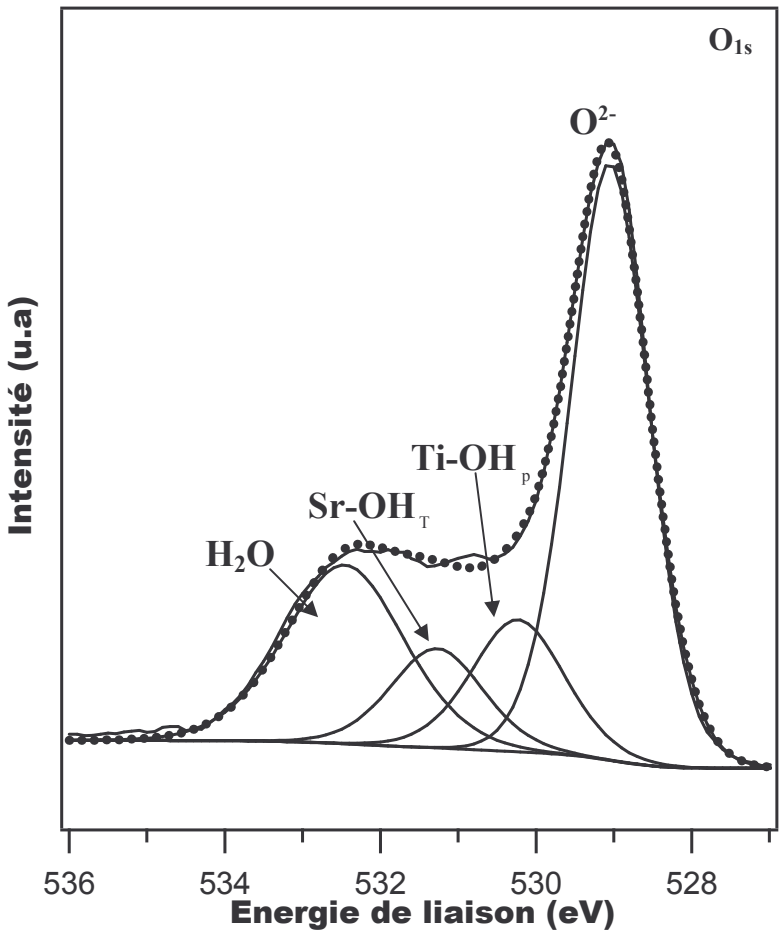


Fig. 6 : Spectre XPS du pic O_{1S} de la poudre $SrTiO_3$ hydraté.

Afin de confirmer l'existence de ces groupements hydroxyle à la surface du matériau, des expériences XPS complémentaires ont été réalisées sur des monocristaux de $SrTiO_3$, (fourni par CERAC), préalablement hydratés suivant la méthodologie appliquée à la poudre de $SrTiO_3$. Ces monocristaux ont été analysés par XPS d'une part avec le faisceau X perpendiculaire à la face du cristal et d'autre part avec un angle de 60° entre le faisceau X et la normale à la surface. Les spectres enregistrés sur la face (100) (Figure 7) ont été décomposés de la même façon que la poudre. Cependant, il faut noter une inversion dans les intensités des pics à 530,1 et 531,5 eV. Les différentes faces constitutives de la poudre polycristalline ne présentant pas toutes les mêmes proportions en groupements ≡Sr-OH et ≡Ti-OH, il n'est de ce fait pas étonnant que les intensités correspondant à la face (100) soient différentes de celles de la poudre.

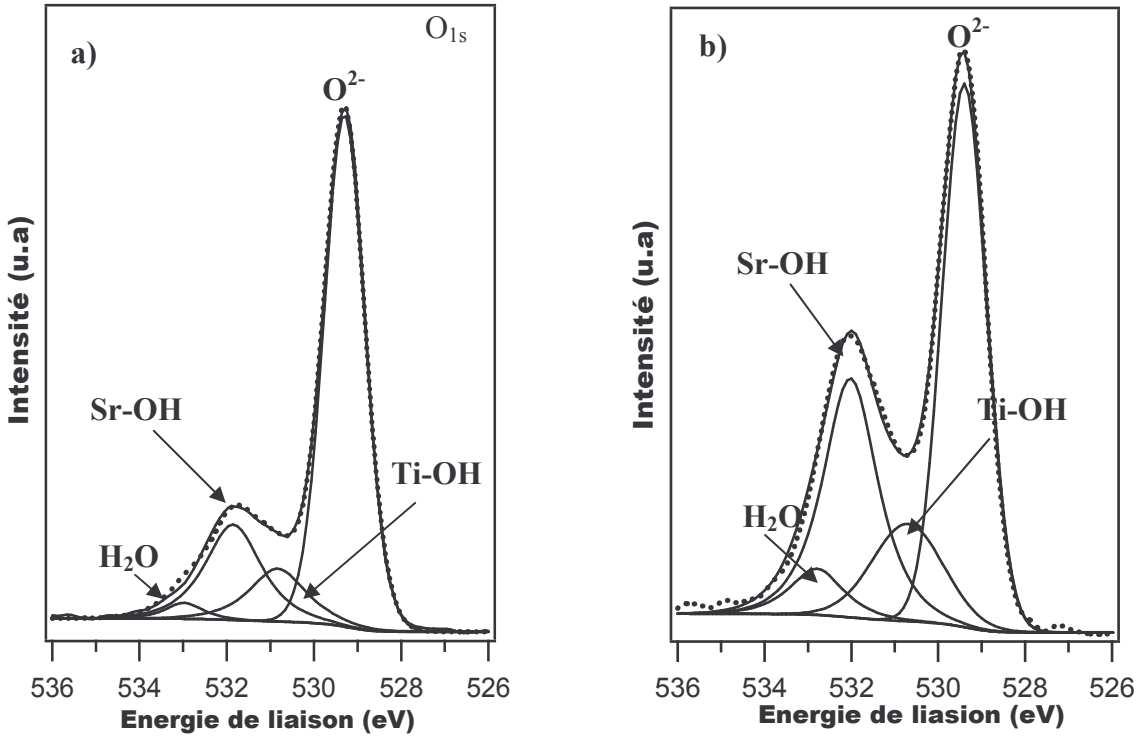


Fig. 7 : Spectre XPS du pic O_{1S} du monocristal face (100) de $SrTiO_3$ hydraté : a) incidence normale b) angle d'irradiation à 60 ° entre la surface de l'échantillon et la normale à l'échantillon.

Le point important ici est l'augmentation, avec l'angle d'incidence, des intensités des pics correspondant aux groupements ≡Sr-OH et ≡Ti-OH par rapport au pic O^{2-} de l'oxyde. Ceci met clairement en évidence que les pics à 530,1 et 531,5 eV sont bien la signature d'entités présentes à la surface du solide.

Nous pourrons donc considérer, au cours de cette étude, que l'hydratation du solide $SrTiO_3$ conduit à l'hydroxylation de la surface et ainsi à la formation de charges de surface dépendant principalement de la valeur du pH de la suspension.

References

[1] J. Brunen, G. Zegenha *Surf. Sci.* 389 (1997) 349.

[2] H. Swanson, Fuyat *Natl. Bur. Stand.* 539/3 (1954) 44.

[3] R. H. Buttner, E.N. Maslen *Acta Crystallogr.* 48 (1992) 639.

[4] E. Heifets, E.A. Kotomin. J. Maier *Surf. Sci.* 462 (2000) 19.

[5] F. Bottin, F. Finnochi, C. Noguera *Surf. Sci.* 532/535 (2003) 468.

[6] J. Padilla, D. Vanderbil *Surf. Sci.* 418 (1998) 64.

[7] T. Sano, C.S. Kim, G.S. Rohrer. *J. Am. Ceram. Soc.* 88 /4 (2005) 993.

[8] B.J. Ameida, A. Pietka, P. Caldelas, J.A. Mendes, J.L. Ribeiro *Thin solid Films* 513 (2006) 275.

[9] R.A. Nyquist and R.O. Kagel, *Infrared Spectra of Inorganic Compounds*, Academic Press, New York (1971).

[10] S. Ferrer, G.A. Somorjai *Surf. Sci.* 94 (1980) 41.

[11] A.G. Thomas, C.A. Muryn, P.J. Hardman., H.A. Durr., I.W. Owen, G. Hornton, F.M. Quinn, R.A. Rosenberg, P.J. Love, V. Rehn. *Surf. Sci.* 307/309 (1994) 355.

[12] I.W. Owen, N.B. Brookes. C.H. Richardson, D.R. Warburton *Surf. Sci.* 178 (1986) 897.

[13] R.A. Evarestov, A.V. Bandura, V.E. Alexandrov *Surf. Sci.* 601 (2007) 1844.

[14] T. Kubo, H. Nozoye *Surf. Sci.* 542 (2003) 177-191.

[15] H.S. Kato, S. Shiraki, M. Nantoh, M. Kawai *Surf. Sci.* 544(2003) L722.

[16] B.J. Almeida, A. Pietka, J.A. Mendes *Appl. Surf. Sci.* 238 (2004) 395.

[17] Z. Fang, K. Terakura *Surf. Sci.* 470 (2000) L75.

[18] S. Sekiguchi, M. Fujimoto, M. Nomura, S.B. Cho, J. Tanaka, T. Nishihara, M.G. Kang, H.H. Park *Solid State Ionics* 108 (1998) 73.

[19] B. Rahmati, J. Fleig. W. Sigle, E. Bischoff, J. Maier, M. Rühle *Science* 595 (2005) 115.

[20] J.M. Pan, B. L. Maschhoff, U. Diebold, T.E. Madey *J. Vac. Sci. Technol.* A10 (1992) 2470.

[21] W. Göpel, J.A. Anderson, D. Frankel, M. Jaehnig, K. Phillips, J.A. Schäfer, G. Rocker *Surf. Sci.* 139 (1984) 333.

[22] T.K. Sham, M.S. Lazarus *Chem. Phys. Lett.* 68 (1997) 426.

[23] J. Vandenborre, Thèse de l'université Paris-Sud-11, Orsay, France, 2005.

[24] H. Perron, J. Vandenborre, C. Domain, R. Drot, J. Roques, E. Simoni, J.J. Ehrhardt, H. Catalette *Surf. Sci.* 601 (2007) 518.

[25] R.W.M. Kwork., XPSpeak95 version 3, The Chinese University of Honk-Kong, 1997.

ACID-BASE PROPERTIES OF STRONTIUM TITANATE SUBSTRATE *versus* TEMPERATURE

G. García-Rosales, R. Drot, F. Mercier-Bion, E. Simoni

Abstract

The behavior of the two kinds of the surface site on the strontium titanate (≡Ti-O and ≡Sr-O) has been investigated *versus* temperature (25, 50, 75 and 90°C). The N_2-BET specific area is measured at 2.4 ± 0.2 $m^2.g^{-1}$. The surface site density has been determined from potentiometric titrations (6 sites/nm^2 for each site ≡Ti-O and ≡Sr-O). The potentiometric titration data have been simulated, for each temperature, using the constant capacitance model and taking into account both protonation of the ≡Sr-OH surface sites and deprotonation of the ≡Ti-OH ones (one pK model). The intrinsic strontium protonation constant increases with an increasing temperature, while the titanate deprotonation one decreases. Moreover, both enthalpy and entropy changes corresponding to the surface acid-base reactions have been evaluated using the vant'Hoff relation.

1. Introduction

In the frame of the depolluting processes [1] and the migration of heavy metal ions in the geosphere [2, 3], the interfacial phenomena are of great importance. Indeed, it is now well-known that the mineral surfaces play an important role in controlling the trace element chemistry of natural waters [4]. A precise description of the surface reactions is therefore needed in the field of geochemistry, material science and corrosion reactions [5]. The characterizations of the interactions between metal ions and a solid in an aqueous suspension have been investigated especially at the oxide/solution interface and at the clay surfaces [6, 7]. These interactions depend mainly on several different geological parameters such as, for instance, redox potential, ionic strength and pH of the suspension, related to the variation of the electrical charges developed by the surface. In order to determine quantitatively the retention constants, two thermodynamic models have mainly been developed, the ion-exchange and the surface complexation models [8, 9]. Nevertheless, although the temperature is an important factor, which could have an effect on both retention and migration of heavy metals, such as, for example, radionuclides in a nuclear disposal [10], most of the acid-base surface properties have been investigated so far mainly under ambient temperature [11-15] and only few have been devoted to the temperature effects on the surface reactivity [16-18].

The aim of this study is to evaluate the effect of the temperature on the surface properties on a simple substrate. The surface site density, the surface acidity constants values and the associated enthalpy and entropy changes, versus temperature (25, 50, 75 and 90°C), are presented in this paper.

The solid $SrTiO_3$ was first characterized using physico-chemical methods (IR, XRD). Then, the temperature variation of the surface site density has been investigated using potentiometric experiments. The potentiometric titration data were then simulated with a constant capacitance surface complexation model, which allows one to determine the surface acidity constants at all studied temperatures. Finally, the associated enthalpy and entropy changes were evaluated from the surface protonation and deprotonation constant values *vs* temperature, using the van't Hoff relation.

2. Materials and methods

2.1. Materials

The studied strontium titanate is a ground powder provided by Aldrich® (EC235-044).

X-ray powder diffraction pattern were recorded on a Bruker® D8 Advance diffractometer using the Cu K_α rays (λ = 1.5418Å). The obtained diffraction pattern was in perfect agreement with the JCPDS file 35-0734 [19], corresponding to the cubic strontium titanate and does not show any secondary phase.

Infrared spectrum was recorded on a Hitachi® I-2001 spectrophotometer, the sample being prepared by diluting 1 wt % of $SrTiO_3$ in KBr. The bands series obtained for the spectrum (not shown here) are characteristics of the $SrTiO_3$ [20], which corroborates the diffraction pattern.

The specific surface area was determined from N_2 adsorption isotherm, using the BET (5-points) method [21] with a Coulter® SA 3100 apparatus. Prior to the measurement, the sample was degassed at 120°C for 2 hours. The obtained specific surface area was 2.4 ± 0.2 $m^2.g^{-1}$.

2.2. Methods

The solubility of $SrTiO_3$ powder was tested in aqueous solution at 25°C by mean of ICP-MS measurements. The samples were prepared under an inert atmosphere in polypropylene tubes. 200 mg of $SrTiO_3$ powder were contacted for 24 hours with 10 mL of a $NaClO_4$ 0.1 M solution adjusted at different pH (1-10) to perform the hydration step of the surface. After centrifugation (3500 rpm, 30 min), 5 mL were removed from the supernatant for ICP-MS analyses to obtain Sr and Ti concentrations.

Sr and Ti concentrations at the different pH were determined by using the spectrometer PlasmaQuad Excell EX 129 (Thermo Electron®) from the laboratory SUBATECH (Ecole de Mines, Nantes, France). Before their analysis, all the solutions were diluted in HNO_3 medium (2% volume) to obtain a concentration close to 10 ppb. The results showed a negligible dissolution of $SrTiO_3$ at all the pH measured.

The potentiometric titration experiments were performed with 100 $g.L^{-1}$ aqueous suspensions of solid in potassium nitrate medium (0.1 M to keep the ionic strength constant), since it is usually admitted that K^+ and NO_3^- ions do not sorb specifically [9]. Both deionized water and argon controlled atmosphere were used in order to avoid the presence of carbonates. Moreover, to minimize the evaporation during the heating, these experiments

were carried out in an autoclave apparatus (Annexe). This device is divided in three parts: i) in the upper part, a closed Teflon reaction vessel to perform the experiments, ii) a central part to filtrate the suspensions and iii) in the lower part, a Teflon vessel to collect the filtrate. The two upper parts are maintained at the temperature under investigation (using a PID (Proportional, Integral, Differential) temperature regulation unit) to prevent any reaction modification during the filtration process. The *in situ* pH values were measured with a combined Fisher Bioblock® glass electrode, with solid electrolyte and double Teflon junction. The calibration was done with three different certified Hanna® buffer solutions. The precision of the measured temperature was estimated to be ± 1°C and the precision on the measured pH values was estimated to be ± 0.1 unit. The sample was continuously shaken to prevent settling.

For the hydration step, the suspensions were shaken for 24 hours at room temperature, followed by 1 hour at the temperature under study. A kinetic study showed that this time is sufficient to reach the hydration equilibrium. After hydration, the suspension was adjusted at on initial pH value close to 2, using a 0.5 M HNO_3 solution, the solution was shaken for 10 min until the pH value was constant and was titrated by adding incremental volumes of a KOH solution (0.1 M). The precision on the concentration of the added OH^- was estimated to be 2 %. Moreover, potentiometric titrations were carried out with the background salt solution alone using identical experimental conditions.

3. Results and Discussion

First, the effects of the temperature (25°C - 90°C) on the surface site density values were investigated. These values were used, by simulating the potentiometric data, to calculate the surface protonation and deprotonation constants *versus* temperature. Secondly, the variation of these constants with the temperature allowed one to determine the corresponding change in enthalpy and entropy.

3.1. Surface acidity constants

As the crystallographic repartition of the different faces of this polycrystalline sample is not known, it is quite difficult to directly use the surface acidity constants calculated, for each planes, by the MUSIC approach [22, 23]. Nevertheless, in order to try to reduce the number of adjustable parameters, the pK values corresponding to the different surface oxygen atoms were calculated, using the Pauling valence bond concept, for both (100) and (110) crystallographic orientations, which are known to be the main ones for the studied substrate.

According to crystallographic considerations, both "≡Sr-OH" and "≡Ti-OH" surface sites are expected to be reactive towards proton sorption/desorption processes [20, 24-26]. The Pauling calculations (not given here) have shown that whatever the crystallographic orientation considered, the pK values are quite similar for a known surface site. Moreover, it was found that the "≡Sr-OH" site is negatively charged and thus is only capable of protonation while the "≡Ti-OH" site, positively charged, is only capable of deprotonation.

Then according to these results, it was chosen to perform the modelling of the potentiometric titration curves by considering two surface reactive sites, each presenting only one pK value, and a charge of -0.5 was assigned to the "≡Sr-OH" site (≡Sr-$OH^{-0.5}$) while a charge of +0.5 was assigned to the "≡Ti-OH" surface site (≡Ti-$OH^{+0.5}$). Thus, the pH dependence of the surface charge can be modelled by two acid-base equilibria with the associated constants K_{Sr} and K_{Ti} referring to the protonation and deprotonation of the ≡Sr-$OH^{-0.5}$, ≡Ti-$OH^{+0.5}$ surface sites respectively:

$$SrOH^{-0.5} + H^{+} \Leftrightarrow SrOH_2^{+0.5} \qquad (K_{Sr}) \qquad [1]$$

$$TiOH^{+0.5} \Leftrightarrow TiO^{-0.5} + H^{+} \qquad (K_{Ti}) \qquad [2]$$

Obviously, the actual surface charge will be a function of the pH value and the constants K_{Sr} and K_{Ti} can be determined by treatment of the experimental potentiometric measurements data and their expressions are:

$$K_{Ti} = \frac{[SrOH_2^{+0.5}]}{[SrOH^{-0.5}][H^{+}]} \times \exp(F\psi / RT) \qquad [3]$$

$$K_{Sr} = \frac{[TiO^{-0.5}][H^{+}]}{[TiOH^{+0.5}]} \times \exp(-F\psi / RT) \qquad [4]$$

Where F is the Faraday constant, Ψ the surface electrostatic potential, R the ideal gas constant and T the temperature expressed in Kelvin.

As a modelling with a minimum number of parameters is required, among all the surface complexation models, the CCM (Constant Capacitance Model), only used in the case of high (and constant) ionic strengths (above 0.1 M), was used. Indeed, this model needs only the surface site density, the inner-layer capacitance value and the surface acidity constants as

adjustable parameters. These surface acidity constants, defined as written in Equations [1] and [2], were calculated by simulating the potentiometric titration data using the simulation code FITEQL 4.0 [27], which is an iterative gradient-directed nonlinear least-squared optimization program based on the Gauss method.

The inner-layer capacitance value ($C = \frac{\varepsilon\varepsilon_0}{d}$; d is the thickness of the electric double layer), needed in the simulation, should vary with the temperature, because it depends on the permittivity ε of the medium, which is temperature dependent. Moreover, although, most of the time, published values for the capacitance range from 1.0 to 1.5 $F.m^{-2}$ for the oxide solids at room temperature [28, 29], the capacitance value, associated to the best fit, was 3.1 $F.m^{-2}$ at the room temperature and was adjusted for higher temperatures. This result is not surprising because the permittivity of the medium being temperature dependent, the capacitance value is expected to vary with the temperature. The site density, calculated from the potentiometric titration experiments of $SrTiO_3$ suspensions was found to be constant whatever the temperature and being equal to 12 sites/nm^2. Crystallographic considerations lead to an equal site density for the terminal oxygen atoms linked to strontium and titanium (Ti-OH and Sr-OH) atoms for the (100 and 110) planes. A total surface sites density around 14 sites/nm^2 was determinated. Considering these results, one could expect an equivalence for the formation of the surface groups on the two faces. Then, experimentally the obtained surface site density of 6 sites/nm^2 was considered for both $\equiv Sr\text{-}OH^{-0.5}$ and $\equiv Ti\text{-}OH^{+0.5}$ surface site in agreement with the crystallographic values, these values being kept constant for all the temperature.

The figure 1 presents the potentiometric titration curves obtained at the four temperatures investigated which allow one to directly visualize the effect of the temperature. The figure 2 presents the comparison between the experimental and simulated curves for 25 and 90 °C. One can notice that the modelling of the potentiometric titration curve obtained at 90°C is not perfect, especially for the lowest pH values (below pH = 5). This is in fact due to the fitting criterion chosen for the modelling step. Indeed, in order to have a more constrained system, it was postulated that the van't Hoff relation (constant enthalpy and entropy changes) is verified in our experimental conditions which appears as a reasonable assumption since we have investigated a limited temperature range (ΔT = 65°C). Then, two criteria were considered to get the best fits: the WSOS/DF factor value (weighed sum of squares over degrees of freedom) which as to be ranged from 0.1 to 20 [27] and the fact that the obtained constants have to respect the van't Hoff relation which means that the R^2 factor for the linear regression of the log(K) = f(1/T) has to be higher than 0.9. Considering these constraints, the

best fits led to the values summarized in Table 1. According to the number of adjustable parameters and considering the results obtained from a sensibility analysis of the goodness of the fit by changing the surface affinity constants values (the fitting procedure), it can be assumed that the average error bars associated to the surface affinity constants is about 0.5 logarithmic unit. While for $\equiv$Sr-OH$^{-0.5}$ site, the protonation constant increases (more than one order of magnitude) with the temperature, the $\equiv$Ti-OH$^{+0.5}$ site deprotonation constant decreases (two orders of magnitude). It is interesting to notice that these results are different from those obtained with γ-alumina [18]. Indeed, in this work, both protonation and deprotonation constants decrease with the temperature. But nevertheless, one important point is that i) the model used for this substrate was not the CCM but the DLM one, ii) only one amphoteric site has been considered.

3.2. Enthalpy and entropy changes

First, as it was discussed above, it was assumed that enthalpy and entropy changes were not temperature-dependent. This assumption seems reasonable and has already been used in previous works with different substrates such as rutile [30] and corundum [31]. The variation of log K with 1/T is presented in the Figure 3 and the $\Delta_r H^0$ and $\Delta_r S^0$ values obtained are summarized in the table 2.

As the $\equiv$Sr-OH$^{-0.5}$ site protonation constant increases with the temperature, the corresponding reaction is endothermic, whereas the titanium site ($\equiv$Ti-OH$^{+0.5}$) deprotonation reaction is exothermic. In the literature, both endothermic and exothermic protonation reactions are reported. For instance, from microcalorimetry measurements, values such as 80 kJ.mol^{-1} and –58 kJ.mol^{-1} have been given for alumina [18] and goethite [14], respectively. A value of 53 kJ.mol^{-1} is proposed for kaolinite [32]. Concerning the deprotonation, endothermic reactions have been reported several times in the literature. For instance, the values given for kaolinite and goethite are 32 and 35 kJ.mol^{-1} respectively [14, 32]. An endothermic behavior of the surface of titanium oxide and alumina has been reported as well [33, 34]. The study on the effect of temperature on the acid-base behaviour of a γ-alumina, using microcalorimetry, gives a value of 5 kJ.mol^{-1} [18], in agreement with the results reported by Halter [31] for corundum (α-Al_2O_3). But, once again, this comparison should be used carefully because the models involved in these results are often different.

The entropy changes are quite high ($|\Delta_R S°| > 300$ J.K^{-1}.mol^{-1}). Nevertheless, while for the protonation of the $\equiv$Sr-OH$^{-0.5}$ site the obtained value is positive, indicating an increase in the disorder of the system, the entropy changes associated to the deprotonation of the $\equiv$Ti-

$OH^{+0.5}$ site is negative, indicating a decrease in the disorder of the system. If the surface acid-base reactions were elementary, the expected values for the entropy change were positive for the deprotonation reaction and negative for the protonation one. Since the result is different with the obtained values, one may conclude that the reactions are not elementary and that the mechanism is probably more complex than the global reactions [1] and [2] presented above. Then, it is difficult to give a definitive interpretation involving a variation of the disorder of the system corresponding to these acid-basic reactions and extensive studies considering the modification of the interfacial double layer has probably to be taken into account more precisely.

4. Conclusion

Considering the crystallographic structure of the $SrTiO_3$ substrate, the surface acidity properties of two different kinds of sites ($\equiv$Sr-$OH^{-0.5}$ and $\equiv$Ti-$OH^{+0.5}$) have been investigated *versus* temperature (25°C - 90°C). The corresponding acid-base reactions constants have been determined by modelling the potentiometric titration data using the constant capacitance model, at all temperatures.

According to crystallographic consideration and potentiometric results, the surface site density was kept constant at 6 sites.nm^{-2} whatever the temperature for both $\equiv$Sr-$OH^{-0.5}$ and $\equiv$Ti-$OH^{+0.5}$ sites. The inner-layer capacitance value varied from 3.1 to 5.5 F.m^{-2}. Whereas the protonation of the $\equiv$Sr-$OH^{-0.5}$ presents an endothermic character, it was found that the deprotonation of the $\equiv$Ti-$OH^{+0.5}$ site is exothermic. Moreover, using the van't Hoff relation, the enthalpy and entropy changes associated to these surface acid-base reactions have been determined. These results will then be used in a further study on the retention mechanisms between uranyl ion and the same substrate $SrTiO_3$, *versus* temperature.

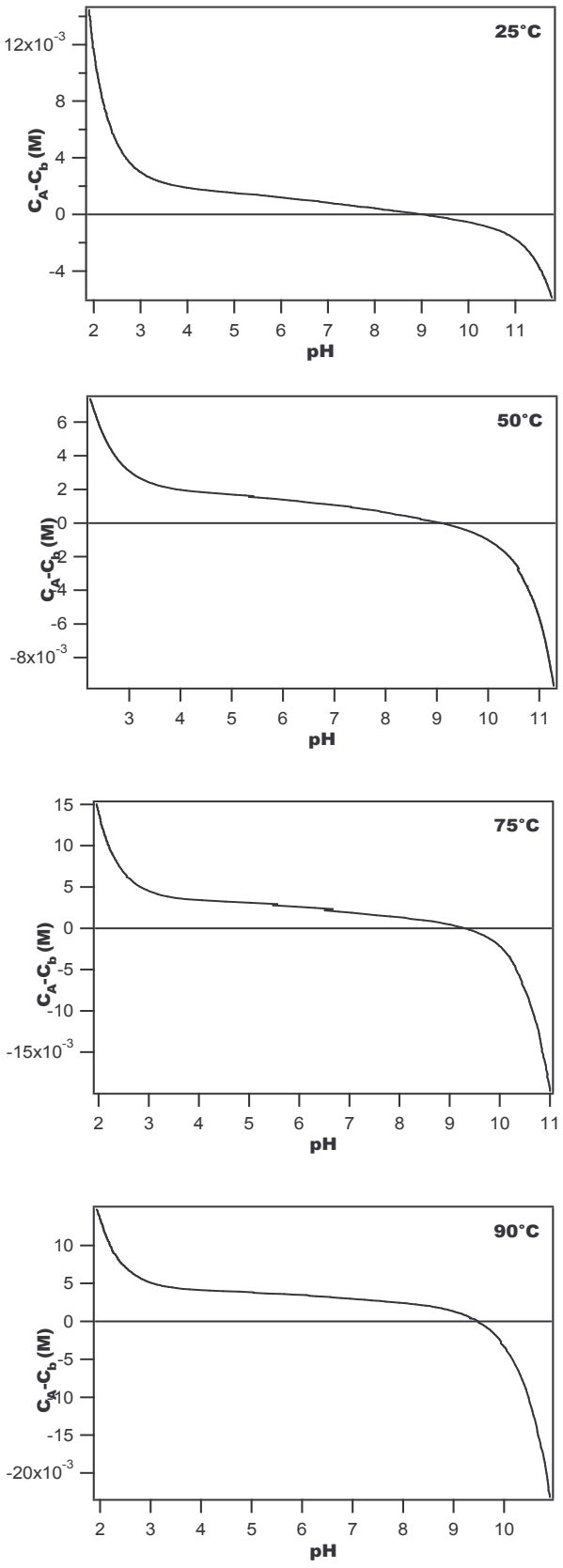


Fig. 1: Potentiometric titration curves of strontium titanate suspensions (100 g.L^{-1}) in KNO_3 0.1 M medium between 25°C and 90°C representing the net number of added base versus the pH.

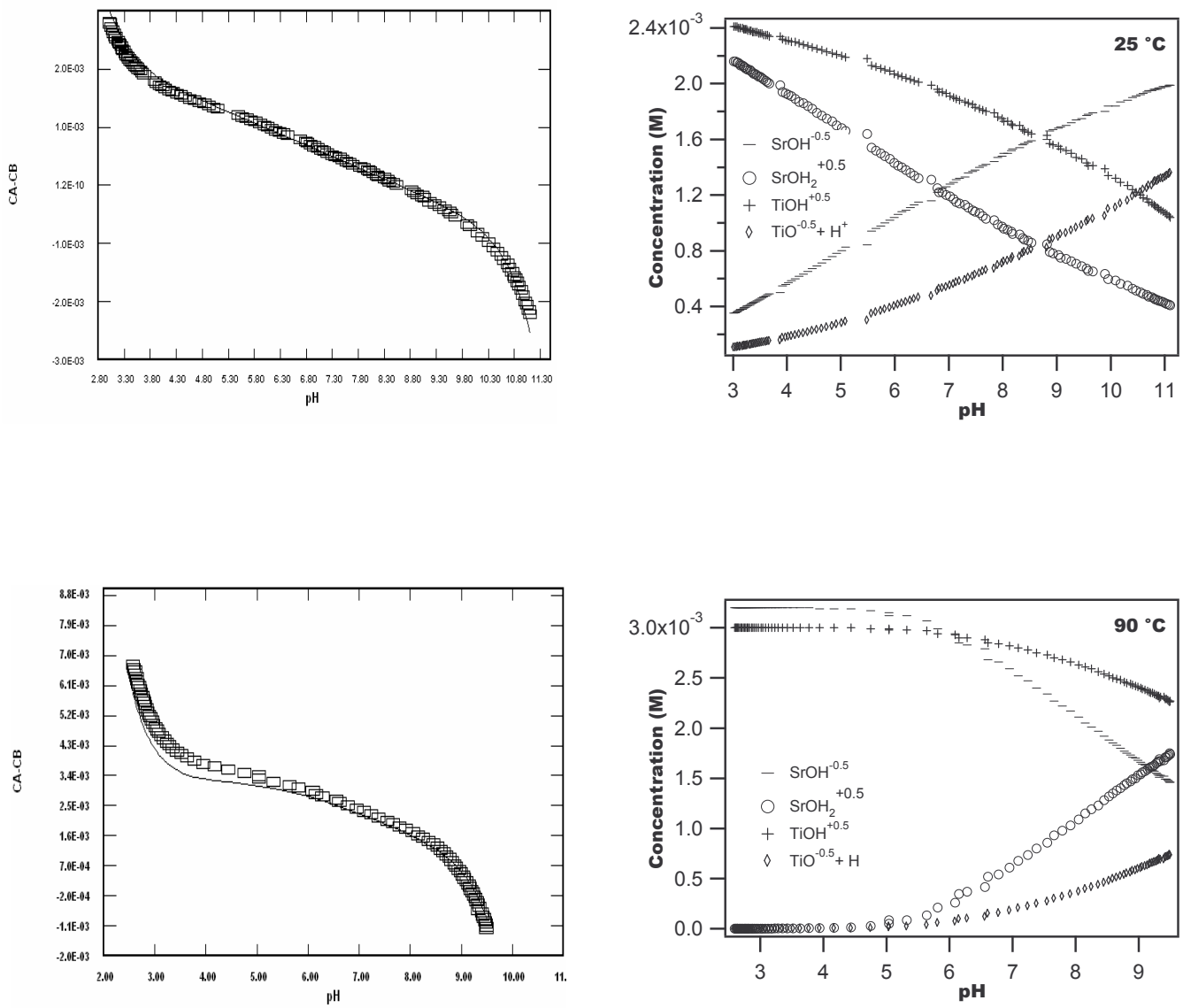


Fig. 2: Potentiometric titrations data of strontium titanate suspensions (100 g.L^{-1}) at 25°C and 90°C in KNO_3 0.1 M medium. Experimental (dots) and CCM calculated curves (line).

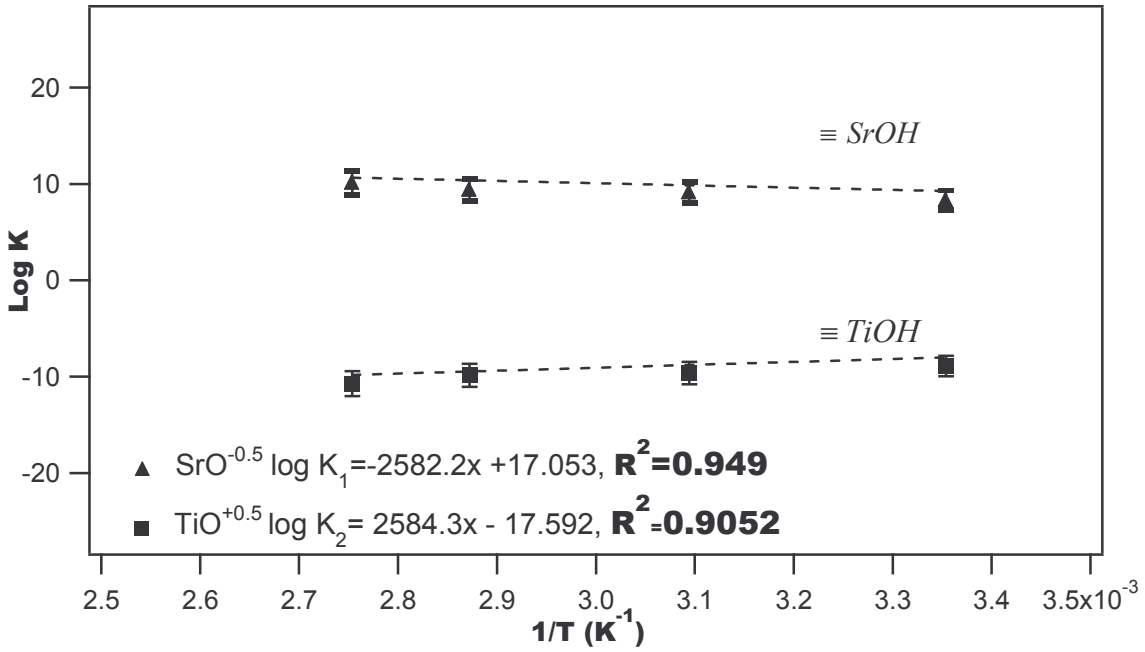


Fig. 3: log K versus 1/T relation for the titanium and strontium surface sites protonation and deprotonation reactions at the $SrTiO_3$ surface.

Table 1: Calculated (intrinsic or chemical) surface reaction constants for the titanium and strontium surface sites, versus temperature.

Temp. (°C)	**C (Fm^{-2})**	**WSOS/DF**	**log $K_{Sr\text{-}O}$ ± 0.5**	**log $K_{\equiv Ti\text{-}O}$ ± 0.5**
25	3.1	1.13	8.3	-8.8
50	3.6	0.90	9.1	-9.6
75	4.8	4.45	9.4	-9.8
90	5.5	3.30	10.1	-10.7

Table 2: Enthalpy and entropy changes values corresponding to the protonation and deprotonation reactions of the titanium and strontium surface sites.

Surface reaction	**$\Delta_r H°$ ($kJ.mol^{-1}$)**	**$\Delta_r S°$ ($J.K^{-1}.mol^{-1}$)**
$SrOH^{-0.5} + H^{+} \Leftrightarrow SrOH_2^{+0.5}$	49 ± 8	325 ± 24
$TiOH^{+0.5} \Leftrightarrow TiO^{-0.5} + H^{+}$	-49 ± 11	-336 ± 34

References

[1] A. Browski *Adv. Colloid Interface Sci.* 93 (2001) 135.

[2] T. Arnold, T. Zorn, G. Bernhardt, H. Nitsche *Chem. Geol.* 151 (1998) 129.

[3] S.J. Morrison, V.S. Tripathi, R.R. Spangler *J. Contam. Hydrol.* 17 (1995) 347.

[4] G. Sposito, *Chemical Equilibria and Kinetics in Soils*, Oxford University Press, Oxford (1994).

[5] W. Stumm, *Chemistry of Solid-Water Interface*, *Processes at the Mineral-Water and Particle-Water Interface in Natural Systems*, J. Wiley & Sons Eds, New York, 1992.

[6] M.H. Bradury, B. Baeyens *J. Contamin. Hydrol.* 27 (1997) 223.

[7] A. Kowal-Fouchard, R. Drot, E. Simoni, N. Marmier, F. Fromage, J.J. Ehrhardt *New J. Chem.* 28 (2004) 864.

[8] N.Z. Misak *Colloids surf. A Physicochem. Eng. Asp.* 97 (1995) 129.

[9] D.A. Dzombak, F.M.M. Morel, *Surface Complexation Modeling: Hydrous Ferric Oxide*, J. Wiley & Sons Eds, New York, 1990.

[10] A. Bauer, T. Rabung, F. Claret, T. Schäfer, G. Buckau, T. Fanghänel *Appl. Clay Sci.* 30 (2005) 1.

[11] E. Ordoñez-Regil, R. Drot, E. Simoni *J. Colloid Interface Sci.* 263 (2003) 391.

[12] N. Marmier, A. Delisee, F. Fromage *J. Colloid Interface Sci.* 211 (1999) 54.

[13] R. Drot, C. Lindecker, B. Fourest, E. Simoni *New J. Chem.* 22 (1998) 1105.

[14] M. J. Angove, J. D. Wells, B. B. Johnson *J. Colloid Interface Sci.* 211 (1999) 281.

[15] A. Kowal-Fouchard, R. Drot, E. Simoni, J.J. Ehrhardt *Environ. Sci. Technol.* 38 (2004) 1399.

[16] E. Tertre, G. Berger, S. Castet, M. Loubet, E. Giffaut *Geochim. Cosmochim. Acta* 69 (2005) 4937.

[17] E. Tertre, G. Berger, E. Simoni, S. Castet, E. Giffaut, M. Loubet, H. Catalette *Geochim. Cosmochim. Acta* 70 (2006) 4563.

[18] J.P. Morel, N. Marmier, C. Hurel, N. Morel-Desrosiers *J. Colloid Interface Sci.* 298 (2006) 773.

[19] R. Buttner, E. Maslen *Acta Crystallogr.* B48 (1992) 639.

[20] B. Almeida, A. Pietka, J. Mendes *Appl Surf. Sci.* 238 (2004) 395.

[21] S. Brunauer, P.H. Emmet, E. Teller *J. Am. Chem. Soc.* 60 (1938) 309.

[22] T. Hiemstra, W.H.V. Riemsdijk, G.H. Bolt *J. Colloid Interface Sci.* 133 (1989) 91.

[23] T. Hiemstra, P. Venema, W. H. V. Riemsdijk *J. Colloid Interface Sci.* 184 (1996) 680.

[24] R. Evarestov, A. Bandura, V. Alexandrov *Surf. Sci.* 601 (2007) 1844.

[25] T. Kubo, H. Nozoye *Surf. Sci.* 542 (2003) 177.

[26] S. Ferrer, G. Somorjai *Surf. Sci.* 94 (1980) 41.

[27] A.L. Herbelin, J.C. Westall, Report 96.01. Department of Chemistry, Oregon State University, Corvallis, OR. USA (1996).

[28] K.F. Hayes, G.Redden, W. Ela, J.O. Leckie *J. Colloid Interface Sci.* 142 (1991) 448.

[29] C. Lomenech, E. Simoni, R. Drot, J.J. Ehrhardt, J. Mielczarski *J. Colloid Interface Sci.* 261 (2003) 221.

[30] M.L. Machesky, D.J. Wesolowski, D.A. Palmer, K. Ichiro-Hayashi *J. Colloid Interface Sci.* 200 (1998) 298.

[31] W.E. Halter *Geochim. Cosmochim. Acta* 65 (1999) 3077.

[32] M.J. Angove, B.B. Johnson, J.D. Wells *J. Colloid Interface Sci.* 204 (1998) 93.

[33] N. Kallay, T. Preocanin, S. Zalac, H. Lewandowski, H.D. Narres *J. Colloid Interface Sci.* 211 (1999) 401.

[34] N. Kallay, T. Madic, L. Kucej, T. Preocanin *Colloids Surf. A: Physicochem. Eng. Asp.* 230 (2004) 3.

RESUME DU CHAPITRE I

La première partie de cette thèse a été consacrée à l'étude des propriétés acido-basiques de la surface de $SrTiO_3$ en fonction de la température (25, 50, 75, 90°C), afin de prévoir l'influence de ce paramètre sur la rétention d'ions métalliques. Préalablement à cette étude, une caractérisation physico-chimique a été effectuée au moyen de plusieurs techniques structurales (DRX, FTIR) et morphologique (MEB) qui nous ont permis de vérifier le degré de pureté du substrat. La surface spécifique de $SrTiO_3$, mesurée par la méthode BET, est de $2,4 \pm 0,2$ m^2/g. Des études de dissolution ont montré une faible solubilité du solide sur toute la gamme de pH considérée. Suite à cette caractérisation, l'état d'hydratation de la surface de $SrTiO_3$ a été étudié par spectroscopie XPS. La comparaison des résultats ainsi obtenus avec ceux enregistrés sur deux solides de référence (TiO_2 et SrO_2) ont permis de mettre en évidence l'hydroxylation de la surface de $SrTiO_3$ hydraté et la présence de deux types de groupements hydroxyle de surface ≡Ti-OH and ≡Sr-OH.

Les titrages potentiométriques réalisés sur des suspensions de $SrTiO_3$ à différentes températures (25, 50, 75 et 90°C) ont conduit à la détermination de la densité de sites actifs, qui reste constante et égale à 6 sites/nm^2 quelle que soit la température. Ensuite, la simulation des titrages potentiométriques, entre 25 et 90°C, a été réalisée à l'aide du code FITEQL en utilisant le modèle de la capacitance constante (CCM). Les constantes de protonation et de déprotonation ont été obtenues en considérant un modèle à 1 pK (conformément au modèle MUSIC) et en prenant en compte les deux sites $\equiv Sr-OH$ et $\equiv Ti-OH$. Les constantes d'équilibre ainsi obtenues montrent une nette variation avec la température : la protonation du site $\equiv Sr-OH$ fait intervenir un processus endothermique tandis que la déprotonation du site $\equiv Ti-OH$ implique un processus exothermique.

A partir de ces constantes d'équilibre, les grandeurs thermodynamiques, enthalpie et entropie d'hydratation ont été calculées en utilisant la relation de van't Hoff. L'ensemble de ces paramètres sera ensuite indispensable pour minimiser le nombre de paramètres ajustables lors de la modélisation des sauts de sorption présentée dans le prochain chapitre de ce mémoire (CHAPITRE II).

CHAPITRE II : SAUTS DE SORPTION ET ETUDE STRUCTURALE EN FONCTION DE LA TEMPERATURE

INTERACTION BETWEEN U(VI) AND $SrTiO_3$ SURFACES *versus* TEMPERATURE

G. García-Rosales, R. Drot, F. Mercier-Bion, G.Lagarde and E. Simoni

Abstract

The purpose of this work is the study of the interaction mechanisms between U(VI) ions and $SrTiO_3$ surfaces as a function of pH and temperature (25, 50, 75 and 90°C), by coupling thermodynamic and spectroscopic approaches. The uranium(VI) ions are sorbed onto $SrTiO_3$ surfaces in the 0.5-5.0 pH range with an initial cation concentration equal to 10^{-4} M. The U(VI) surface complexes were identified by using Time-Resolved Laser-Induced Fluorescence Spectroscopy (TRLIFS). For all the studied samples, the fluorescence spectra and the corresponding lifetime values do not change with the pH and the temperature. Two U(VI) complexes sorbed onto $SrTiO_3$ were detected and the corresponding lifetimes are 60 ± 5 and 12 ± 2 μs at 25, 50, 75 and 90°C for all the samples.

The sorption edges were simulated by using the FITEQL 4•0 software. The sorption equilibrium constants of the U(VI)/$SrTiO_3$ system between 25 and 90°C were obtained with the constant capacitance model (CCM), considering two reactive surface sites and a one pK model. According to the spectroscopic characterization, two types of surface complexes, namely $\left[(\equiv SrOH)(\equiv TiOH)UO_2\right]^{2+}$ and $\left[(\equiv TiOH)(\equiv TiO)UO_2\right]^{2+}$, were considered. Finally, enthalpy ($\Delta_R H°$) and entropy ($\Delta_R S°$) changes were calculated from the temperature-dependent sorption constants, by the application of the van't Hoff formalism. The formation of the $\left[(\equiv SrOH)(\equiv TiOH)UO_2\right]^{2+}$ surface complex was found to present an endothermic character associated to an increase in the disorder of the system. On the contrary, the formation of the $\left[(\equiv TiOH)(\equiv TiO)UO_2\right]^{2+}$ surface complex led to an exothermic process with only a slight increase in the disorder of the system.

Keywords

Sorption, $SrTiO_3$, temperature, uranyl, surface complexation modelling, enthalpy, entropy, TRLIFS.

1. Introduction

Sorption reactions on mineral surfaces are known to decrease the dispersion of pollutants in the geosphere and particularly the migration of U(VI) in the aqueous environment is influenced by sorption onto mineral surfaces [1,2].

Uranium is an element of environmental interest: it exists at various oxidation states. Compared to U(IV), the uranyl ions are particularly mobile [3,4]. In recent years, the adsorption of U(VI) onto solid surfaces, especially on different oxides such as ferrite, ferrihydrite and goethite [5-8], phosphates, aluminates, and silicates [9] has received a great interest. However, most of the studies concerning the U(VI) sorption are carried out at 25°C [10-14]. Indeed, only few experimental studies have been so far performed for the sorption and complexation of U(VI) at temperature outside the 20-30°C range [15]. However, the temperature is an important parameter that should be taken into account in the sorption experiments [16] since in the near-field environment of a spent fuel or vitrified high-level waste repository, the temperature will remain elevated for a long time period: thermal calculations have shown that the temperature in a bentonite may attain 70-90°C for 1000 years after repository closure [17].

The perovskite ($SrTiO_3$) is involved in numerous technological applications [18-21]. The choice of this materiel for our study is based on the presence of many based perovskite compounds in the geosphere. Moreover, the perovskite presents a high chemical stability over a wide range of pH values [22].

The aim of the present paper is to investigate the temperature effects on U(VI) sorption mechanisms onto $SrTiO_3$ (chosen as a model mineral). For the understanding of the sorption process, it is necessary to use structural techniques, which allow one to identify the sorption mechanisms at a molecular scale and thus the identification of the species involved in the retention processes. In this investigation, we present the temperature influence on the sorption of U(VI) onto $SrTiO_3$ at 25, 50, 75 and 90°C by using a thermodynamic approach based on the acquisition of the U(VI) sorption edges coupled to a spectroscopic approach by using Time-Resolved Laser-Induced Fluorescence Spectroscopy (TRLIFS). The structural information obtained from the spectroscopic study at the different temperatures provides information as constraints to fit the macroscopic data using the FITEQL4.0 simulation code (constant capacitance model) [23]. These constraints, coupled with previous results [24] concerning the intrinsic surface parameters characterization at different temperatures, drastically reduced the number of fitting parameters during the simulation of the macroscopic data.

2. Materials and methods

2.1. Materials and characterization

Commercially available $SrTiO_3$ powders provided by Aldrich® (EC235-044) were used. The material was purified by extensive washing with deionized water until the pH and the electrical conductivity were constant. The substrate was then dried at 100°C during 48 h before being used. The XRD data showed pure crystallographic phases, in agreement with JCPDS 35-0734 file of cubic structure. The specific surface area has been determined by N_2-BET method (5 points) and was found to be 2.4 ± 0.2 m^2/g. The average grain size is between 0.4 and 1.2µm.

2.2. Sorption procedure

The sorption experiments were carried out in polypropylene tubes and under argon atmosphere at different temperatures: 25, 50, 75 and 90°C. A shaking thermostated bath was used to keep the samples at constant temperature. For all the experiments, $HClO_4$ and NaOH solutions were prepared to adjust the pH of the suspensions. A 0.025 M uranyl stock solution was prepared by dissolution of solid $UO_2(NO_3)_2.6H_2O$ (Merck™) in a $NaClO_4$ 0.1 M solution previously acidified at pH = 1 to avoid cation hydrolysis. Hydration and sorption experiments were separated. In a first step, 200 mg of $SrTiO_3$ powder were added to 10 mL of $NaClO_4$ (Prolabo™) 0.1 M solutions, adjusted at the desired pH value. The resulting suspension was shaken for 24 hours to allow the hydration of the solid surface. This time was found to be sufficient to reach the equilibrium. In a second step, a negligible volume of the cation stock solution (40 µl) was added to the suspension in order to reach an initial uranyl concentration equal to 10^{-4} M. This concentration was chosen to avoid surface site saturation. The resulting suspension was shaken for 24 hours before being centrifuged at 3500 rpm for 15 minutes. Then, the pH values of the supernatant were measured, at the temperature under investigation, with a combined glass electrode, composed of a solid electrolyte and double Teflon junction (Fisher Bioblock™). The calibration was done using temperature certified buffer solutions (Hanna™). The precision on the measured temperature was estimated to be ± 1°C and the precision on the measured pH values was estimated to be ± 0.1 unit.

The uranium uptake was obtained by determining the initial and final concentrations in solution by mean of α-liquid scintillation counting, using a PACKARD 2700 Tri-Carb Analyser™, after extraction of the uranium from the supernatant by a scintillating-extracting cocktail (Alphaex™).

For the spectroscopic investigations, the *in situ* samples were prepared by directly using the supernatant in a quartz tube while for the dried samples, the suspensions were filtered before analysis of the solid. Note that in the case of the samples prepared at 25°C, the solids were washed with deionized water and air-dried for spectroscopic analysis.

2.3. Time-resolved laser-induced fluorescence spectroscopy (TRLIFS)

TRLIFS is a very selective and sensitive method for actinides and lanthanides analysis and has been widely used [25]. This technique allows the identification of the sorbed complexes from both the fluorescence spectrum (wavelength position, peak shape) and the associated lifetimes.

In our experiments, TRLIFS was applied to study sorbed powders. The fluorescence of the sorbed U(VI) species at different pH was followed at 25, 50, 75 and 90 °C. TRLIFS experiments were performed on dry powders contained in sealed quartz tubes at the temperature under study, using an oven placed on the optical path. A Continuum^{TM} Nd:YAG laser (pulse duration around 7ns) coupled with a Panther^{TM} OPO was used as excitation source at 430 nm to provide the best signal-to-noise ratio. The detection was performed by a Spectra-Pro-300 monochromator (Acton Research Corporation^{TM}) coupled with a CCD camera (Princeton Instruments^{TM}). Emission spectra were recorded between 470 and 570 nm using the Winspec software (Princeton Instruments^{TM}). The decay profiles were fitted to multi-exponential laws with the IGOR^{TM} software to determine the decay times of uranyl surface species fluorescence. The relative precision on the lifetime values is estimated to be 10%.

2.4. Modelling of the sorption results

Uranyl sorption edges onto $SrTiO_3$ as a function of the temperature were modelled with the FITEQL4.0 [23], which is based on a nonlinear least-squared optimization routine [26]. This program allows one to consider different surface complexation models: non-electrostatic or electrostatics ones. Among these, the constant capacitance model (CCM) [27], which was successfully used for other systems [28-30], was preferred. The choice of this model was already discussed in a previous paper [24]. The surface acid-base characteristics of the strontium titanate are summarized in table 1. Thus, since the species involved in the sorption process are known from the spectroscopic investigation, the only remaining parameters to calculate are the sorption constants and the associated number of exchanged protons involved in the sorption equilibria. The number of proton released during the sorption process was determined from the goodness of the fit which can be evaluated with the WSOS/DF ratio where WSOS if the weighed sum of squares and DF the degrees of freedom. According to Westall *et al.* [23], the WSOS/DF ratio has to be ranged from 0.1 to 20. Moreover, the aim of this work was to determine the enthalpy and entropy changes associated to the sorption process. Considering the limited temperature range investigated ($\Delta T = 65°C$), we have postulated that both $\Delta_R H°$ and $\Delta_R S°$ are constant which seems to be a reasonable assumption. Then, we have considered a second criterion for the goodness of the fit which was the linear regression coefficient (R^2) value when plotting log K as a function of 1/T, according to the van't Hoff relation. It was chosen that homogeneous values should give a R^2 value higher than 0.9 which provided us another constraint for the modelling procedure. The uncertainties associated to the sorption constants were estimated to be about 0.5 logarithmic units. One can notice that this value is only estimation since no sensitivity analysis has been carried out.

3. Results and Discussion

Firstly, the effects of the temperature (25°C - 90°C) and pH on the uptake of U(VI) sorption onto $SrTiO_3$ powders were investigated from a macroscopic point of view. Secondly, the spectroscopic study was realised for both *in situ* and dried samples in order to identify the surface complexes formed onto the solid. Finally, the spectroscopic results were used as constraints for the modelling of the sorption edges in order to obtain accurate sorption constant values corresponding to the equilibria involved in the sorption of U(VI) onto $SrTiO_3$.

The variation of these sorption constants with the temperature allowed the determination of the enthalpy and entropy variations by application of van't Hoff equation.

3.1. Uranyl sorption edges

Uranyl sorption edges as a function of pH and temperature were obtained by measuring the concentration of uranium in solution before and after sorption. Sorption edges as a function of the pH value (0.5 to 5) for temperature ranged between 25 and 90°C are displayed on figure 1. The sorption edges spread over four pH units which suggest the presence of different surface complexes. Moreover, considering the pH_{pzc} value of the studied substrate (pH_{pzc} around 9.5 whatever the temperature), we can underline that the position of the obtained sorption edges indicates that the retention process occurs on a globally positive surface. Such a behaviour is commonly observed for U(VI)/oxides and U(VI)/phosphates systems [31-34].

The data show an increasing uptake of U(VI) as a function of the pH and a shift of the sorption edges towards lower pH values as the temperature is increased. Then, an increase in temperature favours the U(VI) retention at constant pH: this trend indicates a global endothermic character of the sorption process. Such a temperature effect on the position of the sorption edge has already been reported for several sorption studies performed at temperature higher than 20°C [35-37] and was explained to be primarily driven by favourable entropic effects, in part due to the increasing release of hydration-sphere water molecules with increasing temperature. This behaviour has also been observed for the sorption of a wide range of metals onto oxide surfaces. Indeed, Angove *et al* [38] showed that metallic sorption increased with the temperature for Cd(II) and Co(II) interaction with goethite between 10 and 70°C. Moreover, similar U(VI) sorption behaviour has been reported on various metal oxides: γ-alumina, ferrihydrite, kaolinite and hematite [39-42]. Finck *et al.* [43] showed an increasing uranyl sorbed amount onto zirconium diphosphate when the pH and the temperature are increased. Almazan *et al* [34] the same trend for the sorption of U(VI) onto zirconium oxophosphate. In the same way, previous studies of Eu(III) sorption onto clay minerals performed by *E. Tertre et al.* between 25 and 150 °C, showed a strong influence of the pH and the temperature on the sorption process [44].

3.2 Spectroscopic measurements

TRLIFS experiments carried out on the U(VI)/$SrTiO_3$ system yield to identify the chemical environment of the sorbed uranyl species from the shape of the fluorescence

spectrum, the position of the emission bands and the associated lifetimes. We have chosen dried samples corresponding to different sorption percentages which covered the entire sorption edge: pH ≅ 2 (25%), pH ≅ 2.5 (50%), pH ≅ 3 (75%), pH ≅ 4 (90%) for all temperatures (25°C - 90°C). In the pH range of the sorption edges, the uranyl speciation diagrams (figure 2) show that only UO_2^{2+} is present in solution at 25°C, but the proportion of hydrolyzed species, particularly $UO_2(OH)^+$, strongly increases with the temperature. One could thus expect that different uranyl aqueous species are sorbed onto the surface. Then, these samples were analysed by using laser spectroscopy to check whether the surface species change or not as the temperature is increased.

The figure 3 showed the fluorescence spectra of the samples prepared at 25, 50, 75 and 90°C for different pH values. For these samples, the emission spectra do not change with the temperature and the pH, considering both emission wavelengths (504, 525 and 545 nm) and relative peak intensities. Nevertheless, the analysis of the decay profiles indicates the presence of two lifetime values: $\tau 1 = 12 \pm 2\mu s$; $\tau 2 = 60 \pm 5\mu s$ (table 2) unchanged with the temperature and the pH. This indicates that whatever the temperature and the pH, only two uranyl species are present on the surface. Thus, since only UO_2^{2+} is present in solution at 25°C over the entire sorption edge, we concluded that only the free aqueous uranyl ion interacts with the $SrTiO_3$ surface for all the temperatures investigated. Consequently, two surface complexes have to be considered for the modelling step.

The same behaviour has been observed for U(VI) sorption onto $Zr_2O(PO_4)_2$ [34] and onto ZrP_2O_7 [43]: two unchanged surface species have been determined between 25 and 90°C for the same pH range as for the U(VI)/$SrTiO_3$ system and have been attributed to the interaction of UO_2^{2+} ions with two types of surface sites ≡Zr-OH and ≡P-OH.

3.3. Modelling of the macroscopic retention data

FITEQL4.0 code was used to calculate the sorption constants corresponding to the experimentally identified equilibria. The spectroscopic investigation led to conclude that only the free uranyl ion is sorbed on the surface whatever the temperature. Moreover, we know from a previous study [24] that the $SrTiO_3$ surface could be described with two kinds of non-amphoteric sites: $\equiv Sr\text{-}OH^{-0.5}$ and $\equiv Ti\text{-}OH^{+0.5}$. A summary of the surface acid-base behaviour is reported on Table 1. Additionally, numerous EXAFS experiments were performed considering sorption processes of U(VI) and other cations onto different types of mineral surfaces. It can be noticed that in most of the cases, the authors concluded that the sorbed cation is doubly coordinated to the surface. For the uranium sorption onto ZrP_2O_7, *Drot et al*

[45] report the formation of mononuclear bidentate inner-sphere complexes. For another substrate, *Gabriel et al.* [46] showed that the adsorption of the uranyl ion onto silica occurs as a bidentate surface complex as well. In the same way, the adsorption of the uranyl ion onto γ-alumina surface appears to occur *via* an inner-sphere, bidentate complexation with the surface sites, with the formation of polynuclear surface complexes occurring only at near-neutral pH conditions [47]. Some experiments performed on the U(VI)/silica gel system suggested that for a pH as low as 4.0, uranyl undergoes inner-sphere, mononuclear, bidentate surface complexation [48]. Finally, Ordóñez *et al* [49] showed that U(VI) sorbed onto lanthanum monophosphate, forms a bidentate complex. Then, according to the literature, it was considered in the modelling procedure that only bidentate surface complexes are formed.

As a conclusion, considering all these results, only the number of proton released associated to the sorption mechanism remains as an adjustable parameter. Moreover, since it is well established that the sorbed U(VI) species are doubly coordinated to the surface and that two kinds of surface sites are considered (Sr-OH$^{-0.5}$ and ≡Ti-OH$^{+0.5}$), the modelling procedure has to define which combination of surface sites is involved in the surface complexes formation. Nevertheless, this approach has allowed one to drastically reduce the total degrees of freedom of the system during the modelling procedure.

The uranium (VI) speciation in solution (figure 2) was described using the constants recommended by Grenthe *et al*. [50], excepted for the $UO_2(OH)_2$ [51]. The speciation constants declared in the FITEQL input file were previously corrected from the ionic strength by using the Davies equation. No more ionic strength corrections were performed during the modelling of the sorption data. Moreover, for 50, 75, and 90°C, the DQuant equation was used to correct the aqueous equilibrium constants from the temperature effect (Table 3). Such a correction has already been described in the literature for uranyl species [43].

The best fits obtained are presented on figure 4 which shows the calculated curves and the corresponding repartition of the surface complexes for all the temperatures considered. They correspond to the following sorption mechanism whose sorption constant values are reported in table 4:

$$(\equiv SrOH^{-0.5}) + (\equiv TiOH^{+0.5}) + UO_2^{2+} \Leftrightarrow \left[(\equiv SrOH)(\equiv TiOH)UO_2\right]^{2+}$$

$$2(\equiv TiOH^{+0.5}) + UO_2^{2+} \Leftrightarrow \left[(\equiv SrOH)(\equiv TiO)UO_2\right]^{2+} + H^+$$

As discussed above, these results where obtained by considering the WSOS/DF factor together with the R^2 coefficient from the linear regression when plotting log K as a function of 1/T. One can notice that the stability of the first complex is favoured (compare to the second one) with an increasing temperature since the stability of the second one decreases as the temperature increases. Consequently, the resulting proportion of these two surface complexes is affected by the temperature. For 25°C, the sorption mainly occurs onto the titanium site (*e.g.* reaction of U(VI) with 2 ≡Ti-$OH^{+0.5}$ sites) while at 90°C the sorption onto the titanium/strontium site (e.g. reaction of U(VI) with one ≡Ti-$OH^{+0.5}$ and one ≡Sr-$OH^{-0.5}$ sites) is equivalent in term of quantities to the sorption onto the titanium/titanium site (figure 4).

The plots of log K versus 1/T are shown in figure 5 and the enthalpy and entropy values associated to both surface complexes are reported in table 5. The enthalpy value is positive for the $\left[(\equiv SrOH)(\equiv TiOH)UO_2\right]^{2+}$ complex formation ($\Delta_R H°$ = 33 kJ.mol^{-1}), showing an endothermic sorption process. On the opposite, the formation of the $\left[(\equiv TiOH)(\equiv TiO)UO_2\right]^{2+}$ complex involves an exothermic process. The entropy values are positive whatever the surface complex formation which indicate an increase in the disorder of the system during the sorption of uranyl ion onto $SrTiO_3$. One possible explanation for these positive values is that the sorption of UO_2^{2+} led to the decrease of the number of water molecules surrounding the ion and thus the increase of the degrees of freedom of the system.

Metal sorption onto perovskite structures was not already reported in the literature, but nevertheless, a great number of studies concerning the sorption of different metals onto various matrices from a thermodynamic point of view, can be useful to compare to our results.

Finck *et al.* [43] and Almazan-Torres *et al* [34] works dealt with the sorption of uranyl onto ZrP_2O_7 and $Zr_2O(PO_4)_2$, respectively, for temperature ranged from 25 to 90°C. They found positive values for both entropy and enthalpy changes. Moreover, Angove *et al* [52] have investigated the sorption of Cd^{2+} and Co^{2+} onto goethite between 10 and 70 °C: the retention of these two cations increased with the temperature and this phenomenon was quantified by determining the sorption enthalpy value from the modelling. Pivovarov *et al* [53] studied the sorption of Cd^{2+} by hematite between 25 and 100 °C where the enthalpy and entropy values were both positive, indicating that the sorption process was entropy driven. The values of ΔH^0_{ads} and ΔS^0_{ads} obtained by Ridley *et al* [54] for the Ca^{2+} sorption onto rutile between 25 and 250 °C are 7.93 ± 0.54 kJ·mol^{-1} and 363.48 ± 1.71 J·mol^{-1}, indicating an

endothermic character of the adsorption process and an increase in the disorder of the system due to the sorption. In the same conditions, Ridley studied the Nd^{3+} sorption onto rutile between 25 and 250°C and obtained the values of ΔH^0_{ads} and ΔS^0_{ads} of 45.2 kJ·mol^{-1}and 591.3 J·mol^{-1}, respectively [55].

Even if no result is reported in the literature for the U(VI) sorption onto $SrTiO_3$, the thermodynamic data values reported for different metallic ions sorbed onto various mineral surfaces are in the same order of magnitude than those corresponding to our system, and all these studies evidence an increase in the disorder of the system regarding sorption reactions.

4. Conclusion

The sorption of U(VI) onto $SrTiO_3$ was investigated, as a function of the pH and the temperature, between 25 and 90 °C. Experimental data show that the sorption of U(VI) onto $SrTiO_3$ was strongly temperature-dependent since the percentage of sorbed uranium increases with the temperature, indicating that the global process is endothermic. The results obtained by TRLIFS spectroscopy showed the formation of two types of U(VI) surface complexes. The nature of these surface species were not affected by the pH and the temperature considered.

These structural results were used as constraints for the simulation of the sorption edges for the overall temperature range (from 25 to 90 °C). Moreover, the results obtained from the modelling of the potentiometric titrations (site density, nature of the surface sites, acidity constants and the capacitance values) were also used, and led to have only as remaining free parameters: the sorption equilibrium constants and the number of exchanged protons. The experimental data were fitted with the constant capacitance model (CCM) and, according to the structural results, the two following equilibria led to the best fits:

$$(\equiv SrOH^{-0.5}) + (\equiv TiOH^{+0.5}) + UO_2^{2+} \Leftrightarrow \left[(\equiv SrOH)(\equiv TiOH)UO_2\right]^{2+}$$

$$2(\equiv TiOH^{+0.5}) + UO_2^{2+} \Leftrightarrow \left[(\equiv TiOH)(\equiv TiO)UO_2\right]^{2+} + H^+$$

The quantification of both ΔH^0_{ads}, ΔS^0_{ads} values was realized by using the classical van't Hoff relation. The formation of the first complex was found to be endothermic while the process was exothermic for the second one. Moreover, for both cases, the sorption process induces an increase of the disorder of the system which is probably due to the lost of hydration water molecules surrounding the cation, involved in the surface complex formation.

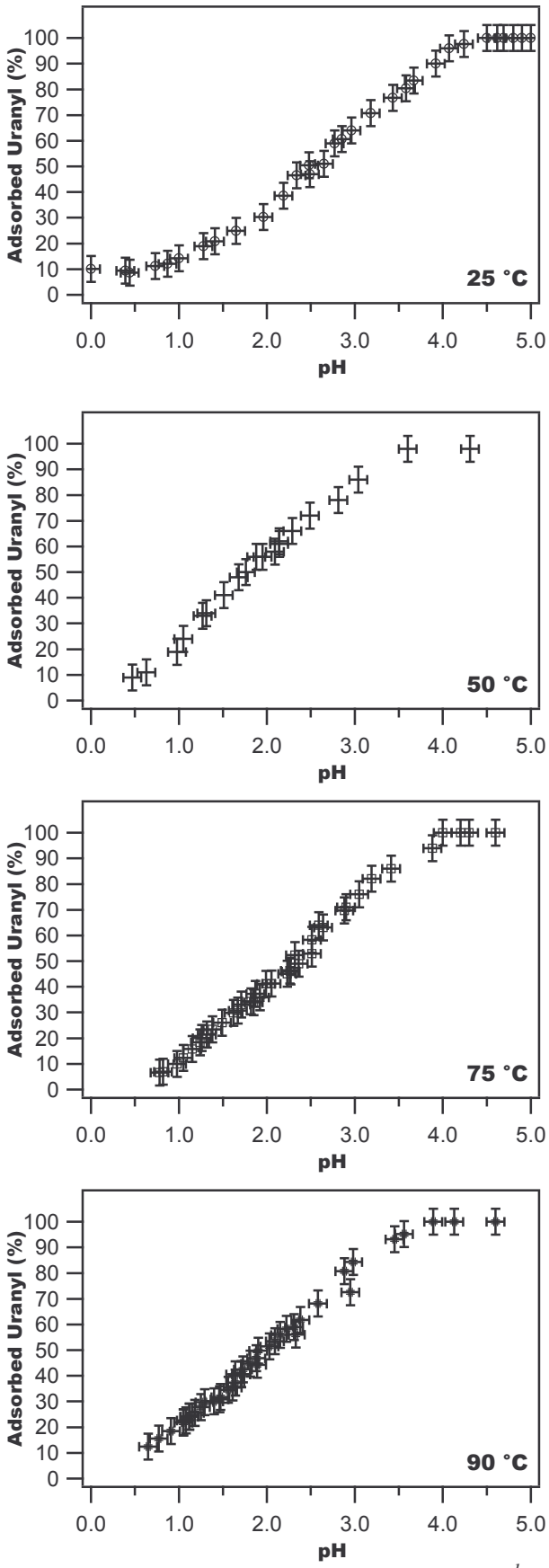


Fig. 1: Sorption edges of strontium titanate suspensions (20 g.L^{-1}) in $NaClO_4$ 0.1 M initial concentration of 10^{-4}M, between 25°C and 90°C representing the adsorbed uranyl % versus the pH.

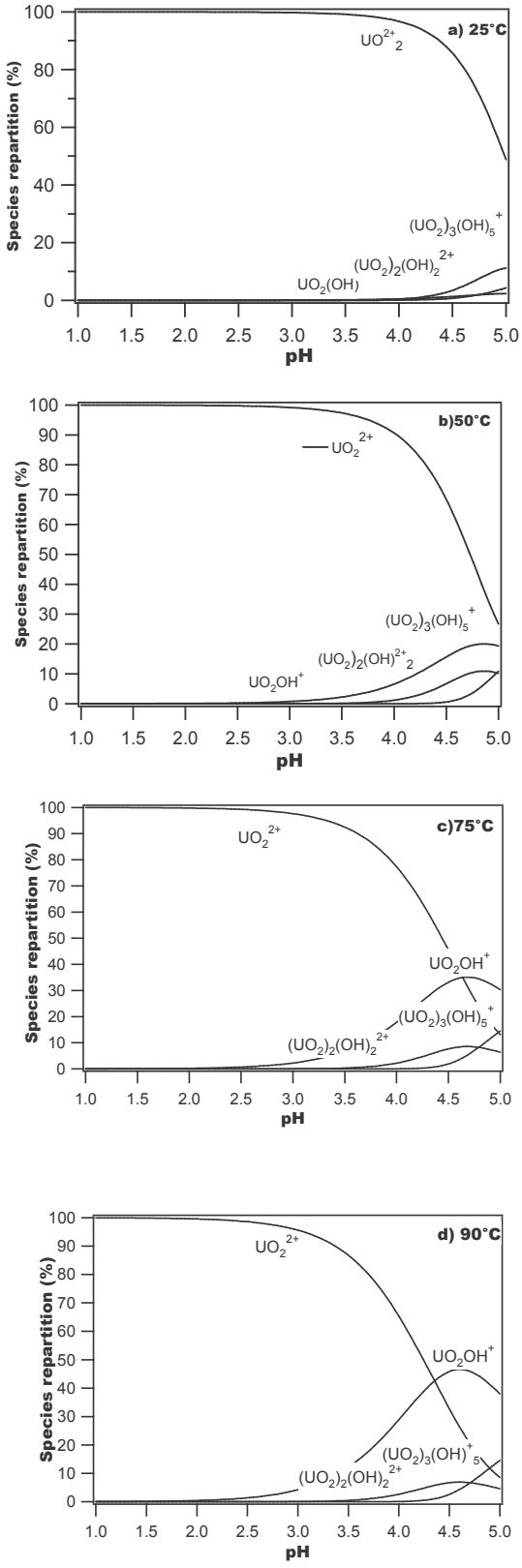


Fig. 2: Calculated U profile as a function of pH between 25 and 90°C. Solution composition: $U_{Total}=10^{-4}M$, $NaClO_4$ 0.1M. Values calculated using data Grenthe et al (1992). Activity correction made with the Davis equation.

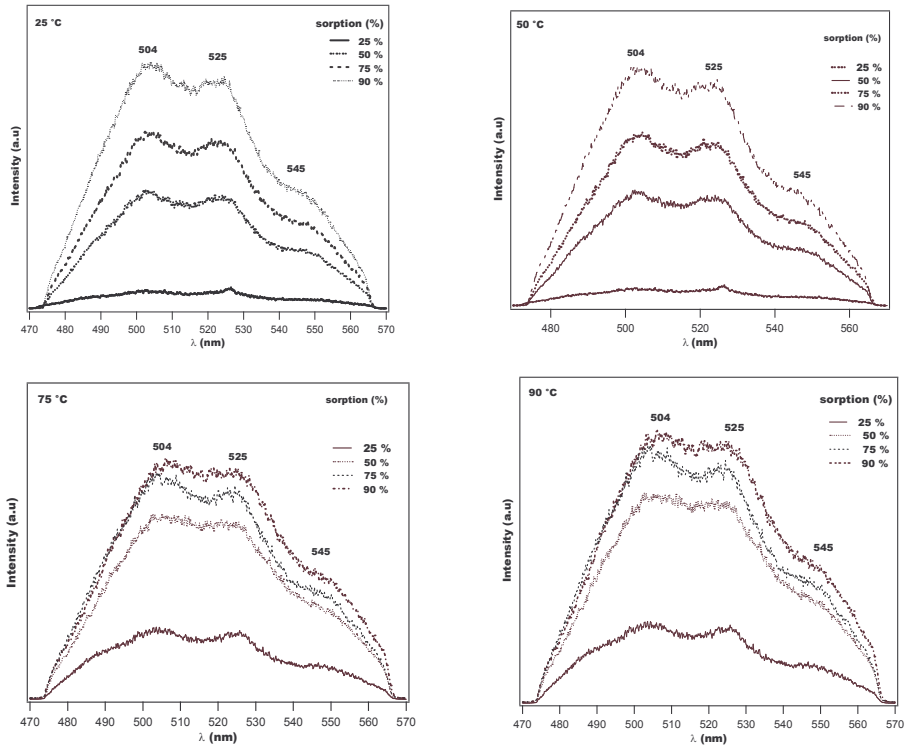


Fig. 3: a) Fluorescence spectra of the uranyl ions sorbed onto $SrTiO_3$, λ_{ex}= 430 nm between 25 and 90°C for different retention rates.

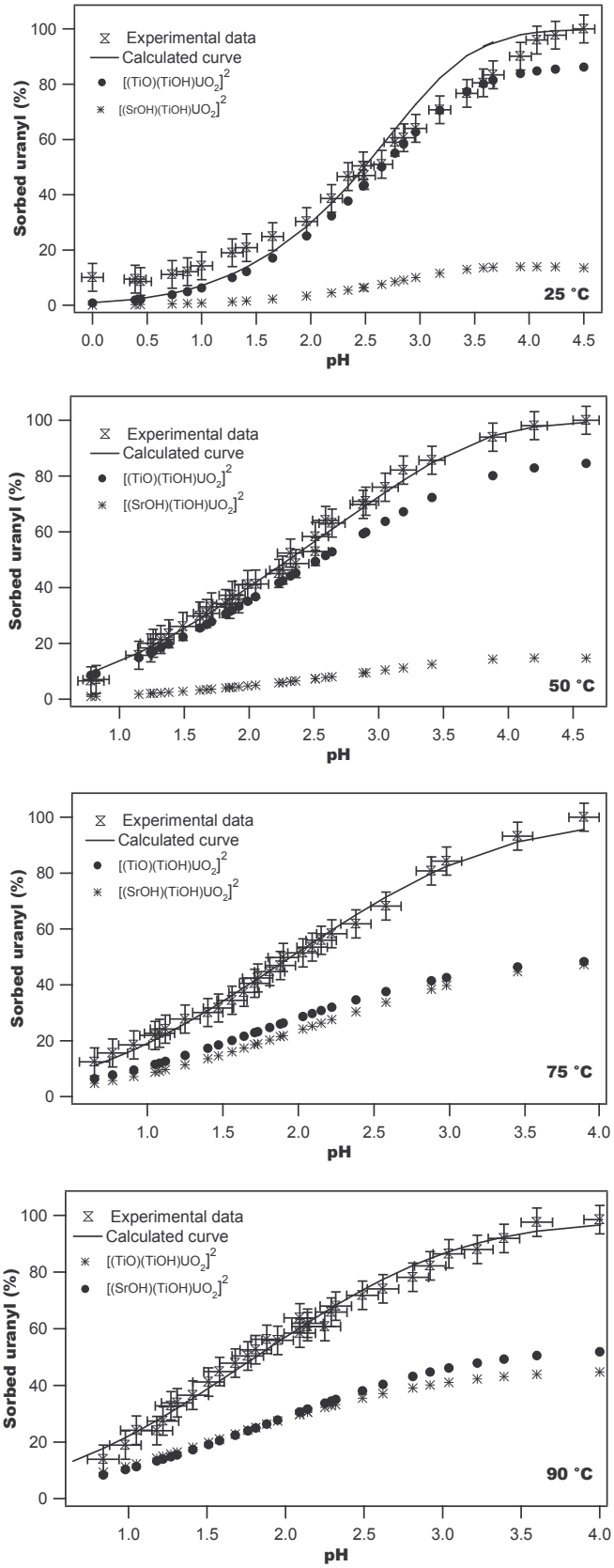


Fig. 4: Experimental data and calculated curves for uranyl sorption onto Sr-OH/UO_2^{2+} and Ti-OH /UO_2^{2+} (10 mL of uranyl solution 10^{-4}M and 0.2 g. of $SrTiO_3$ powder) between 25 and 90°C.

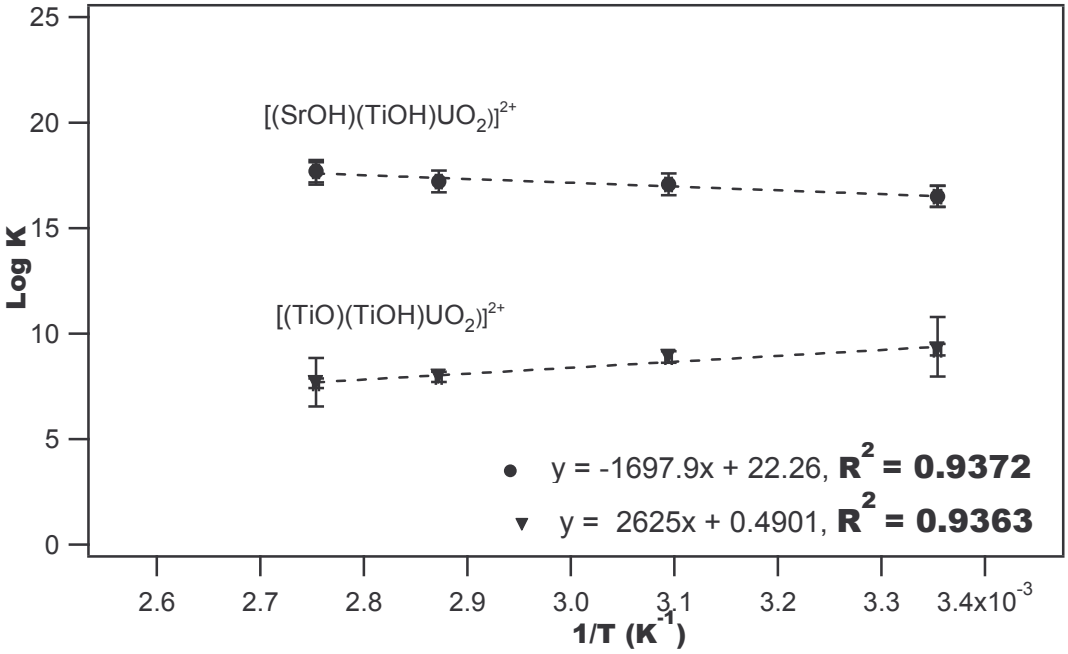


Fig. 5: log K versus 1/T relation for the titanate strontium ($SrTiO_3$/ UO_2^{2+}) reactions sorption.

Table 1: Calculated (intrinsic or chemical) surface reaction constants for the titanium and strontium surface sites, versus temperature.

Temp. (°C)	**C (Fm^{-2})**	**WSOS/DF**	**log $K_{\equiv Sr\text{-}O}$ ± 0.5**	**log $K_{\equiv Ti\text{-}O}$ ± 0.5**
25	3.1	1.13	8.3	-8.8
50	3.6	0.90	9.1	-9.6
75	4.8	4.45	9.4	-9.8
90	5.5	3.30	10.1	-10.7

Table 2: Emission lifetimes recorded for U(VI) ions sorbed onto $SrTiO_3$ in $NaClO_4$ at 25, 50, 75 and 90 % sorption.

$SrTiO_3$ Powder								
25 °C		**50 °C**		**75 °C**		***90 °C***		
pH	*% sorption*	*pH*	*% sorption*	*pH*	*% sorption*	*pH*	*% sorption*	***Emission Lifetimes*** (μs)
1.9	3	1,4	17	1,6	28	1.0	28	12 ± 2 and 60 ± 5
2.5	47	2,3	51	2.0	46	1.5	47	12 ± 2 and 60 ± 5
3.2	70	2,9	55	2.7	48	1.9	58	12 ± 2 and 60 ± 5
4.0	90	3,5	65	2.9	57	2.7	78	12 ± 2 and 60 ± 5

Table 3: Calculated U equilibrium constants between 25 and 90°C. Solution composition: $U_{Total}=10^{-4}M$, $NaClO_4$ 0.1M. Values calculated using data Grenthe et al (1992). Activity correction made with the Davis equation.

Equilibrium Reaction	**Log K^0 (25 °C)**	**Log K^0 (50 °C)**	**Log K^0 (75 °C)**	**Log K^0 (90 °C)**
$UO_2^{2+} + H_2O \Leftrightarrow UO_2(OH)^+ + H^+$	-5.20	-4.60	-4.07	-3.77
$UO_2^{2+} + 2H_2O \Leftrightarrow UO_2(OH)_{2\,(aq)} + 2H^+$	-12.9	-9.41	-8.63	-8.21
$UO_2^{2+} + 3H_2O \Leftrightarrow UO_2(OH)_3^- + 3H^+$	-19.20	-17.76	-16.53	-15.88
$UO_2^{2+} + 4H_2O \Leftrightarrow UO_2(OH)_4^{2-} + 4H^+$	-33.00	---	---	---
$2UO_2^{2+} + H_2O \Leftrightarrow (UO_2)_2(OH)^{3+} + H^+$	-2.70	---	---	---

Table 4: Sorption constant calculated values of uranium sorption onto $SrTiO_3$, versus temperature.

Temp. (°C)	**C (Fm^{-2})**	**log $K_{[(\equiv SrOH)(\equiv Ti\text{-}OH)UO_2]^{2+}}$ ± 0.2**	**log $K_{[(\equiv TiO)(\equiv TiOH)UO_2]^{2+}}$ ± 0.2**	**WSOS/DF**
25	3.1	16.5	9.3	29.4
50	3.68	17.1	8.9	1.8
75	4.8	17.2	8.0	1.5
90	5.5	17.7	7.7	2.9

Table 5: Enthalpy and entropy changes values corresponding to the uranium sorption reactions of the titanium and strontium surface sites.

Surface reaction	**$\Delta_r H°$ (kJ.mol^{-1})**	**$\Delta_r S°$ (J.K^{-1}. mol^{-1})**
$(\equiv SrOH^{-0.5}) + (\equiv TiOH^{+0.5}) + UO_2^{2+} \Leftrightarrow \left[(\equiv SrOH)(\equiv TiOH)UO_2\right]^{2+}$	33 ± 6	425 ± 18
$2(\equiv TiOH^{+0.5}) + UO_2^{2+} \Leftrightarrow \left[(\equiv TiOH)(\equiv TiO)UO_2\right]^{2+} + H^+$	-50 ± 9	9 ± 1

References

[1] M. Walter, T. Arnold, G. Geipel, A. Scheinost and G. Bernhard *J. Colloid Interface Sci.* 282 (2005) 293.

[2] T.E. Payne, J.A. Davis, G.R. Lumpkin, R. Chisari and T.D. Waite *Appl. Clay Sci.* 26 (2004) 151.

[3] M. Dossot, S. Cremel, J. Vandenborre, J. Grausem, B. Humbert, R. Drot, E. Simoni. *Langmuir* 22 (2006) 140.

[4] O.M. Barnett, P.M. Jardine, S.C.Brooks *Environ Sci. Technol.* 36 (2002) 937.

[5] T.E. Payne, J.A. Davis, T.D.Waite *Geochim. Cosmochim. Acta* (1994) 5465.

[6] R.J. Murphy, J.J. Lenhart, B.D. Honeyman *Colloid Surf.* 157 (1999) 47.

[7] D.E. Glammar, J.G. Hering *Environ. Sci. Technol.* 35 (2001) 3332.

[8] M. Wazne, G.P. Korfiatis, X. Meng *Environ. Sci. Technol.* 37 (2003) 3619.

[9] E.R. Sylvester, E.A. Hudson, P.G. Allen *Geochim. Cosmochim. Acta.* 64 (2000) 2431.

[10] C. Lomenech, E. Simoni, R. Drot, J.J. Ehrhardt and J. Mielczarski. *J. Colloid Interface Sci.* 261 (2003) 221.

[11] P. Toulhoat *C. R. Physique* 3 (2002) 975.

[12] A. Mellah, S. Chegrouche, M. Barkat *J. Colloid Interface Sci.* 296 (2006) 434.

[13] N. Baumann, V. Brendler, T. Arnold, G. Geipel, Bernhard *J. Colloid Interface Sci.* 290 (2005) 318.

[14] C.J. Chisholm-Brause., J.M.Berg, K.M. Little, R.A. Matzner, D.E. Morris *J. Colloid Interface Sci.* 277 (2004) 366.

[15] L. Rao, J. Jiang, P. Zanonato *Radiochim. Acta* 90 (2002) 581.

[16] S. García-García, M. Jonsson, S. Wold *J. Colloid Interface Sci.* 98 (2006) 694.

[17] A. Bauer, T. Rabung, F. Claret, T. Schäfer, G. Buckau, T. Fanghänel *Appl. Clay Sci.* 20 (2005) 1.

[18] R.H. Butter, E.N. Maslen *Acta Crystallogr.* B48 (1992) 639.

[19] R. Astala, P.D. Bristowe Comput. Mater. Sci. 22 (2001) 81.

[20] O. M. Parkash Kumar, C.C. Chistopher *Chem. Sci.* 115 (2003) 649.

[21] B. Meyer, J. Padilla, D. Vanderbildt *Faraday Discuss.* 114 (1999) 395.

[22] S. Soulet, J. Chaumont, C. Sabatier., J.C. Krupa *Mater. Res.* 17 (2002) 9.

[23] A.L. Herbelin, J.C. Westall, Report 96-01, Department of Chemistry, Oregon State University, Corvallis, OR. USA (1996).

[24] G. García Rosales, R. Drot, F. Mercier-Bion, E. Simoni (2007). In course.

[25] C. Moulin, P. Decambox *Anal. Chem.* 67 (1995) 348.

[26] S. Goldberg *Soil Sci. Soc. Am.* 3 (2004) 676.

[27] K.F. Hayes, G. Redden, W. Ela and J.O. Leckie *J. Colloid Interface Sci.* 142 (1991) 448.

[28] R. Drot, E. Simoni *Langmuir* 15 (1999) 4820.

[29] J.J. Lenhart, L.A. Figueroa, D.H. Bruce, D. Kaneko. *Colloids and Surfaces A: Physicochem. Eng. Asp.* 120 (1997) 243.

[30] N. Finck, R. Drot, F. Mercier-Bion, E. Simoni, H. Catalette *J. Colloid Interface Sci.* 312 (2007) 230.

[31] J. Vandenborre, PhD thesis, University of Paris-Sud-11, Orsay, France (2005).

[32] R. Drot, PhD thesis, University of Paris-Sud-11, Orsay, France (1998).

[33] C. Lomenech, E. Simoni, R. Drot, J.J. Ehrhardt, J. Mielczarski *J. Colloid Interface Sci.* 261 (2003) 221.

[34] M.G. Almazan-Torres, PhD thesis, University of paris-Sud-11, Orsay, France (2007).

[35] M.J. Angove, B.B. Johnson, J.D. Wells *J. Colloid Interface Sci.* 204 (1998) 93.

[36] O.A. Karasyova, L.I. Ivanova, L.Z. Lakshtanov, L. Lövgren. *J. Colloid Interface Sci.* 220 (1999) 419.

[37] M. Kosmulski *J. Colloid Interface Sci.* 192 (1997) 215.

[38] M.J. Angove J.D. Wells, B.B. Johnson *J. Colloid Interface Sci.* 296 (2006) 30.

[39] J.D. Prikril *Radiochim. Acta.* 66/77 (1994) 291.

[40] T.D.Waite, J.A. Davis, T.E. Payne, G.A. Waychunas *Geochim. Cosmochim. Acta.* 58 (1994) 5465.

[41] T E. Payne, J.A. Davis, T.D. Waite, *Adsorption of Metals by Geomedia*, Academic Press, New York (1998).

[42] J.R. Bargar, R. Reitmeyer, J.J. Lenhart, J.A. Davis *Geochim. Cosmochim. Acta.* 64 (2000) 2737.

[43] N. Finck, PhD thesis, University of Paris-Sud-11, Orsay, France (2006).

[44] E. Tertre, G. Berger, E. Simoni, S. Castel, E. Giffaut, M. Loubet, H. Catalette *Geochim. Cosmochim. Acta* 70 (2006) 4563.

[45] R. Drot, E. Simoni, C. Denauwer *C. R. Acad. Sci.- Series IIC* 2 (1999) 111.

[46] U. Gabriel, L. Charlet, C.W. Schlapfer, J.C. Vial, A. Brachmann, G. Geipel *J. Colloid Interface Sci*. 239 (2001) 358.

[47] T. Reich, H. Moll, A. Denecke, G. Geipel, G. Bernhard, H. Mitche, P.G. Allen, J.J. Bucher, N. Kaltsoyannis, N.M. Edelstein, D.K. Shuh *Radiochim. Acta.* 74 (1996) 219.

[48] T. Reich, H. Moll, T. Arnold, M.A. Denecke, C. Hennig, G. Geipel, G. Bernhard, H. Mitche, P.G. Allen, N.M. Edelstein, D.K. Shuh *J. Elec. Spec Related Phenom.* 96 (1998) 237.
[49] E. Ordoñez-Regil, R. Drot, E. Simoni *J. Colloid Interface Sci.* 263 (2003) 391.
[50] I. Grenthe, J. Furger, R. Konings, R.J. Lemire, A.B. Muller, C. Nguyen-Trung, H. Wanner, *Chemical Thermodynamics of Uranium, Vol 1 of Chemical Thermodynamics*. Elsevier, Amsterdam, 1992.
[51] I. Pashalidis, J.I. Kim, T. Ashida, I. Grenthe. *Radiochim. Acta.* 68 (1995) 99.
[52] M.J. Angove, J.D. Wells, B.B. Johnson *J. Colloid Interface Sci.* 296 (2006) 30.
[53] S. Pivovarov *J. Colloid Interface Sci.* 234 (2001) 1.
[54] M K. Ridley, M.L. Machachesky, D.J. Weselowski, D.A Palmer *Geochim. Cosmochim. Acta* 68 (2004) 239.
[55] M. K. Ridley, M.L. Macheski, D.J. Weselowski, D.A Palmer *Geochim. Cosmochim. Acta* 69 (2005) 63.

RESUME DU CHAPITRE II

L'acquisition des données expérimentales de sorption de l'ion uranyle sur le solide $SrTiO_3$, en fonction de la température et du pH, a fait l'objet de cette partie de notre étude.

Les sauts de sorption de l'ion uranyle (concentration initiale de 10^{-4} M) ont été réalisés en milieu $NaClO_4$ 0,1 M, pour des valeurs de pH comprises entre 0,5 et 5 et pour des températures de 25 à 90 °C. Les sauts de sorption obtenus montrent une augmentation du pourcentage de sorption avec l'augmentation de la température, traduisant un phénomène globalement endothermique. Pour caractériser les complexes de l'U(VI) formés en surface, des enregistrements des spectres de fluorescence ainsi que des temps de vie correspondants ont été réalisés sur les systèmes $UO_2^{2+}/SrTiO_3$, en fonction de la température. Deux sites de sorption différents, caractérisés par deux temps de vie, respectivement de 12 ± 2 et 60 ± 5 μs, ont été identifiés à la surface du solide. L'ion uranyle aquo est la seule espèce à se sorber quelle que soit la température envisagée. La présence des mêmes types de complexes de surface, sur toute la gamme de pH et de température étudiée, semble indiquer que le processus de sorption n'est sensible ni à la spéciation du cation en solution, ni à la température.

Après l'identification expérimentale des équilibres mis en jeu dans le processus de rétention, les sauts de sorption ont été modélisés à l'aide du code FITEQL en utilisant le modèle à capacitance constante. Cette simulation des sauts de sorption a été réalisée en tenant compte : i) des résultats de l'étude structurale (deux sites de surface $\equiv Ti-OH$ et $\equiv Sr-OH$ et formation de complexes surfaciques de sphère interne bidentate, mononucléaire) ; ii) des données obtenues dans le précédent chapitre de ce mémoire (densité de sites de surface, valeur de la capacitance à différentes températures et constantes de protonation/déprotonation obtenues par modélisation des courbes de titrages potentiométriques). La correction des constantes de formation des espèces de l'uranium (VI) en solution aqueuse à une force ionique de 0,1 M entre 25 et 90°C, a été effectuée au moyen de l'équation de Davies pour les corrections de force ionique et par l'équation DQuant pour les corrections de température. Les meilleurs résultats de cette modélisation ont été obtenus en considérant deux équilibres de complexation de surface à caractère bidentate :

$$(\equiv SrOH^{-0.5}) + (\equiv TiOH^{+0.5}) + UO_2^{2+} \Leftrightarrow \left[(\equiv SrOH)(\equiv TiOH)UO_2\right]^{2+}$$

$$2(\equiv TiOH^{+0.5}) + UO_2^{2+} \Leftrightarrow \left[(\equiv TiOH)(\equiv TiO)UO_2\right]^{2+} + H^+$$

La complexation par le site mixte « $(\equiv SrOH^{-0.5})(\equiv TiOH^{+0.5})$ » ne s'accompagne pas de la libération de protons, contrairement à la complexation par le seul site $(\equiv TiOH^{+0.5})$ pour former le second complexe de surface. La répartition des différentes formes $\left[(\equiv SrOH)(\equiv TiOH)UO_2\right]^{2+}$ et $\left[(\equiv TiOH)(\equiv TiO)UO_2\right]^{2+}$ varie assez sensiblement avec l'augmentation de la température. En effet, la formation du complexe $\left[(\equiv SrOH)(\equiv TiOH)UO_2\right]^{2+}$ est fortement favorisée par rapport à l'autre complexe lorsque la température augmente. Suite à l'obtention des constantes thermodynamiques par simulation des sauts de sorption, la relation de van't Hoff a été appliquée pour déterminer les variations d'enthalpie et d'entropie associées au processus de sorption.

CHAPITRE III

TRANSFERT D'ENERGIE ENTRE DES IONS Tb^{3+} ET Eu^{3+} SORBES SUR $SrTiO_3$

ENERGY TRANSFER FROM Tb^{3+} TO Eu^{3+} IONS SORBED ONTO $SrTiO_3$ SURFACE

G. García-Rosales, R. Drot, G.Lagarde, F. Mercier-Bion, J. Roques and E. Simoni

Keywords: surface energy transfer, Tb^{3+}, Eu^{3+}, strontium titanate, TRLIFS.

Abstract

In this work, the energy transfer at room temperature between Tb^{3+} and Eu^{3+} ions sorbed onto $SrTiO_3$ powders has been investigated, by using Time-Resolved Laser-induced Fluorescence Spectroscopy (TRLIFS). This study is particularly innovating as, to our knowledge, no publication concerning the energy transfer between two ions sorbed onto a solid surface has been reported. The only studies published in the literature mainly concern the energy transfer between two lanthanide ions in co-doped matrices. Our results have shown that the energy transfer between Tb^{3+} and Eu^{3+} ions sorbed onto $SrTiO_3$ is a non-radiative process and follows a dipole-dipole type interaction. Moreover, the more the acceptor ions Eu^{3+} concentration is high, the more the energy transfer is efficient.

As we proved that there is no energy migration between the Tb^{3+} donor ions, a formalism based on the theories of Dexter and of Inokuti-Hirayama, taking into account the energy transfer between a donor and an acceptor ion, has allowed one to fit the decay curves of Tb^{3+} and consequently to access to the distance between Tb^{3+} and Eu^{3+} sorbed onto $SrTiO_3$. The calculated distances are similar to those obtained for other couples of donor-acceptor lanthanide ions reported in the literature.

1. Introduction

The investigation of Fluorescence Resonance Energy Transfer (FRET) between a donor and an acceptor (ions or molecules) in solutions and solids has considerably increased in the last decades. FRET is the process by which the extra energy of a molecule (or an ion) in an excited electronic state (called the donor D) is transferred to an acceptor A (molecule or ion). The necessary conditions for this mechanism occurs are: the fluorescent emission spectrum of the donor overlaps the absorption spectrum of the acceptor, and the separation distance (noted R) between D and A is sufficiently short, as the energy transfer efficiency varies as $1/R^6$. The direct application of FRET provides distances between the two fluorophores spaced from 0.5 to 10 nanometers. The D→A energy transfer is not due to the emission-absorption of a photon but there is a Coulomb charge-charge interaction between the D and A molecules [1].

The main applications of FRET are focused on biology and on the development of lasers components to increase their efficiency.

FRET provides a unique means of measuring interatomic distances in biological molecules in real time. For example, recent advances have been made in the application of this technique to studies of conformational changes in proteins [2]. New ways of introducing fluorescence probes into biological molecules and progress in the technologies for fluorescence signal detection have greatly expanded the range of applications of FRET. So, due to their spectral properties (high luminescence yield and particularly their long fluorescence lifetimes compared to conventional fluorophores), and to their ability to be linked to various organic compounds, rare earth ions are often introduced in biomolecules as fluorescent probes to permit the energy transfer between these ions and then to access to distances between biomolecules and conformation changes [3, 4].

In addition to its applications to biological science, the non-radiative energy transfer has played a major role in increasing the pumping efficiency of active ions in solid state laser materials. Studies concerning the energy transfer between lanthanide ions or between UO_2^{2+} and rare-earth ions and particularly Eu^{3+} are numerous in the literature. Some publications report the energy transfer in liquids as between UO_2^{2+} and Eu^{3+} in $POCl_3/SnCl_4$ solutions [5], or in inorganic solvents as D_2O [6, 7], polyphosphoric [8] and sulphuric [9] acids. Numerous works mention the energy transfer in co-doped solids and some examples can be cited among this exhaustive literature: transfer between UO_2^{2+} and Eu^{3+} in silica glasses [10], between UO_2^{2+} and Sm^{3+} in zinc phosphate glass with uranyl acetate and samarium oxide used as dopants [11], between Nd^{3+} and U^{3+} in $LiYF_4$ co-doped with these two ions [12] and from

Tm^{3+} to Ho^{3+} and Nd^{3+} in doped zinc phosphate glass [13], yttrium fluorides doped with lanthanides [14], potassium lanthanum ternary halides K_2LaX_5 (with X=Cl, Br, I) co-doped with different lanthanide ions [15].

Among the donor-acceptor pairs studied in the energy transfer, Tb^{3+} and Eu^{3+} are known to show an effective energy transfer from Tb^{3+} to Eu^{3+}. This energy transfer from Tb^{3+} to Eu^{3+} was investigated in several hosts as for example in co-doped solids: tungstates [16], zeolite-Y [17], Y_2O_2S [18], Y_2O_3 crystals [19], porous silicon matrix [20], in doped alumina films [21] or in $LiREP_4O_{12}$ (where RE=Tb and Eu) [22].

Even if the applications of FRET are numerous, to our knowledge, no publication concerning the energy transfer between two ions adsorbed onto solids or present in surface films has been reported in the literature. In this paper, the energy transfer between Tb^{3+} and Eu^{3+} ions sorbed onto strontium titanate ($SrTiO_3$) surface has been investigated, by using Time-Resolved Laser-induced Fluorescence Spectroscopy (TRLIFS) for obtaining the decay fluorescence of Tb^{3+} and consequently to identify the responsible interaction for the energy transfer $Tb^{3+} \rightarrow Eu^{3+}$ and to determine the distance between Tb^{3+} and Eu^{3+} sorbed ions onto $SrTiO_3$. This work is related to the research of interaction mechanisms between an ion in aqueous solution (as UO_2^{2+} or a lanthanide) and a solid surface, in the general context of environmental studies. In this work, $SrTiO_3$ has been chosen as a methological solid for retention experiments of cations: it is a well-known material because of its advantageous properties such as its chemical and physical stability, its high storage capacities and its crystallographic structure perfectly identified [23].

2. Experimental details

2.1. Samples preparation

The studied strontium titanate samples are ground powders (grain diameter varying from 0.4 to 1.2 µm) provided by Aldrich® (reference: EC235-044). X-Ray Diffraction data (not shown) evidenced pure crystallographic phase, in agreement with the JCPDS file n° 35-0734. Further assessments on purity of this material were performed by EDS, which showed the absence of any secondary phase. The N_2-BET specific surface area was found to be 2.4 m^2/g.

Stock solutions of Tb^{3+} and Eu^{3+} were prepared by dissolving the corresponding rare-earth oxides with pure $HClO_4$ at pH=1 in $NaClO_4$ 0.1 M medium.

The sorption experiments of Tb^{3+} and Eu^{3+} ions onto $SrTiO_3$ samples were carried out under an inert atmosphere and at room temperature in polypropylene tubes, which allow one

to avoid rare-earth ions sorption onto their walls. 100 mg of $SrTiO_3$ were firstly hydrated for 24 h with 5 mL of $NaClO_4$ 0.1 M aqueous solution adjusted at pH = 4. After centrifugation (3500 rpm, 24 h), 2 mL were removed from the supernatant and replaced by the same volume of rare-earth ions solutions: Tb^{3+}, Eu^{3+} or Tb^{3+}/Eu^{3+} mixtures and adjusted to the same pH. After a contact time of 24h (necessary to reach the thermodynamic equilibrium between ions and the $SrTiO_3$ surface) and under a constant stirring, a centrifugation at 3000 rpm during 15 minutes allows one to separate the solution from the solid: the suspension is then filtrated onto a sintered glass to recover the solid phase that is washed with distilled water and dried at room temperature then placed in quartz tubes to be analyzed by TRLIFS and the supernatant is removed for ICP-MS analyses (to obtain Tb^{3+} and Eu^{3+} concentrations sorbed onto $SrTiO_3$). The sorption experiments for the energy transfer studies were performed with an initial Tb(III) concentration of 10^{-4} M in $NaClO_4$ medium 0.1 M. The $SrTiO_3$ samples (100 mg) have been contacted at 25°C during 24 hours, at pH = 4 and in $NaClO_4$ medium 0.1 M with 5 mL of Tb^{3+} solution 10^{-4} M concentration, and with mixed solutions of Tb^{3+}/Eu^{3+} for whose the concentrations of Eu^{3+} vary from 10^{-6} M to 10^{-2} M. The value of pH = 4 was chosen to favour the maximal uptake of Tb (III) and Eu (III) by strontium titanate and to avoid the hydrolysis of Tb^{3+} ions.

2.2 Techniques

2.2.1 Time-Resolved Laser-induced Fluorescence Spectroscopy (TRLIFS)

The energy transfer between Tb^{3+} and Eu^{3+} ions sorbed onto $SrTiO_3$ surfaces has been investigated, by using the Time-Resolved Laser-induced Fluorescence Spectroscopy (TRLIFS) of the Radiochemistry Group (Nuclear Physics Institute, University of Orsay, France). Laser spectrofluorimetry experiments were carried out at room temperature, using a tunable OPO Panther Continuum® laser as excitation source whose wavelength varies from 200 to 2000 nm. The detection was made by a Spectra-Pro-300 monochromator (Acton Research Corporation®) coupled with a CCD Camera (Princeton Instruments®). Emission spectra were recorded using the software WINSPEC (Princeton Instruments®). Lifetime values from the fluorescence decays have been obtained with the software IGOR®. The emission spectra of Tb^{3+} and Eu^{3+} were recorded by using an excitation wavelength of 487 nm.

2.2.2 Ion Coupled Plasma Mass Spectrometry (ICPMS)

Tb and Eu concentrations in the different solutions, before and after contact with $SrTiO_3$ samples, have been determined by using the experimental spectrometer PlasmaQuad Excell EX 129 (Thermo Electron®) of the Laboratory SUBATECH (Ecole des Mines, Nantes, France). Before their analysis, all the solutions were diluted in HNO_3 medium (2% volume) to obtain a concentration close to 10 ppb.

3. Results and discussion

3.1 Sorption of Tb^{3+} and Eu^{3+} onto $SrTiO_3$ surfaces

Sorption percentages of terbium and europium have been calculated from the ICP-MS concentrations in the liquid phase before and after contact with the solid.

As reported in the literature for different mineral surfaces [24-26], the sorption of Eu^{3+} and Tb^{3+} increases with pH. These results justify the choice of pH = 4 for energy transfer experiments as it corresponds to the maximal uptake of the ions (sorption percentage: around 30 %) by avoiding the formation of Tb^{3+} and Eu^{3+} precipitates in our experimental conditions.

3.2 Evidence of the energy transfer between Tb^{3+} and Eu^{3+} sorbed onto $SrTiO_3$ surfaces

On the Figure 1, the emission spectrum of Tb^{3+} sorbed onto $SrTiO_3$ (10^{-4} M) with an exciting wavelength of 487 nm (a) and the excitation spectrum of Eu^{3+} sorbed onto $SrTiO_3$ (10^{-4} M) by monitoring the luminescence of the transition ($^5D_0 \rightarrow {}^7F_4$) at 700 nm (b) are reported. As it can be seen on this figure and from that showing the energy levels diagrams of Tb^{3+} and Eu^{3+} (Figure 2), an energy transfer can be envisaged from Tb^{3+} to Eu^{3+} since Tb^{3+} luminescence bands $^5D_4 \rightarrow {}^7F_5$ and $^5D_4 \rightarrow {}^7F_4$ at respectively 540 and 580 nm overlap Eu^{3+} absorption bands $^7F_0 \rightarrow {}^5D_1$ (530 nm) and $^7F_0 \rightarrow {}^5D_0$ (around 580 nm).

Figure 3 shows different excitation spectra: that of Tb^{3+} obtained by monitoring the emission line $^5D_4 \rightarrow {}^7F_5$ at 544 nm for $SrTiO_3$ sorbed with Tb^{3+} 10^{-4} M (a), that of Eu^{3+} by following the fluorescence line $^5D_4 \rightarrow {}^7F_4$ at 700 nm (chosen to avoid spectral interferences with the Tb^{3+} emission lines) for $SrTiO_3$ sorbed with Eu^{3+} 10^{-4} M (b) and that of Eu^{3+} by following the fluorescence line $^5D_4 \rightarrow {}^7F_4$ at 700 nm for $SrTiO_3$ sorbed with Tb^{3+} 10^{-4} M / Eu^{3+} 10^{-4} M (c). The excitation spectrum of Tb^{3+} for $SrTiO_3$ only sorbed with Tb^{3+} (a) shows a single peak at 487 nm corresponding to the transition $^7F_6 \rightarrow {}^5D_4$ of Tb^{3+} whereas on the excitation spectrum of Eu^{3+} for $SrTiO_3$ sorbed with Eu^{3+} 10^{-4} M (b), three absorption lines of Eu^{3+} attributed to the transition bands from the ground state $^7F_0$ are observed : a major peak at 464 nm ($^7F_0 \rightarrow {}^5D_2$) and two minor peaks at 530 nm and at 580 nm (corresponding

respectively to the transitions $^7F_0 \rightarrow {}^5D_1$ and $^7F_0 \rightarrow {}^5D_0$). The excitation spectrum of Eu^{3+} for $SrTiO_3$ sorbed with Tb^{3+} 10^{-4} M / Eu^{3+} 10^{-4} M (c) displays the three absorption lines of Eu^{3+} at 464, 525 and 580 nm (also observed on figure b) and an additional peak at 487 nm corresponding to the absorption line of Tb^{3+} ($^7F_6 \rightarrow {}^5D_4$ transition), indicating clearly a resonant energy transfer from Tb^{3+} to Eu^{3+} ions.

Figure 4 shows the luminescence spectra at an excitation wavelength of 487 nm of Tb^{3+} to Eu^{3+} ions for a wavelength ranged from 440 to 610 nm: for only Tb^{3+}.
10^{-4} M sorbed onto $SrTiO_3$, for only $Eu^{3+}10^{-4}$ M sorbed onto $SrTiO_3$ and for Tb^{3+}/Eu^{3+} M sorbed onto $SrTiO_3$. For $SrTiO_3$ sorbed with the Tb^{3+}/Eu^{3+} mixture, an intensity decrease of the peaks assigned to Tb^{3+} (transitions $^5D_4 \rightarrow {}^7F_5$ and $^5D_4 \rightarrow {}^7F_4$ around 540 and 580 nm respectively) occurs simultaneously to a raise of the bands corresponding to Eu^{3+} transitions ($^5D_0 \rightarrow {}^7F_3$ at 651 nm and $^5D_0 \rightarrow {}^7F_4$ around 700 nm), relatively to the samples only sorbed with Tb^{3+} and Eu^{3+}. These results still suggest an energy transfer between Tb^{3+} and Eu^{3+} ions, all the more efficient as the acceptor ions Eu^{3+} concentration is high.

The logarithmic plot of the fluorescence decay profiles of Tb^{3+} ions obtained by monitoring the emission line at 544 nm for the samples only contacted with Tb^{3+} of 10^{-4} M concentration of and contacted with Tb^{3+}/Eu^{3+} mixtures for whose $[Tb^{3+}] = 10^{-4}$ M and $[Eu^{3+}]$ vary from 10^{-6} M to 10^{-2} M, is displayed on Figure 5. It is observed that the decay curves are affected by the presence of Eu^{3+} ions: when Eu^{3+} is introduced into the system, the fluorescence decay becomes faster than for Tb^{3+} alone and we observe, for short times, a deviation of the decay curve from the exponential law, indicating a non-radiative process between both ions [12, 27-30]. The more the acceptor ions Eu^{3+} concentration is high, the more this tendency is obvious.

Our results are in agreement with the literature, even if the studies connecting the decay curves of the donor ions and the possibility of a non-radiative energy transfer are relatively poor and not completely explained. The data of Balda *et al.* [29] showed a non-exponential behaviour and a shortening of the lifetime of Nd^{3+} ions in disordered potassium bismuth molybdate laser crystals co-doped with Nd^{3+}/Eu^{3+} if compared to the single doped crystals, because the additional probability for relaxation by non-radiative energy transfer to Yb^{3+} ions. The same observations have also been reported by Louis *et al.* [12]: these authors noticed that in $LiYF_4$ crystals doubly doped with Nd^{3+}/U^{3+}, the decay curves of Nd^{3+} are affected by the presence of U^{3+} ions, which indicates a non-radiative transfer process. Moreover, with the increase of the U^{3+} ions concentration, it has been observed a deviation, at short time, from the exponential law. From the same manner, W. Ryba-Romanowki *et al*. [28] observed the

same phenomenon in fluorindate glass singly doped with thulium and co-doped with Tm^{3+} and Tb^{3+} ions: terbium ions influence the decay curve feature of Tm^{3+} ions with a shortening of the lifetime of these latters and the deviation from the exponential law of the fluorescence decay. In the same way, Lin *et al.* [27] reported the effect of the presence or not of the acceptor ions Eu^{2+} and the concentration of these ions on the fluorescence decay curves of Ce^{3+} in co-doped Ce^{3+}/Eu^{2+} co-doped calcium magnesium chlorosilicates, such as a non-exponential behaviour, indicating a nonradiative energy transfer from Ce^{3+} to Eu^{2+} all the more efficient as the Eu^{2+} ions concentration is high.

By the time-dependent behaviour of the Tb^{3+} fluorescence in the doubly-contacted $SrTiO_3$, our results have shown the existence of a non-radiative energy process from Tb^{3+} to Eu^{3+}.

4. Application of the energy transfer process: determination of the distance between Tb^{3+} and Eu^{3+} ions sorbed onto $SrTiO_3$

4.1 Presentation of the formalism used for the calculations

The energy transfer between a donor D and an acceptor A has a double aspect: (1) the direct interaction between the donor (Tb^{3+}) and the acceptor (Eu^{3+}) and, (2) the energy migration between the Tb^{3+} ions. The typical decay profiles can be described as follows: for times $t<t^*$, the direct D→A energy transfer process dominates, while for $t>t^*$, the diffusion energy process dominates [1].

Tb^{3+} ions themselves have a small self-overlap and to see if there is any self-quenching effects due to the energy migration between these ions, the lifetimes of Tb^{3+} were measured for different systems: $SrTiO_3$ samples sorbed with Tb^{3+} aqueous solutions of concentrations of 10^{-5}, 10^{-4} and 10^{-3} M at pH 4 in 0.1 M $NaClO_4$ medium (table 1). For this Tb^{3+} concentration range corresponding to our energy transfer experiments, there is no evidence of a non-radiative Tb^{3+}→Tb^{3+} energy transfer as all the Tb^{3+} fluorescence decays can be fitted with two exponential functions giving the lifetimes (and the statistical dispersion on measurements in brackets) of: 110 (± 5) and 481 (± 25) µs. These calculated values of Tb^{3+} lifetimes are perfectly reliable as that we obtained for the lifetime of Tb^{3+} ions in aqueous solutions (in the absence of complexing reagents), adjusted to an ionic strength of 0.1 M with $NaClO_4$, is of 395 µs, in agreement with the values reported in the literature [31, 32], corresponding to fully coordinated Tb^{3+} ions in water, with nine coordination H_2O molecules.

Therefore, by assuming that the energy diffusion between Tb^{3+} ions is negligible in the concentration range studied, the following step of calculations consists in fitting the total

fluorescence decay curve of Tb^{3+} in presence of Eu^{3+}, for sorbed $SrTiO_3$ samples prior sorbed with Tb^{3+}/Eu^{3+} mixtures with different concentrations of Eu^{3+}, according to the Inokuti-Hirayama equation [33]:

$$I_t = I_0 \exp[-t/\tau_0 - At^{3/s}] \quad (1)$$

where I_0 is the fluorescence intensity of the donor at t = 0, τ_0 is the radiative lifetime of the donor in the absence of the acceptor, s traduces the nature of the multipolar interactions donor-acceptor and A is a function of the transfer constant C_{DA} (expressed in $cm^6.\mu s^{-6}$) as follows :

$$A = 4\pi/3\ \Gamma\ (1-3/s)\ N_A C_{DA}^{3/s} \quad (2)$$

where $\Gamma(1-3/s)$ is the Euler integral whose value is 1.77 for s = 6 (dipole-dipole interaction), 1.43 for s = 8 (dipole-quadrupole interaction) and 1.3 for s = 10 (quadrupole - quadrupole interaction), N_A is the number of acceptor ions per cm^3 onto the surface and C_{DA} (expressed in $cm^6.\mu s^{-6}$) is the transfer constant.

So, the fitting of the total fluorescence decay curve of Tb^{3+} in presence of Eu^{3+} to the Inokuti-Hirayama equation will allow one to determine the nature of the multipolar interaction between Tb^{3+} and Eu^{3+} ions and to obtain the value of the transfer constant C_{DA}. Before fitting the fluorescence decay, the number of Eu^{3+} ions (per cm^3) sorbed onto $SrTiO_3$ must be determined. The difference between the measured ICPMS concentrations (obtained in ppb) of Eu in aqueous solutions before and after contact with $SrTiO_3$ gave the quantity (in ppb) of Eu sorbed onto $SrTiO_3$ (table 2). The conversion of this quantity in atoms per cm^3 takes into account the specific surface area of $SrTiO_3$ determined by N_2-BET method (2.4 m^2/g), the mass of $SrTiO_3$ used for the sorption experiments (100 mg) and the assumed thickness of the sorbed layer constituted by Eu^{3+} ions sorbed onto $SrTiO_3$.

It is difficult to estimate the thickness of the adsorbed layer constituted by Tb^{3+} and Eu^{3+} sorbed onto $SrTiO_3$. Previous EXAFS studies concerning the sorption of cations whose Eu^{3+} onto different mineral matrices (phosphates and oxides) imply the formation of inner-sphere, mononuclear, bidentate surface complexes onto surfaces, showing two well-separated equatorial oxygen coordination shells around 2.3 and 2.5 Å [34-36]. Moreover, taking account the measured surface area (2.4 m^2/g), an average site density of 6 sites/nm^2 for $SrTiO_3$, an aqueous solution volume of 5 mL and a solid mass of 100 mg for sorption experiments, all samples were assumed to have a surface coverage of less than 100% of a sorbed monolayer.

So, taking account that the surface coverage by Tb^{3+} and Eu^{3+} is less than a sorbed monolayer and that the sorbed ions onto oxide surfaces forms inner-sphere, mononuclear, bidentate surface complexes, we can assume that the sorbed layer is close to 5 Å. In our calculations, the thickness of the adsorbed layer has been authorized to take values of 3, 5 and 10 Å.

As two radiative lifetimes of Tb^{3+} (109 and 482 µs) for $SrTiO_3$ samples sorbed with Tb^{3+} aqueous solutions of concentrations of 10^{-4} at pH 4 in 0.1 M $NaClO_4$ medium (table 1) have been determined for the studied system, the mathematic term developed in the equation (1), has been applied for each lifetime, which induces that the expression of the fluorescence decay is the sum of two terms, each term corresponding to each radiative lifetime of Tb^{3+}. So, for each calculation used in this study, the developed formalism given for an unique fluorescence lifetime of the donor ions, has been applied for two lifetimes of Tb^{3+}.

The experimental curves are impossible to be fitted by considering dipole-quadrupole and quadrupole-quadrupole interactions between Tb^{3+} and Eu^{3+} ions. The best agreement between the experimental decay and the theoretical expression of the decay is obtained for a dipole-dipole interaction. These results are in agreement with the literature as it has been demonstrated that the dominant non-radiative energy transfer between rare-earth ions is found to be electric dipole-dipole interaction [12, 27, 29, 37]. As the interaction between Tb^{3+} and Eu^{3+} ions is a dipole-dipole type, the equation (1) simplifies as follows:

$$I_t = I_0 \exp[-t/\tau_0 - At^{3/6}] \qquad (3)$$

with:

$$A = 4\pi/3\ 1.77\ N_A C_{DA}^{1/2} \qquad (4)$$

The experimental radiative decay times of Tb^{3+} in the absence of Eu^{3+} ions, Γ=1.77 (because s = 6) and the concentrations of Eu^{3+} extracted from ICP-MS measurements (table 2) permit to obtain the best agreement between the experimental decay and the theoretical expression for all the systems Tb^{3+}/Eu^{3+} with a same value of C_{DA} = $3.23*10^{-48}$ $cm^{-6}.\mu s^{-1}$, according to the equation (3). In our calculations, the thickness of the adsorbed layer has been authorized to take values of 3, 5 and 10 Å which induces a same value of C_{DA} of $3.23\ 10^{-48}$ $cm^6.\ \mu s^{-6}$.

In the following text, a brief summary of theories of Dexter [38] and of Inokuti and Hirayama [33] and detailed in references [39, 40] is given to show the formalism adopted to determine the distance between a donor and an acceptor ions when a non radiative energy transfer occurs between these two ions.

So, for electric multipole interaction between a donor and an acceptor, the energy transfer probability P_{DA} is given by:

$$P_{DA}(R) = C_{DA}R^{-s} \quad (5)$$

where C_{DA} is the transfer constant between D and A, s traduces the nature of multipole interactions between D and A and R is the separation between the donor and the acceptor.

A critical distance R_0 and a critical concentration C_0 are defined as follows:

$$P_{DA}(R_0) = 1/\tau_0 \quad (6)$$

$$C_0 = (3/4\pi)\, R_0^{-3} = (3/4\pi)\, (\tau_0 C_{DA})^{-3/s} \quad (7)$$

C_0 corresponds to a situation for which another ion than the donor ion is localized in a sphere of influence of radius R_0 in which the donor ion is surrounded by the acceptor ions.

So, from the value of the C_{DA} microparameter extracted from the best agreement between the experimental decay and the theoretical expression for all the $SrTiO_3$ samples doubly sorbed with Tb^{3+}/Eu^{3+}, such as $3.23.10^{-48}$ $cm^6.\ \mu s^{-1}$ and by choosing one of the two independent lifetimes of the intrinsic Tb^{3+} lifetimes (109 ± 11 μs or 482 ± 48 μs), we can calculate the value of the critical concentration $C_0 = 1.24.10^{22}$ $/cm^3$ (by the choice of 109 μs for the Tb^{3+} lifetime) and $C_0 = 6.03.10^{21}$ $/cm^3$ (by the choice of 482 μs for the Tb^{3+} lifetime), we obtain the two values of the radius R of the sphere of influence of 2.7 and 3.4 Å for the two lifetimes 109 and 482 μs respectively. We report on Table 5 the values of R calculated in this work for the energy transfer from Tb^{3+} to Eu^{3+} sorbed onto $SrTiO_3$ and the comparison to the other values obtained from the literature for interactions between lanthanide ions such as $Pr^{3+} \rightarrow Nd^{3+}$, $Er^{3+} \rightarrow Er^{3+}$ and $Nd^{3+} \rightarrow Yb^{3+}$ in co-doped solids as LaF_3 and $LiLaP_4O_{12}$. Even if the data reported concern co-doped solids, it appears that our values are similar to those obtained for other donor-acceptor lanthanide ions.

Conclusion

This paper studied the energy transfer, at room temperature, between Tb^{3+} and Eu^{3+} ions sorbed onto $SrTiO_3$ by using TRLIFS. A non-radiative energy transfer from Tb^{3+} to Eu^{3+} has been evidenced with an interaction of dipole-dipole type between the donor and acceptor ions. Moreover, the more the acceptor ions Eu^{3+} concentration is high, the more the energy transfer is efficient.

The energy transfer is all the more efficient as the acceptor concentration is high. This study is particularly innovating as in the literature no publication reports the energy transfer between ions adsorbed onto mineral surfaces. These results have permitted to calculate distances between Tb^{3+} and Eu^{3+} ions sorbed onto $SrTiO_3$ powders. As we proved that there is no energy migration between the Tb^{3+} donor ions, the Inokuti-Hirayama model, taking into account the energy transfer between a donor and an acceptor ion, has allowed to fit the decay curves of Tb^{3+} and consequently to access to the distance (close to 3 Å) between Tb^{3+} and Eu^{3+} sorbed onto $SrTiO_3$. The calculated distances are similar to those obtained for other couples of donor-acceptor lanthanide ions reported in the literature.

In the following of this study, the same approach will be applied to $SrTiO_3$ single crystals sorbed with $Tb^{3+} \rightarrow Eu^{3+}$ which will permit one both to confront the distances between $Tb^{3+}$and Eu^{3+} ions obtained from energy transfer experiments with the perfectly known crystallographic structures of $SrTiO_3$. These results could be directly correlated with theoretical calculations to access to the interactions mechanisms between ions and solid surfaces.

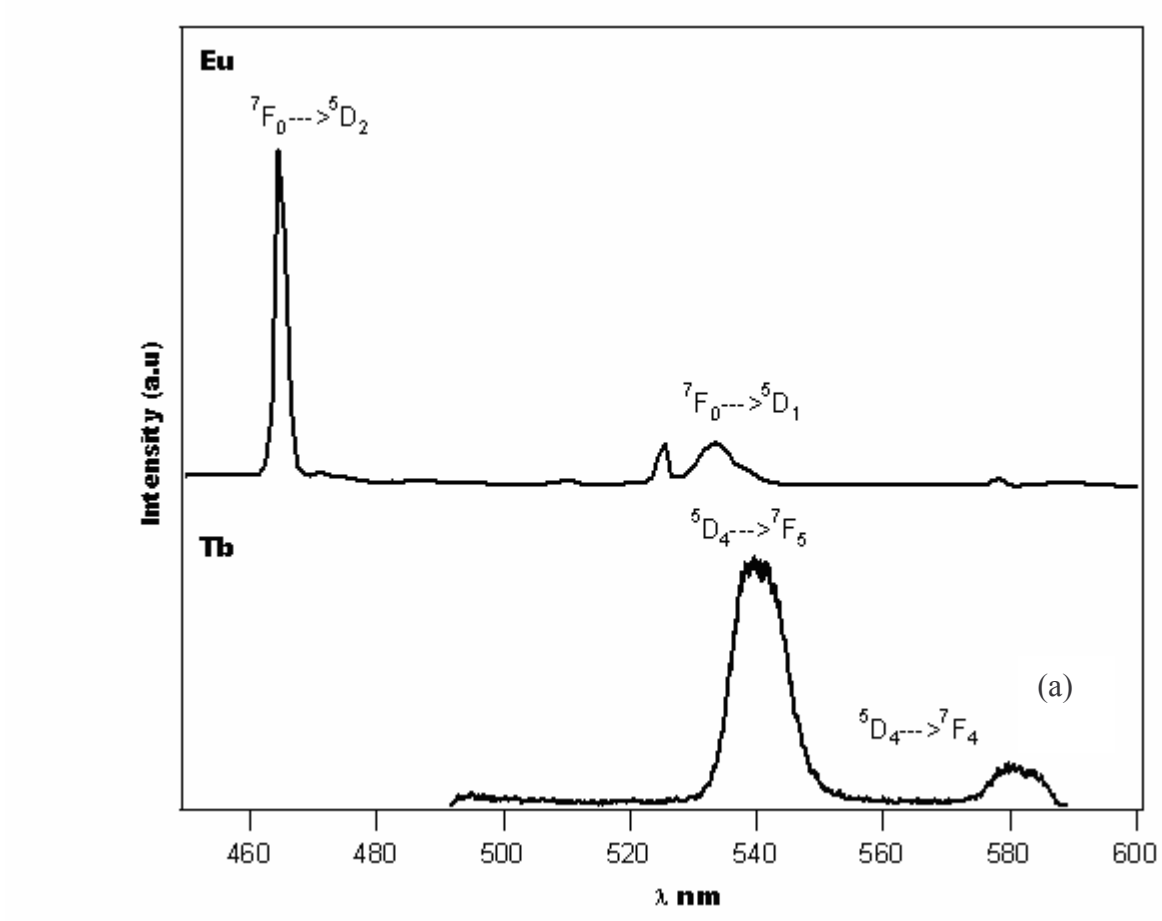


Fig. 1: (a) Emission spectrum at 25°C of Tb^{3+} sorbed onto $SrTiO_3$ (10^{-4} M) under 487 nm excitation; (b) excitation spectrum of Eu^{3+} sorbed onto $SrTiO_3$ (10^{-4} M) by monitoring the transition $^5D_0 \rightarrow {}^7F_4$ of Eu^{3+} at 700 nm. The spectra correspond to 1000 accumulations.

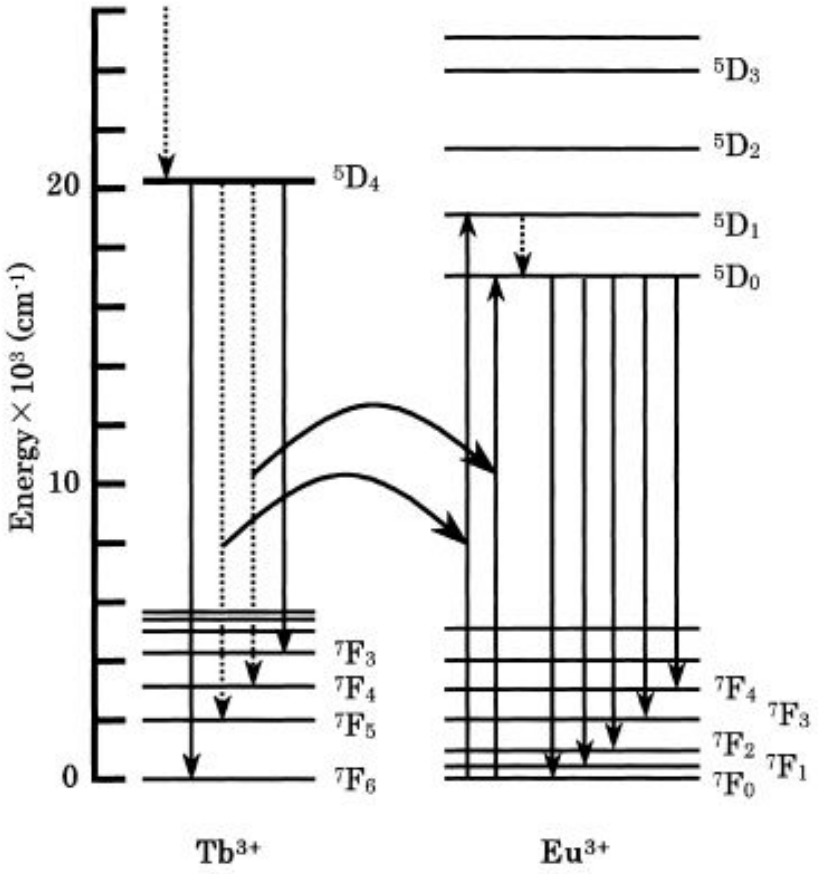


Fig. 2: Energy level diagrams of Tb^{3+} and Eu^{3+} ions (from reference [22]).

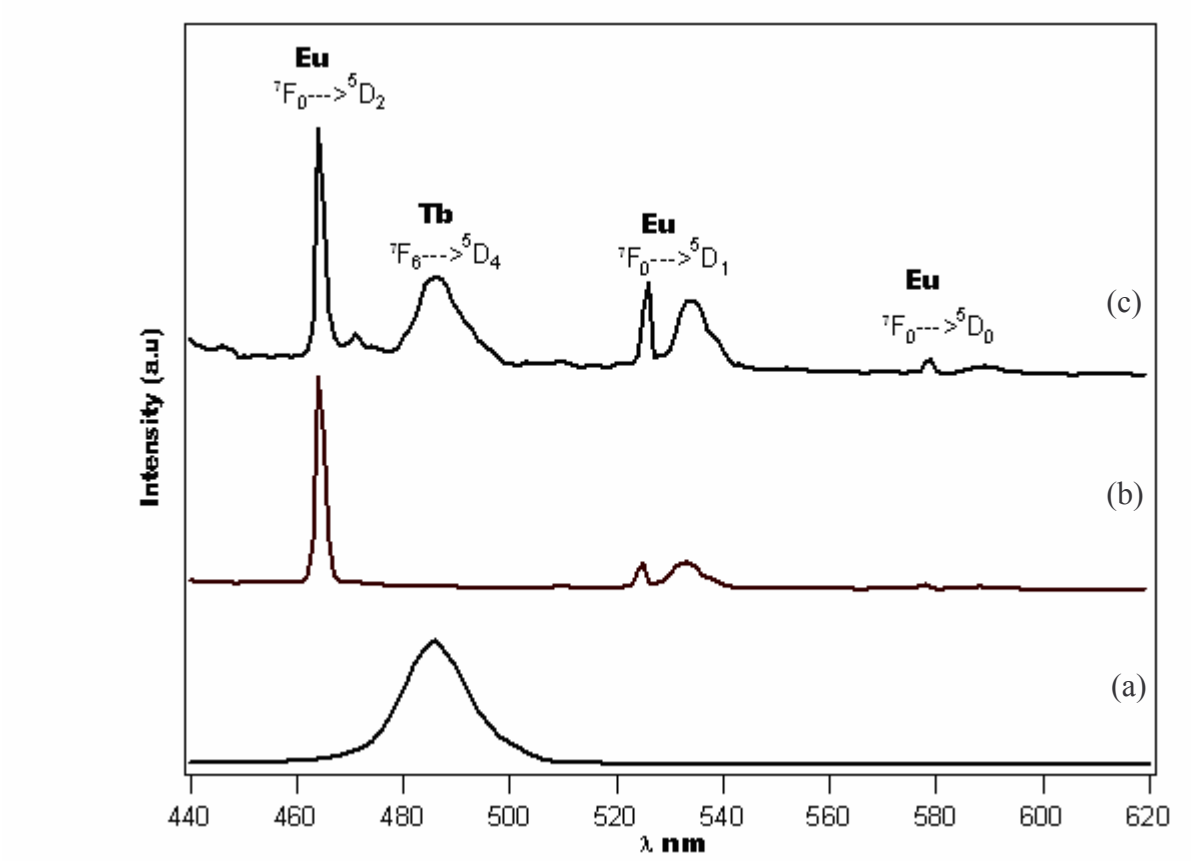


Fig. 3: Comparison of different excitation spectra: (a) that of Tb^{3+} (by monitoring the emission line $^5D_4 \rightarrow {}^7F_5$ of Tb^{3+} at 544 nm) for $SrTiO_3$ sorbed with Tb^{3+} 10^{-4} M; that of Eu^{3+} (by monitoring the emission line $^5D_4 \rightarrow {}^7F_4$ of Eu^{3+} at 700 nm) for $SrTiO_3$ sorbed with Eu^{3+} 10^{-4} M; (c) that of Eu^{3+} (by monitoring the emission line $^5D_4 \rightarrow {}^7F_4$ of Eu^{3+} at 700 nm) for $SrTiO_3$ sorbed with the mixture Tb^{3+} 10^{-4} M / Eu^{3+} 10^{-4} M.

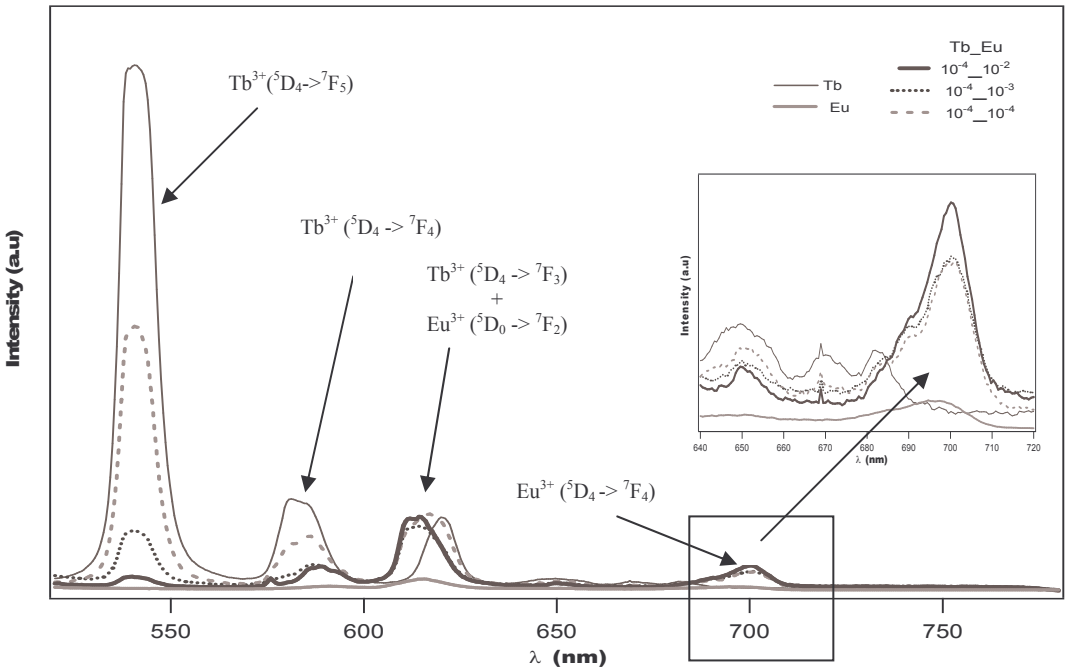


Fig. 4: Luminescence spectra at 25°C (at an excitation wavelength of 487 nm) for only Tb^{3+} sorbed onto $SrTiO_3$, for only Eu^{3+} sorbed onto $SrTiO_3$ and for Tb^{3+}/Eu^{3+} sorbed onto $SrTiO_3$.

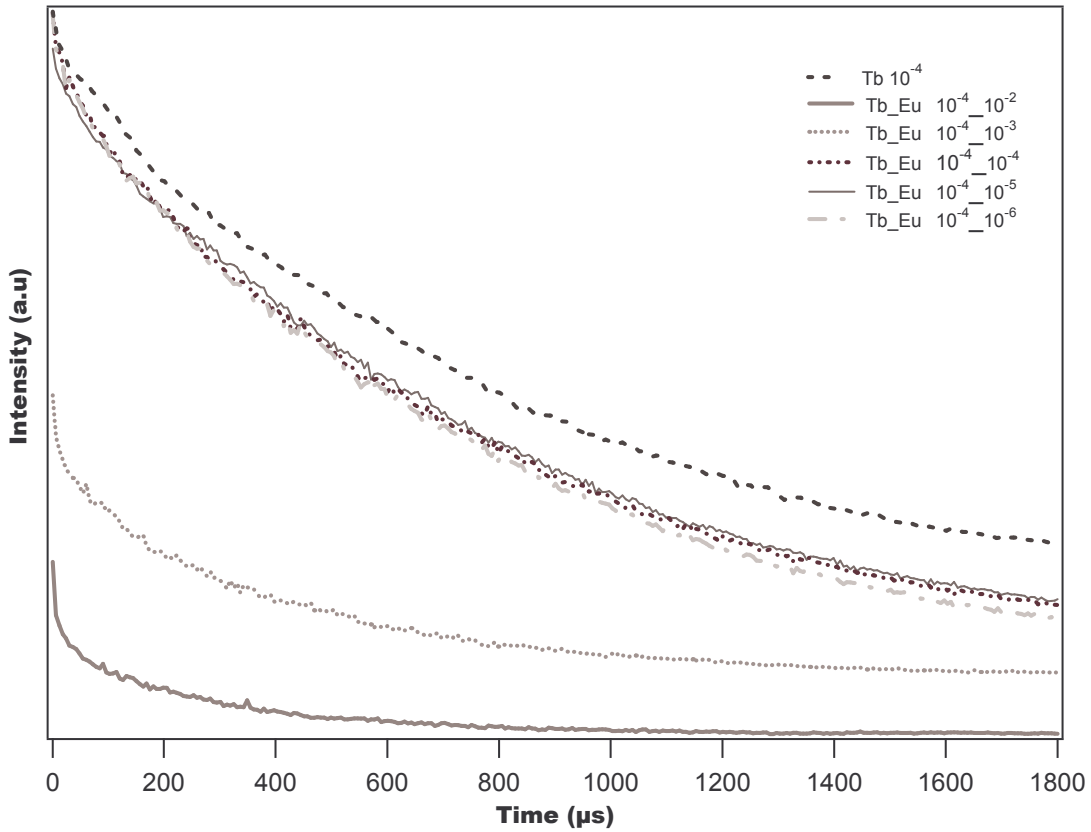


Fig. 5: Logarithmic plot of the fluorescence decay of Tb^{3+} ions at room temperature for different systems: for $SrTiO_3$ only sorbed with Tb^{3+} and for $SrTiO_3$ sorbed with Tb^{3+} 10^{-4} M /Eu^{3+} mixtures ([Eu^{3+}] from 10^{-6} M to 10^{-2} M) by monitoring the emission line $^5D_4 \rightarrow {}^7F_5$ of Tb^{3+} at 544 nm. The excitation wavelength is of 487 nm.

Table 1: Lifetimes of Tb^{3+} ions (by monitoring the fluorescence at 544 nm) in $SrTiO_3$ only contacted with Tb^{3+} at different aqueous concentrations and at pH = 4 in $NaClO_4$ 0.1 M

Tb^{3+} concentration (M)	τ_1 (µs)	τ_2(µs)
10^{-3}	116 ± 16	506 ± 50
10^{-4}	109 ± 11	482 ± 48
10^{-5}	106 ± 10	456 ± 45

Table 2: Number of acceptor ions Eu^{3+} sorbed onto $SrTiO_3$ (in atoms per cm^3) obtained from ICPMS measurements.

$SrTiO_3$ doubly sorbed with Tb^{3+}/Eu^{3+} at pH = 4 in $NaClO_4$ 0.1 M	$N_{Eu}{}^{3+}$
10^{-4}_10^{-2} M	$2.23 \cdot 10^{22}$
10^{-4}_10^{-3} M	$3.96 \cdot 10^{21}$
10^{-4}_10^{-4} M	$3.17 \cdot 10^{20}$
10^{-4}_10^{-5} M	$6.0 \cdot 10^{19}$
10^{-4}_10^{-6} M	$2.09 \cdot 10^{18}$

Table 3: Values of R calculated in this work for the energy transfer from Tb^{3+} to Eu^{3+} sorbed onto $SrTiO_3$ and comparison to the other values obtained from the literature for interactions between lanthanide ions such as $Pr^{3+} \rightarrow Nd^{3+}$, $Er^{3+} \rightarrow Er^{3+}$ and $Nd^{3+} \rightarrow Yb^{3+}$ in co-doped solids as LaF_3 and $LiLaP_4O_{12}$

System	Radius of the sphere of influence (in Å)
$LaF_3 \rightarrow Er^{3+} \rightarrow Er^{3+}$	3.7
$LiLaP_4O_{12} : Nd^{3+} \rightarrow Yb^{3+}$	5.8
$SrTiO_3 : Tb^{3+} \rightarrow Eu^{3+}$	2.7-3.4

References

[1] B. Di Bartolo, G. Armagan, M. Buoncristiani *Opt. Mater.* 4 (1994) 11.

[2] T. Heyduk *Curr. Opin. Biotechnol.* 13 (2002) 292.

[3] E. Soini, T. Lovgren *Crit. Rev. Anal. Chem.* 18 (1987) 105.

[4] E. Soini, I. Hemmilä *Clin. Chem.* 25 (1979) 353.

[5] E.A. Seregina, A.A. Seregin, G.V. Tikhonov *J. Alloys Compounds* 341 (2002) 283.

[6] J. Kropp *J. Chem. Phys.* 46 (1967) 843.

[7] S.P. Tanner, A.P. Vargenas *Inorg. Chem.* 20 (1981) 4384.

[8] G.M. Gaevoy, M.E. Zhabotinskiy, Y.I. Krasilov, Y.I. Rudnitskiy, G.V. Ellert, V.A. Kuzel. *Neorg. Mater.* 5 (1969) 691.

[9] A.V. Stepanov, S.A. Nikitin, N.I. Golovkina *Radiohkimiya* 6 (1993) 36.

[10] S. Dai, W. Xu, D.H. Metcalf, L.M. Toth *Chem. Phys. Lett.* 262 (1996)315.

[11] B.C. Joshi, R. Lohani, B. Pande *J. Non-cryst. Solids* 337 (2004) 97.

[12] M. Louis, S. Hubert, E. Simoni, J.Y. Gesland *Opt. Mater.* 6 (1996) 121.

[13] B.C. Joshi, R. Lohani *J. Non-cryst. Solids.* 215 (1997) 103.

[14] H. W. Kui, D. Lo, Y.C. Tsang, N.M. Khaidukov, V.N. Makhov *J. Lumin.* 117 (2006) 29.

[15] J. Cybinska, J. Legendziewicz, G. Boulon, A. Bensalah, G. Meyer *Opt. Mater.* 28 (2006) 41.

[16] W.W. Holloway, M. Kestigian, R. Newman *Phys. Rev. Lett.* 11 (1963) 458.

[17] W. Chen, R. Sammynaiken, Y. Huang *J. Appl. Phys.* 88 (2000) 1424.

[18] S.H. Park, S.I. Mho, K.W. Lee *Bull. Korean Chem. Soc.* 17 (1996)487.

[19] T. Kim Anh, T. Ngoc, P. Thu Nga, V.T. Bich, P. Long, W. Strek *J. Lumin.* 39 (1988) 215.

[20] A. Moadhen, H. Elhouichet, B. Canut, C.S. Sandu, M. Oueslati, J.A. Roger *J. Mater. Sci. Eng. B* 105 (2003) 157.

[21] T. Ishizaka, R. Nozaki, Y. Kurokawa *J. Phys. Chem. Solids* 63 (2002) 613.

[22] G. Schierning, M. Batentschuk, A. Osvet, A. Winnacker *Radiat. Meas.* 38 (2004) 529.

[23] H. Yamamoto, S. Okamoto, H. Kobayashi *J. Lumin.* 100 (2002) 325.

[24] H. Catalette, J. Dumonceau, P. Ollar *J. Contamin. Hydrol.* 35 (1998) 151.

[25] D. Wenming, W. Xiangke, B. Xiaoyan, W. Aixia, D. Jingzhou, Z. Tao *Appl. Radiat. Isot.* 54 (2001) 603.

[26] T. Rabung, H. Geckeis, J. Kim, H.P. Beck *J. Colloid Interface Sci.* 208 (1998)153.

[27] H. Lin, X.R. Liu, E.Y.B. Pun *Opt. Mater.* 18 (2002) 397.

[28] W. Ryba-Romanowski, S. Golab, G. Dominiak-Dzik, M. Zelechower, J. Gabrys-Pisarska. *J. Alloys Compound* 325 (2001) 215.

[29] R. Balda, J. Fernandez, I. Iparraguirre, M. Al-Saleh *Opt. Mater.* 28 (2006) 1247.

[30] A. Rodenas, D. Jaque, J. Garcia Sole, A. Speghini, M. Bettinelli, E. Cavalli *Opt. Mater.* 28 (2006) 1280.

[31] S. Lis, T. Kimura, Z. Yoshida *J. Alloys Compound* 323-324 (2001) 125.

[32] N. Arnaud, J. Georges *Spectrochim. Acta A* 59 (2003) 1829.

[33] M. Inokuti, F. Hirayama *J. Chem. Phys.* 43 (1965)1978.

[34] T. Reich, H. Moll, T. Arnold, M.A. Denecke, C. Hennig, G. Geipel, G. Bernhard, H. Nitsche, P.G. Allen, N.M. Edelstein, D.K. Shuh *J. Elec. Spec. & Rel. Phen.* 96 (1998)237.

[35] E.R. Sylwester, E.A. Hudson, P.G. Allen *Geochim. Cosmochim. Acta* 64 (2000) 2431.

[36] R. Drot, Sorption des ions U(VI) et Eu(III) à l'interface solution-solides phosphatés : étude structurale et mécanismes, PhD Thesis, Université Paris-Sud-11, Orsay, France (1998).

[37] U.R. Rodriguez-Mendoza, V.D. Rodriguez, I.R. Martin, V. Lavin, J. Mendez-Ramos, P. Nunez. *J. Alloys Compound* 323-324 (2001) 759.

[38] D.L. Dexter *J. Chem. Phys.* 21 (1953) 836.

[39] J. Ferguson, H. Masui *J. Phys. Soc. Jpn.* 42 (1977)1640.

[40] J.M. Breteau, Etude de matériaux dopés Ni^{2+} et Co^{2+} pour laser accordable à fonctionnement continu dans le proche infrarouge, PhD Thesis, Université Paris VI, France (1986).

RESUME DU CHAPITRE III

Dans ce chapitre, a été présentée une étude sur les transferts d'énergie non radiatifs entre deux ions lanthanides sorbés sue le solide $SrTiO_3$, afin d'obtenir une évaluation de la distance entre deux ions métalliques sorbés sur la surface d'un minéral.

Trois systèmes ont été testés initialement (UO_2^{2+} → Eu^3, Sm^{3+}, Er^{3+}). Cependant, les résultats (spectres de fluorescence et de temps de vie) ont montré l'impossibilité d'appliquer les théories de Förster et Dexter pour le calcul de la sphère d'interaction entre les ions (superposition des déclins de fluorescence entre les différents systèmes). Ainsi, dans ce chapitre, le transfert d'énergie entre des ions Tb^{3+} et Eu^{3+} sorbés sur la surface de $SrTiO_3$, a été étudié. Les résultats ont montré que le transfert d'énergie de l'ion Tb^{3+} vers l'ion Eu^{3+} s'effectue selon un processus non radiatif et que l'interaction entre ces deux ions est de nature dipôle-dipôle. L'application du modèle de Förster et Inokuti-Hirayama a conduit à l'évaluation du rayon de la sphère d'interaction (2,7–3,4 Å) entre les deux ions (Tb^{3+} et Eu^{3+}) sorbés sur $SrTiO_3$ et la confirmation de la présence de complexes de surface isolés.

CONCLUSION GENERALE

CONCLUSION GENERALE

Dans le cadre du stockage de déchets radioactifs en formation géologique profonde, la stabilité à long terme d'un colis de déchets nucléaires dépend principalement de la capacité de différentes barrières géologiques à retenir des éléments radioactifs qui peuvent être accidentellement relâchés dans l'environnement, en cas d'infiltration d'eaux souterraines. Le principal facteur pouvant retarder la migration des radionucléides dans l'environnement est leur sorption sur des surfaces minérales. Ainsi, pour prédire la mobilité des radionucléides, il est indispensable de comprendre leurs mécanismes d'interaction avec ces surfaces minérales. L'objectif de ce travail était l'étude, en fonction de la température (25-90°C), des mécanismes d'interaction entre l'ion U(VI) et le titane de strontium $SrTiO_3$.

Tout d'abord, nous avons présenté les caractéristiques physico-chimiques du composé $SrTiO_3$, et l'interaction de la surface du solide avec les molécules d'eau, pendant le processus d'hydratation de la surface. La poudre de $SrTiO_3$ a été caractérisée par différentes techniques telles que DRX et MEB, ce qui a permis de contrôler la pureté et le degré de cristallinité du substrat mais aussi de connaître sa morphologie, sa granulométrie et sa surface spécifique (BET). De plus, des études préliminaires de dissolution ont montré une faible solubilité du matériau sur toute la gamme de pH étudiée. Deux sites de surface ont été définis par spectroscopie XPS : $\equiv Ti-OH$ et $\equiv Sr-OH$, en supposant que le mécanisme d'interaction entre la molécule d'eau et la surface est de type dissociatif.

Suite à ces études, les propriétés acido-basiques du substrat ont été déterminées aux différentes températures, à partir de titrages potentiométriques pour des températures variant de 25 à 90°C. La détermination de la densité de sites de surface a été réalisée à partir de ces titrages (25-90°C). La valeur obtenue (6 sites/nm^2) n'a présenté aucune variation avec l'augmentation de la température. L'acquisition des courbes de dosages potentiométriques et l'ensemble de tous les résultats obtenus à partir de la caractérisation physico-chimique ont servi à simuler les données expérimentales à l'aide du code FITEQL et à déterminer ainsi les constantes acido-basiques en fonction de la température (modèle à 1pK et à capacitance constante CCM). Les résultats ont montré une évolution des constantes de protonation et de déprotonation : la protonation du site $\equiv Sr-OH$ suit un processus endothermique tandis que la déprotonation du site $\equiv Ti-OH$ est quant à elle exothermique. Avec les constantes d'acidité obtenues à partir de la modélisation, les variations d'enthalpie et d'entropie associées aux réactions ont été déterminées à partir de la relation de van't Hoff.

La deuxième partie de ce mémoire a été consacrée aux études de sorption de U(VI) sur $SrTiO_3$. Les sauts de sorption des ions uranyle sur la surface du solide en fonction de la température, ont mis en évidence une nette augmentation du pourcentage de rétention des ions avec l'augmentation de la température. Des échantillons sorbés préparés à pH $\leq$ 4 ont été étudiés par SLRT. L'obtention de deux valeurs de temps de vie (12 ± 2 et 60 ±5 μs) constantes pour tous les systèmes étudiés, indique clairement la formation de deux espèces sorbées à la surface du substrat, où seul l'ion uranyle est susceptible de se sorber, dans les conditions de pH étudiées, sur les sites $\equiv Ti-OH$ et $\equiv Sr-OH$. De plus, considérant les données bibliographiques portant sur la sorption des ions uranyle sur d'autres oxydes, nous avons considéré la formation de complexes de sphère interne, mononucléaires bidentates.

De cette manière, l'information obtenue dans cette première partie nous a permis d'établir, sur des bases expérimentales, les équilibres de sorption mis en jeu lors du processus de rétention. Les sauts de sorption ont été simulés en considérant le modèle de la capacitance constante (CCM) ainsi que les données acquises pendant la modélisation des titrages potentiométriques à différentes températures. La meilleure simulation a été obtenue en considérant la formation de deux complexes : $\left[(\equiv SrOH)(\equiv TiOH)UO_2\right]^{2+}$ qui ne s'accompagne pas de libération de protons et $\left[(\equiv TiOH)(\equiv TiO)UO_2\right]^{2+}$ qui implique la libération d'un seul proton. La constante de formation du premier complexe augmente avec la température alors que la stabilité du second complexe décroit lorsque la température augmente, induisant une modification des proportions relatives des deux complexes de surface à un pH donné lorsque la température augmente. A l'aide de la relation de van't Hoff, les variations d'enthalpie et d'entropie ont été également quantifiées. Pour la formation des deux espèces de surface, une augmentation de l'entropie du système a été obtenue, probablement en raison de la perte d'une partie de la sphère d'hydratation du cation.

Finalement, la dernière partie de ce mémoire consacrée à l'étude des transferts d'énergie entre les ions lanthanides ($Tb^{3+} \rightarrow Eu^{3+}$) par SLRTIF nous a permis d'accéder au rayon de la sphère d'interaction entre les deux ions sorbés, à partir de l'application des modèles de Inokuti-Hirayama et Dexter. Le rayon de la sphère d'influence a été trouvé entre 2,7 et 3,4 Å. De plus, l'ensemble des temps de vie mesurés rend bien compte de la présence de deux complexes de surface. Préalablement à l'étude des transferts d'énergie entre les deux ions lanthanides, trois systèmes $U(VI) \rightarrow Ln^{3+}$: $UO_2^{2+} \rightarrow Eu^{3+}$, Er^{3+} et Sm^{3+} ont été testés. Cependant, les résultats obtenus ont montré une superposition des déclins de fluorescence

pour les différents systèmes avec le déclin de fluorescence du donneur seul ne permettant pas le calcul de la sphère d'interaction entre ces ions puisqu'il n'y a pas de transfert non radiatif entre le donneur et l'accepteur. C'est la raison pour laquelle notre étude sur le transfert d'énergie s'est focalisée sur le choix du système $Tb^{3+} \rightarrow Eu^{3+}$.

Les résultats obtenus lors de l'étude de l'interaction des ions sorbés à la surface de $SrTiO_3$ en fonction de la température, nous ont permis de déterminer certains paramètres thermodynamiques tels que l'enthalpie et l'entropie pour le système $SrTiO_3/UO_2^{2+}$. Cependant, l'utilisation de la relation de van't Hoff nécessite de connaître l'évolution des valeurs des constantes d'équilibre en fonction de la température, qui sont, elles, déterminées à l'aide de modèles faisant intervenir plus au moins de paramètres ajustables. Il serait donc certainement très intéressant et utile de pouvoir comparer ces résultats avec ceux obtenus à l'aide de mesures plus directes comme des mesures microcalorimétriques. Cette technique permettrait en effet d'accéder directement aux chaleurs mises en jeu lors des processus d'hydratation et de rétention. De plus, cela pourrait conduire éventuellement, en cas de fort désaccord, à un réexamen non seulement des valeurs des constantes, mais également du modèle employé pour la description de l'interface solide/solution et la détermination de ces constantes.

L'étude des transferts d'énergie non-radiatifs, sur des échantillons pulvérulents, pourrait être complétée par des investigations analogues sur des faces monocristallines, pour lesquelles l'agencement cristallographique des atomes de surface est parfaitement connu. Cela mènerait probablement à une description plus précise de la répartition des complexes métalliques sorbés à la surface du substrat. Cette information à l'échelle moléculaire serait certainement utilisable pour des futures études de chimie quantique sur la stabilité de ces systèmes surfaciques.

ANNEXE

DESCRIPTION DE L'AUTOCLAVE

Le dispositif expérimental « autoclave » utilisé pour les expériences de titrages potentiométriques en température (25 - 90°C) est composé de deux parties : La partie basse, séparée par un dispositif de filtration composé d'une grille servant de support au filtre, toutes les parties en contact avec la solution ou la suspension sont en téflon. La partie haute, où se déroule la réaction, est entourée d'un ruban chauffant et comprend un bol en téflon amovible. Un piston coulissant traverse le centre du bol : maintenu en position basse par un ressort, il ferme hermétiquement le bol. La filtration est réalisée en tirant sur le piston et en admettant une surpression de gaz argon en partie haute. Le filtrat es récupéré en partie basse, par pipetage de la solution. Parallèlement, le solide est récupéré sur le filtre (Whatman, acétate de cellulose, d=25mm, porosité= 0,2 µm). La mise en suspension est assurée par une table agitante. L'utilisation d'une électrode combinée à l'électrolyte solide et double jonction téflon Fisher Bioblock® N54535 permet la mesure du pH *in situ* en température.

Le contrôle de la température est assuré par un thermocouple situé dans le ruban chauffant au niveau du filtre. Un système de commande de régulation PID (Proportionnel, Intégré, Dérivé) permet de maintenir le milieu réactionnel à la température de consigne. En accord avec les tests réalisés, une heure est nécessaire pour atteindre la température de consigne. L'autoclave utilisé permet d'atteindre des conditions de température et de pression supérieures à 200 °C et 10 bars.

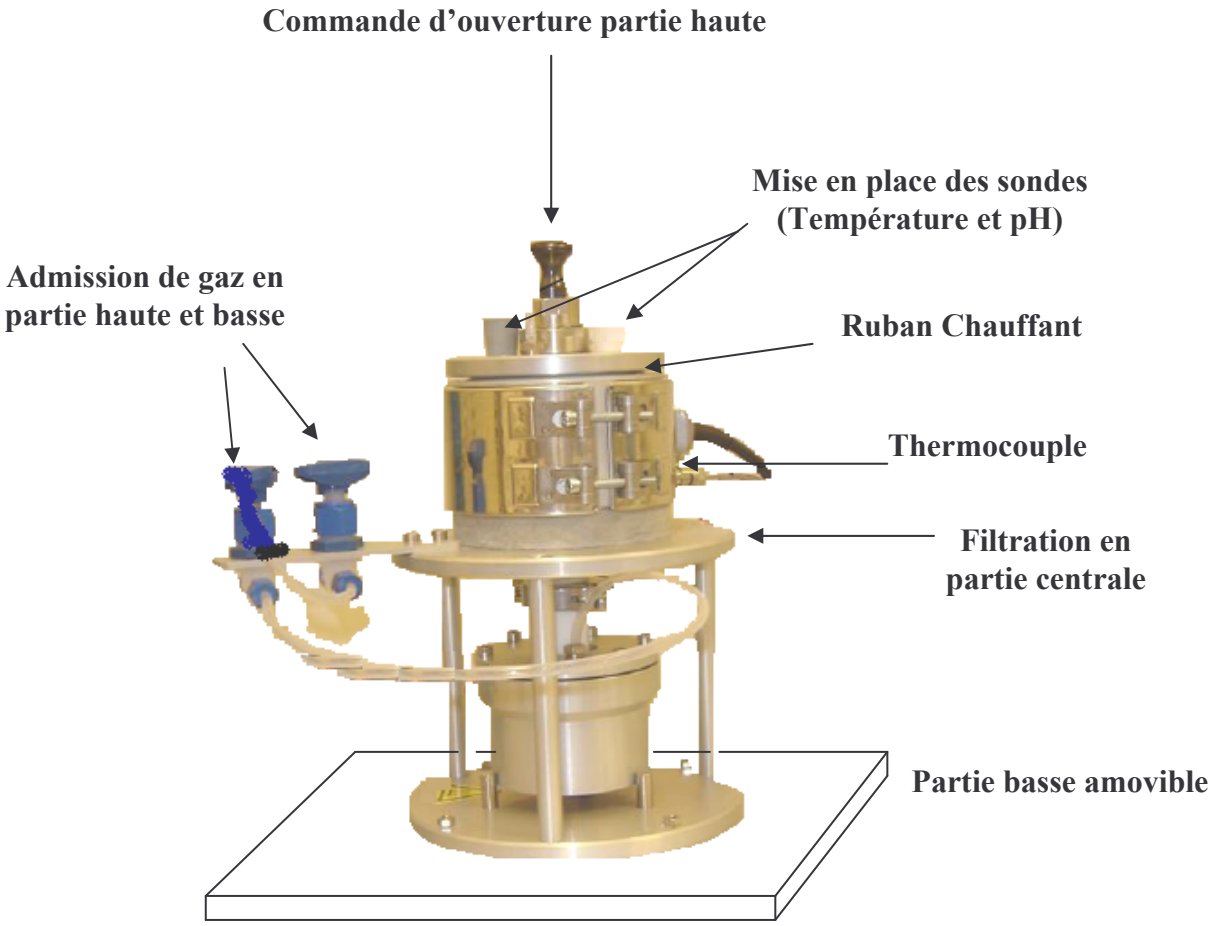


Fig. 1 : Dispositif expérimental (autoclave) permettant de réaliser les expériences de titrage et de sorption en température.

RESUME GENERALE

L'étude des mécanismes de sorption de l'ion uranyle sur le substrat $SrTiO_3$ en fonction de la température a fait l'objet de cette étude. Tout d'abord, une caractérisation physico-chimique a été réalisée à l'aide de plusieurs techniques structurales (DRX, FTIR) et morphologique (MEB). La spectroscopie XPS a permis d'identifier deux sites de surface (Ti-OH et Sr-OH). En utilisant les titrages potentiométriques de $SrTiO_3$ à différentes températures, les caractéristiques acido-basiques ont été déterminées. Ensuite, la simulation des titrages potentiométriques, entre 25 et 90°C, a été réalisée à l'aide du code FITEQL, les constantes d'équilibre ainsi obtenues montrent une nette variation avec la température : la protonation du site $\equiv Sr-OH$ suit un processus endothermique tandis que la déprotonation du site $\equiv Ti-OH$ implique un processus exothermique. A partir de ces constantes d'équilibre, les grandeurs thermodynamiques, enthalpie et entropie de protonation/déprotonation ont été calculées en utilisant la relation de van't Hoff.

Les études de sorption de l'ion uranyle sur le substrat $SrTiO_3$ ont été réalisées dans un intervalle de pH de 0.5 à 5. Les sauts de sorption ainsi obtenus montrent une nette augmentation du pourcentage de sorption avec l'augmentation de la température, traduisant un phénomène globalement endothermique. Deux sites de sorption différents ont été identifiés à la surface du solide par SLRTIF. Ils sont associés aux temps de vie de fluorescence de l'uranyle sorbé de 12 ± 2 et 60 ± 5 μs. Les sauts de sorption ont été modélisés à l'aide du code FITEQL en utilisant le modèle à capacitance constante. Cette simulation des sauts de sorption a été réalisée en tenant compte des résultats de l'étude structurale (deux sites de surface $\equiv Ti-OH$ et $\equiv Sr-OH$ et formation de complexe surfacique de sphère interne bidentate, mononucléaire) et des données obtenues dans la modélisation des titrages potentiométriques. Les équilibres de sorption modélisés ont confirmé la formation de deux complexes de surface de caractère bidentate : $\left[(\equiv SrOH)(\equiv TiOH)UO_2\right]^{2+}$ et $\left[(\equiv TiOH)(\equiv TiO)UO_2\right]^{2+}$. Suite à l'obtention des constantes thermodynamiques obtenues par cette simulation, la relation van't Hoff a été appliquée pour déterminer les variations d'enthalpie et d'entropie associées au processus de sorption.

Finalement, une étude sur les transferts d'énergie a été présentée entre deux ions sorbés sur le solide $SrTiO_3$. Ainsi, le transfert d'énergie non-radiatif des ions Tb^{3+} vers les ions Eu^{3+} a été étudié. L'application du modèle de Inokuti-Hirayama et Dexter a conduit à l'évaluation du rayon de la sphère d'interaction (2,7–3,4 Å) entre les deux ions (Tb^{3+}et Eu^{3+}) sorbés sur $SrTiO_3$ et la confirmation de la présence de complexes de surface.

ABSTRACT

The purpose of this research was the study of the interaction mechanisms between U(VI) ions and $SrTiO_3$ surfaces *versus* pH and temperature: 25, 50, 75 and 90°C. Firstly, a physicochemical characterization was realized (DRX, MEB, FTIR) and the surface site density was determined. The potentiometric titration data were simulated, for each temperature, using the constant capacitance model and taking into account both protonation of the ≡Sr-OH surface sites and deprotonation of the ≡Ti-OH ones (one pK_a model). Both enthalpy and entropy changes, corresponding to the surface acid-base reactions, were evaluated using the van't Hoff relation. U(VI) was sorbed onto $SrTiO_3$ powder in the pH range 0.5-5.0 with an U(VI) initial concentration $1 \cdot 10^{-4}$ M. By TRLIFS two U(VI) complexes were detected associated with two lifetime values (60 ± 5 and 12 ± 2 μs at 25°C). The sorption edges were simulated using FITEQL 4.0 software. The surface complexation constants of the system $SrTiO_3$/U(VI) between 25 and 90°C temperature range were thus obtained with the constant capacitance model considering two reactive surface sites. It reveals that two types of surface complex, namely $\left[(\equiv SrOH)(\equiv TiOH)UO_2\right]^{2+}$ and $\left[(\equiv TiOH)(\equiv TiO)UO_2^{+}\right]^{2+}$, are needed to properly describe the experimental observations. By application of the van't Hoff equation, $\Delta_R S^{\circ}$ and $\Delta_R H^{\circ}$ were obtained, which indicated an endothermic sorption process. Finally, an energy transfer study was realised by TRLIFS. The energy transfer between $Tb^{3+}$and Eu^{3+} ions sorbed onto $SrTiO_3$ powders were investigated. The results showed that the energy transfer between Tb^{3+} and Eu^{3+} is a non-radiative process and follows a dipole-dipole type interaction. A formalism based on the Dexter and the Inokuti-Hirayama theories was used to calculate the distances (2,7–3,4 Å) between $Tb^{3+}$and Eu^{3+}onto $SrTiO_3$ surface.